HYDROGEOLOGIC STUDY OF THE BRYCE CANYON CITY AREA, INCLUDING JOHNS AND EMERY VALLEYS, GARFIELD COUNTY, UTAH

by Janae Wallace, Trevor H. Schlossnagle, Hugh Hurlow, Nathan Payne, and Christian Hardwick

OPEN-FILE REPORT 733
UTAH GEOLOGICAL SURVEY
a division of
UTAH DEPARTMENT OF NATURAL RESOURCES
2021

Blank pages are intentional for printing purposes.

HYDROGEOLOGIC STUDY OF THE BRYCE CANYON CITY AREA, INCLUDING JOHNS AND EMERY VALLEYS, GARFIELD COUNTY, UTAH

by

Janae Wallace, Trevor H. Schlossnagle, Hugh Hurlow, Nathan Payne, and Christian Hardwick

Cover photo: *View to the northwest of the pink and white members of the Claron Formation in Bryce Canyon National Park. Photo by Trevor Schlossnagle*

Suggested citation:

Wallace, J., Schlossnagle, T.H., Hurlow, H., Payne, N., and Hardwick, C., 2021, Hydrogeologic study of the Bryce Canyon City area, including Johns and Emery Valleys, Garfield County, Utah: Utah Geological Survey Open-File Report 733, 55 p., 6 appendices, 2 plates, scale 1:62,500, https://doi.org/10.34191/OFR-733.

UTAH DNR GEOLOGICAL SURVEY

OPEN-FILE REPORT 733
UTAH GEOLOGICAL SURVEY
a division of
UTAH DEPARTMENT OF NATURAL RESOURCES
2021

STATE OF UTAH
Spencer J. Cox, Governor

DEPARTMENT OF NATURAL RESOURCES
Brian Steed, Executive Director

UTAH GEOLOGICAL SURVEY
R. William Keach II, Director

PUBLICATIONS
contact
Natural Resources Map & Bookstore
1594 W. North Temple
Salt Lake City, UT 84116
telephone: 801-537-3320
toll-free: 1-888-UTAH MAP
website: utahmapstore.com
email: geostore@utah.gov

UTAH GEOLOGICAL SURVEY
contact
1594 W. North Temple, Suite 3110
Salt Lake City, UT 84116
telephone: 801-537-3300
website: geology.utah.gov

CONTENTS

FIGURES

TABLES

PLATES

ABSTRACT

Groundwater resources development and the threat of future drought in Garfield County, southwestern Utah, prompted a study of groundwater quality and quantity in the environs of Bryce Canyon National Park and Bryce Canyon City in Johns and Emery Valleys. Water quality, water quantity, and the potential for water-quality degradation are critical elements determining the extent and nature of future development in the valley. The community of Bryce Canyon City is an area of active tourism and, therefore, of potential increase in growth (likely from tourism-related development). Groundwater exists in Quaternary valley-fill and bedrock aquifers (the Tertiary Claron Formation and Cretaceous sandstone). Increased demand on drinking water warrants careful land-use planning and resource management to preserve surface and groundwater resources of Johns and Emery Valleys and surrounding areas that may be hydrologically connected to these valleys including Bryce Canyon National Park.

We constructed four geologic cross sections within the study area to help us understand the groundwater system. The cross sections assist in interpreting valley-fill and bedrock stratigraphy and thickness, water levels, flow paths, groundwater-surface water interactions, and constructing the conceptual flow model. The valley fill in Johns and Emery Valleys is divided into predominantly coarse, predominantly fine, and mixed grain size units.

We compiled existing gravity data and conducted a gravity survey to delineate valley-fill thickness and subsurface structures. A total of 124 new gravity stations were acquired during the 2019 field season. Broad, sequential steps in the gravity anomaly are a result of density contrasts between geologic units bounding Emery Valley. The shape of the anomaly is elongated and shelf-like, the main axis trending south-southwest to north-northeast, situated between the towns of Panguitch and Tropic, and the steepest gradients in the gravity field are on the southeastern margins. The central part of Emery Valley, where the anomaly is widest, is likely the area of thickest valley fill.

We measured water levels during two different seasons for four different measuring campaigns: autumn 2018 and 2019, and spring 2019 and 2020. Drought was recorded for the 2018 season, but 2019 and 2020 winters recorded heavier snowpack, especially as reflected in the increase in overall water levels in the valley-fill well sites and discharge measurements from the East Fork Sevier River. We also measured or estimated discharge along the East Fork Sevier River and tributaries, and on the Tropic Ditch canal during the same measuring campaigns. We measured 8 locations along the East Fork Sevier River, 3 locations on the Tropic Ditch canal, and 25 springs and seeps.

We evaluated water quality in streams, wells, and springs based on three different sampling seasons: autumn 2018, spring 2019, and autumn 2019. We collected additional water quality data from select wells during spring 2020. Overall water quality in the valley is excellent and is classified as Pristine based on the Utah Division of Water Quality Board's Groundwater Quality Classification scheme.

We collected samples for stable isotopes of water analysis from 76 unique locations, including from wells and springs, surface water, and precipitation, as well as limited sampling of the radiogenic isotopes tritium and carbon-14. Stable isotope ratios of water from precipitation, surface water, and groundwater range from -126‰ to -24.7‰ for δ^2H and -16.7‰ to -3.4‰ for δ^{18}O. Data for δ^2H and δ^{18}O ratios in groundwater in the study area indicate that evaporative enrichment is a dominant process, affecting most wells and springs in the valley-fill and Claron aquifers. Groundwater in the Cretaceous bedrock aquifer is less affected by this process and likely reflects recharge composition. We collected water samples for tritium analysis from nine wells and four springs. Tritium concentrations measured in groundwater range from 0.01 to 5.60 TU with a mean of 2.35 TU. Eight samples have tritium concentrations considered modern, whereas three samples have concentrations between 0.19 and 1.7 TU and are considered mixed. The two remaining samples are considered pre-modern and are from wells screened in the Cretaceous bedrock aquifer. The modern and mixed samples are from the alluvial aquifer or Claron bedrock aquifer. We collected water samples for radiocarbon analysis from nine wells and four springs. ^{14}C values ranged from 12.0 to 105.6 pmC. Two bedrock well samples have calculated ^{14}C ages of 4800 ±500 and 8600 ±500 ^{14}C yr B.P. Bomb-peak ^{14}C is present in the remainder of samples, which is another indicator of modern water. Water from the valley-fill aquifer, as well as water from the four springs discharging from the Claron Formation, consists of modern groundwater recharged since or slightly prior to 1952. By contrast, water from wells completed in the Cretaceous bedrock aquifer consists of old groundwater, recharged at least 4000 to 5000 years ago.

Data show overall excellent water quality and fluctuating water levels in wells. Wells completed in alluvium recorded water-level rises during spring 2019 and spring 2020; water levels dropped during autumn measurements, and showed slight fluctuations, regardless of season and year, in bedrock wells.

INTRODUCTION

We investigated the hydrogeology of southwestern Johns Valley, Garfield County, Utah, with emphasis on the area of Bryce Canyon City, including Bryce Canyon National Park (BCNP) and the topographic bench (Johnson Bench) and valley (Emery Valley) north of the city (figure 1). Bryce Canyon City occupies part of eastern Emery Valley in central Utah, adjacent to BCNP. Due to projected increase in tourism-related development, we are conducting an ongoing study to understand the hydrogeology of the area, including the relationship between groundwater and surface water from wells, streams, and springs in the southwestern Johns Valley drainage basin. Local government planners are concerned about the impact of past (most recently 2018 and 2021) and potential future droughts on water resources (Garfield County Economic Development Plan, 2019). The State of Utah and the National Park Service (NPS) are additionally concerned about the potential impacts to water rights and water-dependent resources from increased groundwater withdrawals in the study area.

The primary goals of this study are to: 1) characterize the hydrogeology of the southwestern Johns Valley drainage basin as it pertains to the occurrence and flow of groundwater, with emphasis on delineating the valley-fill aquifer thickness and lithology and determining the bedrock hydrostratigraphy, and 2) characterize groundwater levels, chemistry, flow paths, and connection to surface water, principally the East Fork Sevier River.

Water quality, quantity, and the potential for water-quality degradation are critical elements determining the extent and nature of future development in the basin. Most development is on unconsolidated valley-fill deposits, the primary source of groundwater. The community of Bryce Canyon City is an area of active tourism and, therefore, has a potential for increase in growth (likely from tourism-related development). Increased demand on drinking water warrants careful land-use planning and resource management to preserve surface and groundwater resources of Johns and Emery Valleys and surrounding areas that may be hydrologically connected to these valleys including BCNP.

We measured water levels and sampled water during autumn 2018, spring and autumn 2019, and spring 2020 in selected wells, springs, and streams. We analyzed water samples from 10 wells and 4 springs for carbon isotopes and tritium, 76 unique locations (springs, streams, and wells) for stable isotopes of water, and 42 locations for general solute chemistry.

BACKGROUND

Location and Geography

Southwestern Johns Valley is in eastern Garfield County, central Utah, between latitudes 37° 24′ and 38° N. and longitudes 112° 15′ and 111° 52′ W. The main focus of the study is Bryce Canyon City and the gently rolling, forested slope to the northwest and north; the East Fork Sevier River below Tropic Reservoir and associated side drainages, particularly East Creek; and Johnson Bench and Emery Valley, which comprise the southwestern end of Johns Valley (figure 1). Bryce Canyon City is about 20 miles (32 km) southeast of Panguitch, the county seat. The northwest rim of Bryce Canyon itself forms the southeastern boundary of the study area. Emery Valley is an intermontane basin that is bounded by the Sevier Plateau on the north and the Paunsaugunt Plateau on the southwest and opens to Johns Valley to the northeast. The East Fork Sevier River flows through Emery Valley from southwest to northeast and continues northeast through Johns Valley. The hand-dug Tropic Ditch taps into the East Fork Sevier River and transports water east through Water Canyon toward Tropic Valley (Davis and Pollock, 2010). The entire length of the mostly underground ditch is 14 miles (22.5 km) and the ditch is listed on the National Register of Historic Places. Wells serving BCNP are in shallow aquifers south of Bryce Canyon City.

Geologic Setting

The study area is within the Panguitch 30′ x 60′ quadrangle which was geologically mapped and described by Biek and others (2015) (plate 1), the primary source for the geologic summary below. Johns and Emery Valleys are in the Colorado Plateau physiographic province. Johns Valley, situated between the Escalante Mountains and Sevier Plateau, is a topographic depression in which valley-fill sediment has accumulated from the East Fork Sevier River and alluvial fans and side drainages emanating from the surrounding hills. Emery Valley, a southwestern extension of Johns Valley, is situated between the Sevier and Paunsaugunt plateaus. The valley fill forms the principal aquifer of both valleys. Bryce Canyon is a major geologic feature to the south of both valleys.

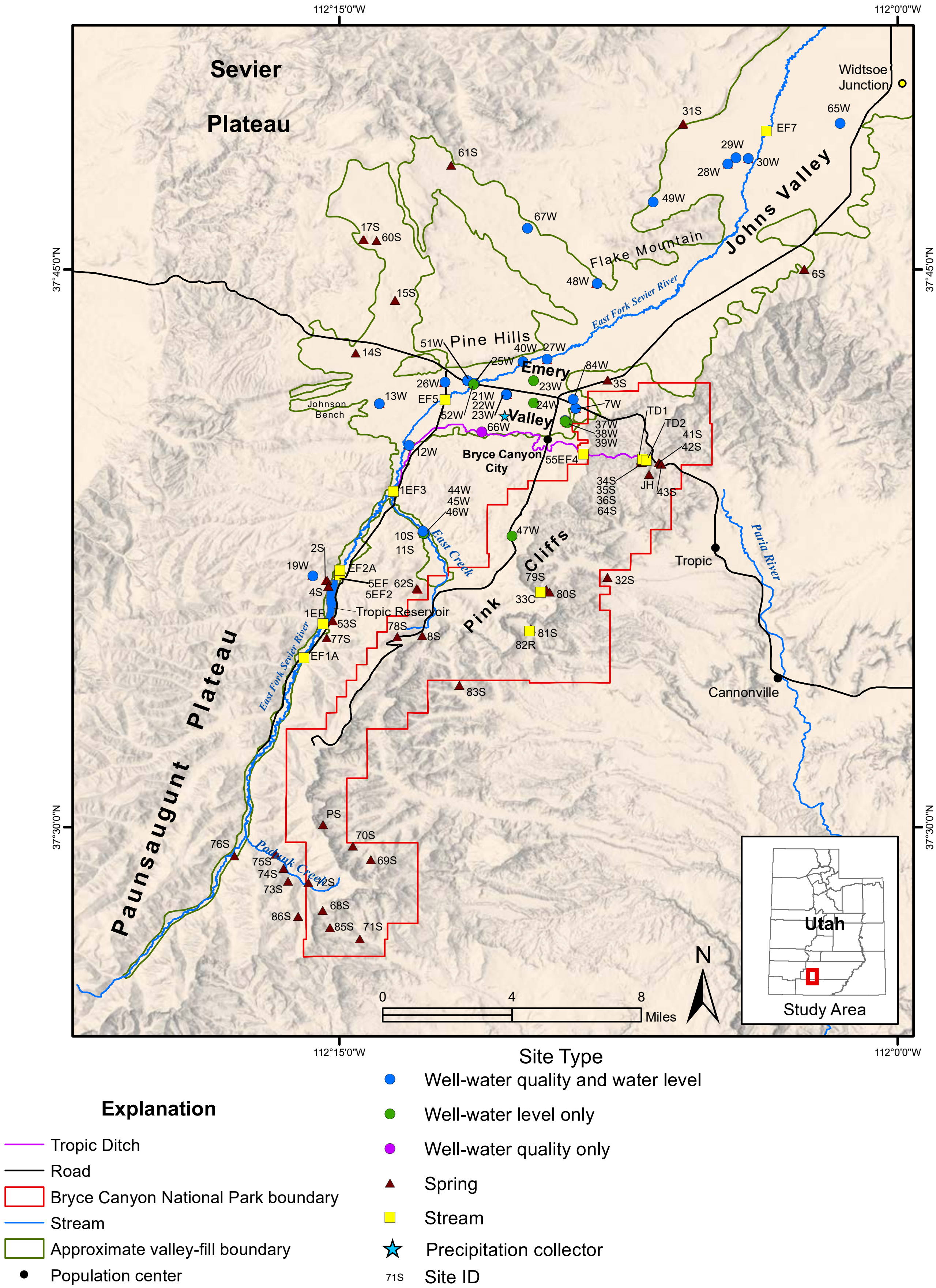

***Figure 1.** Location map of Johns and Emery Valleys, Garfield County, showing sampling locations for wells, springs, and streams, including the East Fork Sevier River.*

Geologic units in the study area are Quaternary unconsolidated deposits, Tertiary volcanic and sedimentary rocks, and Cretaceous sedimentary rocks. The predominant geologic units are Quaternary valley fill, the Tertiary Mount Dutton, Brian Head, and Claron Formations, and the Cretaceous Kaiparowits, Wahweap, and Straight Cliffs Formations.

The Quaternary unconsolidated deposits include gravel, sand, and clay derived from adjacent hills and mountains that were deposited in alluvial-fan, fluvial, and mass-movement environments.

The Oligocene-Miocene Mount Dutton Formation is moderately resistant to nonresistant volcanic mudflow breccia consisting of angular to subrounded, matrix-supported, pebble- to boulder-sized clasts of dacitic to andesitic volcanic rock in a muddy to sandy matrix (Mackin and Rowley, 1976; Maldonado and Williams, 1993a, 1993b; Rowley and others, 1994). In the northwestern part of Johns Valley in the Sevier Plateau, the Mount Dutton Formation is light- to dark-gray and brown, andesitic to dacitic volcanic mudflow breccia and lesser interbedded volcaniclastic conglomerate and tuffaceous sandstone (Biek and others, 2015). Exposures in the Sevier Plateau are the alluvial facies of the Mount Dutton Formation, re-interpreted as part of the Markagunt gravity slide, about 2000 feet (600 m) thick on the southern end of the Sevier Plateau (Rowley and others, 2013; Biek and others, 2015).

The Eocene-Oligocene Brian Head Formation is non-tuffaceous sandstone and conglomerate, volcanic mudflow breccia, mafic lava flows, volcaniclastic sandstone with minor limestone and chalcedony, and ash-flow tuff (Biek and others, 2015). The unit consists dominantly of yellowish-gray and light-gray, cross-bedded, tuffaceous sandstone with interbedded pebble- to boulder-sized conglomerate, sandstone, and minor limestone and mudflow breccia (Maldonado and Moore, 1995).

The Eocene-Paleocene Claron Formation in the study area consists of mudstone, siltstone, sandstone, limestone, and minor conglomerate deposited in fluvial, floodplain, and lacustrine environments of an intermontane basin (Mullet, 1989; Ott, 1999; Biek and others, 2015).

The Claron Formation is divided into the younger white member that was deposited in both fluvial and lacustrine environments and the older pink member that is dominantly fluvial (Goldstrand,1994; Bown and others, 1997). The upper limestone unit of the white member is white, pale-yellowish-gray, pinkish-gray, and very pale orange micritic limestone and uncommon pelmicritic limestone, and is typically about 80 to 100 feet (24–30 m) thick on the southern flank of the Sevier Plateau (Biek and others, 2015). The lower part of the white member consists of micritic limestone similar to the upper white limestone interval and forms a cliff or steep, ledgy, white slope. The lower limestone unit has a maximum thickness of about 300 feet (91 m) at Bryce Point in BCNP (Bowers, 1991), and about 160 feet (49 m) thick to the north on the southwestern flank of the Sevier Plateau (Biek, 2015). Within BCNP at Inspiration Point, the lower limestone unit of the White Member is mostly white, pink, and pale-orange, slope-forming mudstone and siltstone with only minor limestone (Knudsen and others, in preparation).

The pink member of the Claron Formation consists of micritic limestone, calcite-cemented sandstone, calcareous mudstone, and minor pebbly conglomerate that weather to colluvium-covered ledgy slopes. The pink member is about 600 feet (183 m) thick at BCNP (Biek and others, 2015).

The Kaiparowits Formation is a light-brown, very fine grained sandstone and gray sandy mudstone that crops out above the capping sandstone member of the Wahweap Formation southwest of Tropic Reservoir (Bowers, 1991). The Kaiparowits Formation was deposited as an eastward-prograding clastic wedge in a relatively wet, subhumid alluvial plain with periodic to seasonal aridity near the western margin of the Late Cretaceous Western Interior Seaway (Roberts, 2007).

The Late Cretaceous Wahweap Formation overlies the Straight Cliffs Formation in the drainage basin; these two units are very similar, especially near their contact, and are commonly lumped together as an undivided map unit. The Wahweap Formation is mostly fine-grained sandstone, siltstone, and mudstone deposited in braided and meandering river and floodplain environments of a coastal plain (Lawton and others, 2003). Around Tropic Reservoir, because of extensive vegetative cover and poor geomorphic expression, three members of the Wahweap Formation are mapped as undivided, except for the distinctive capping sandstone (Knudsen and others, in preparation).

The Late Cretaceous Straight Cliffs Formation consists of the Drip Tank and John Henry Members in the study area. On the Paunsaugunt Plateau, the Drip Tank Member is white to light-gray, fine- to medium-grained quartzose sandstone, and, in the upper part of the unit, pebbly sandstone and pebbly conglomerate (Biek and others, 2015). The John Henry Member consists of variegated, gray, brown, and reddish-brown mudstone and thin- to thick-bedded, grayish-orange to yellowish-brown, fine-grained subarkosic sandstone and forms ledgy slopes on the eastern margin of the BCNP boundary; in the area around Bulldog Hollow near the town of Tropic, the John Henry Member is stacked or amalgamated sandstone in the upper part of the unit. North of Tropic, a prominent 20- to 40-foot-thick (6–12 m) coal-rich interval is mapped as a marker bed (Knudsen and others, in preparation).

The principal structural elements of Johns Valley (Biek and others, 2015) include the Paunsaugunt fault zone, a northwest-side-down Quaternary normal fault that strikes northeast through Johns Valley along the eastern margin of the study area; the Pine Hills and Rubys Inn thrust faults, which strike east-west and form the northern and southern boundaries, respectively, of Emery Valley; and the Johns Valley thrust fault northwest of Flake Mountain, which strikes northeast through the central part of Johns Valley in the northern part of the study area.

Groundwater is present in the Quaternary sediments of the shallow valley-fill aquifer. Pre-Quaternary sedimentary deposits and Tertiary and Cretaceous rocks also yield water to wells. The limestone in the Claron Formation forms a karst aquifer on the Markagunt Plateau to the west of the study area and may form an aquifer in the Emery Valley area. The East Fork Sevier River is sourced in the Paunsaugunt Plateau, enters the study area from the south, and flows northeast through the study area in Emery Valley and Johns Valley.

Previous Work

Water-Level and Water Quality Data

The U.S. Geological Survey (USGS) has water quality or water level measurement records for five wells and eight springs in the study area, determined from a search of their National Water Information System (NWIS) database. Four of the five wells have at least one water level measurement, and a well located at the Bryce Canyon airport has decades of water level measurements. Most wells are used for domestic, commercial (tourism), and stock supply; two well fields (having a cluster of more than two wells on site) serve as public supply wells to Bryce Canyon City (Ruby's Inn wells) and BCNP (NPS well field).

Limited data for groundwater levels and flow directions have been documented in the study area (Thiros and Brothers, 1993; NWIS data for four wells). The groundwater level measured sporadically since the early 1950s at the Bryce Canyon airport (figure 2) (USGS site 374205112091501) averaged 29 feet (9 m) below ground surface (bgs) over the past 5 years (USGS NWIS data). Most additional groundwater-level data are about 20 to 30 years old. Based on topography and surface hydrology, the regional direction of groundwater flow is likely northeast toward Otter Creek Reservoir (35 miles [56 km] to the north of Bryce Canyon City).

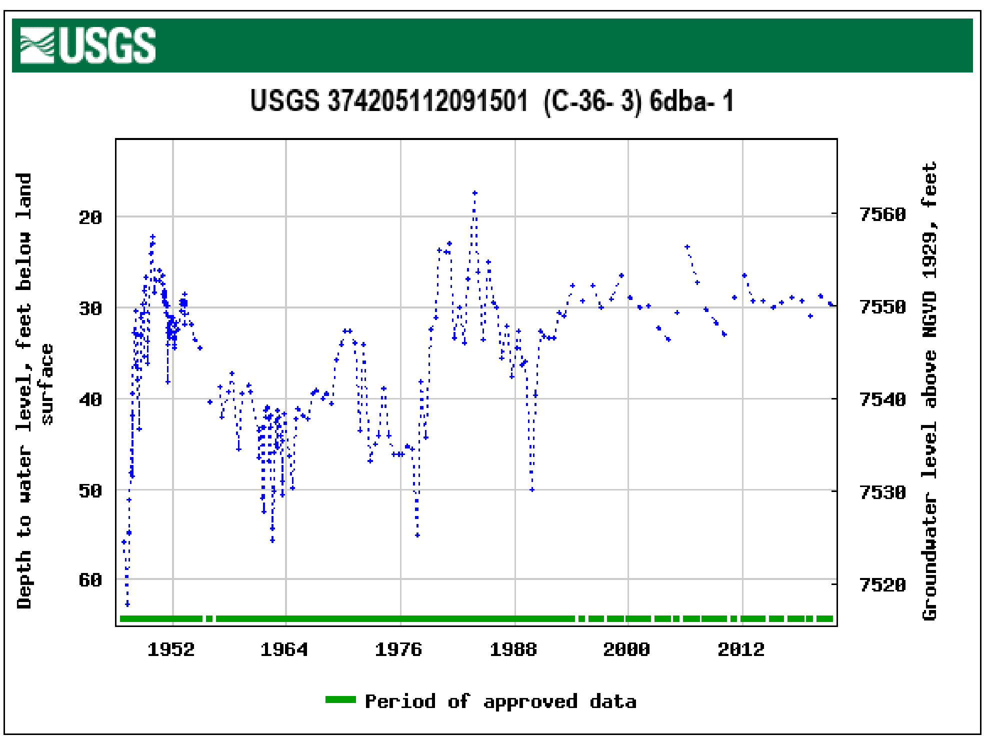

Figure 2. *Historical airport well water levels from the USGS NWIS website (https://nwis.waterdata.usgs.gov/nwis/gwlevels/?site_no=374120112084201&agency_cd=USGS&amp).*

A search of water-quality data for the study area yielded only one sample from the Utah Department of Agriculture and Food (UDAF) and 13 sites from the NWIS database for 5 wells and 8 springs. The UDAF sample was from a well in the northeastern corner of the study area taken in 2003 and had a total-dissolved-solids (TDS) concentration of 218 ppm, a pH of 8.5, and no constituents that exceeded secondary drinking-water or agricultural standards, including pesticides. The 13 NWIS sites (some sampled over several years) measured TDS concentrations for all sites (ranging from 167 to 422 mg/L) and a few sites for arsenic, boron, and barium (all yielded values below maximum contaminant level [MCL]).

Water-Yielding Characteristics

No previous study has addressed in detail the water-yielding characteristics of the Johns and Emery Valleys valley-fill aquifers. Thiros and Brothers (1993) described the larger Sevier watershed including the Panguitch and Otter Creek areas and provided some information on the Bryce area (which they refer to as "East Fork Valley").

Thiros and Brothers (1993) summarized the water-yielding characteristics of the East Fork Valley that includes Johns and Emery Valleys. They identified the sand and gravel deposits of the Emery Valley valley-fill aquifer as having the highest hydraulic conductivity. Transmissivity based on an aquifer test in Emery Valley yielded 6 ft^2/day (0.56 m^2/day). Aquifer tests yielded hydraulic-conductivity values of 0.2 ft/day (0.06 m/day) from an alluvial fan in Johns Valley and 1500 ft/day (457 m/day) for a well in Emery Valley completed in gravel and sand. Hydraulic-conductivity values were estimated from specific capacity data from 21 drillers' logs and ranged from 6 to 20 ft/day (1.8 to 6 m/day), and specific yield was estimated to be 0.13 (Thiros and Brothers, 1993).

Surface Water

The East Fork Sevier River originates within the Paunsaugunt Plateau in the study area and flows north toward Tropic Reservoir. It continues to flow north-northeast through Emery Valley and Johns Valley from October to March; during April to October, most of the East Fork Sevier River is diverted to the Tropic Ditch about 1.5 miles (2.4 km) north of Tropic Reservoir dam to irrigate agricultural operations near the community of Tropic to the east. This diversion is unusual in that it transports water across a major hydrographic boundary—water flowing in the Tropic Ditch ends up in the Paria River drainage, which flows to the Colorado River and ultimately the Gulf of California, whereas water in the East Fork Sevier River flows toward the Sevier Dry Lake terminus in the Great Basin.

Outside of irrigation season and during heavy snowpack years, the river flows past the diversion and continues north out of Johns Valley to Black Canyon where it continues north to meet the main stem of the Sevier River near Kingston in Circle Valley (37 miles [59.5 km] north-northwest of Bryce Canyon City). Tributaries to the East Fork in the study area just south and north of Tropic Reservoir include Kanab, Skunk, Podunk, East, and Daves Hollow Creek to the east and King, Blue Fly, and Ahlstrom Hollow intermittent creeks to the west; farther northwest, Hunt Creek joins the East Fork near Tom Best Spring. The Sevier River, along a tortuous path, eventually drains to the northwest toward Sevier Lake. In BCNP, few perennial streams exist. The streams with flowing water (East, Podunk, Daves Hollow) are quite low during portions of the year. Intermittent creeks include Campbell, East, Sheep, Swamp, and Yellow Creeks. Approximately twelve ephemeral creeks emanate from the park's steeper east escarpment and flow toward the Paria River drainage and eventually toward the Colorado River.

HYDROSTRATIGRAPHY

Regional Hydrostratigraphy

Biek and others (2015) defined the regional stratigraphy of the Panguitch 30′ x 60′ quadrangle which includes the study area for this project (plate 1). We derived hydrostratigraphy for the geologic units in our project area (figure 3) based on their work, water-well data, and limited field observations. Defining hydrostratigraphic units involves grouping or splitting of geologic formations based on their known or inferred water-yielding characteristics. The scheme used here includes aquifer, heterogeneous (mixed confined/unconfined or intercalated fine and coarse sedimentary layers) unit, and confining unit. The valley fill, Claron Formation, and Cretaceous formations (Kaiparowits, Wahweap, and Straight Cliffs Formations) yield water to wells and springs in the study area.

Quaternary and late Tertiary deposits are primarily alluvial and coarse- to medium-grained, include comparatively thin and laterally discontinuous fine-grained layers, and are classified as aquifer units. The next section provides more detail about

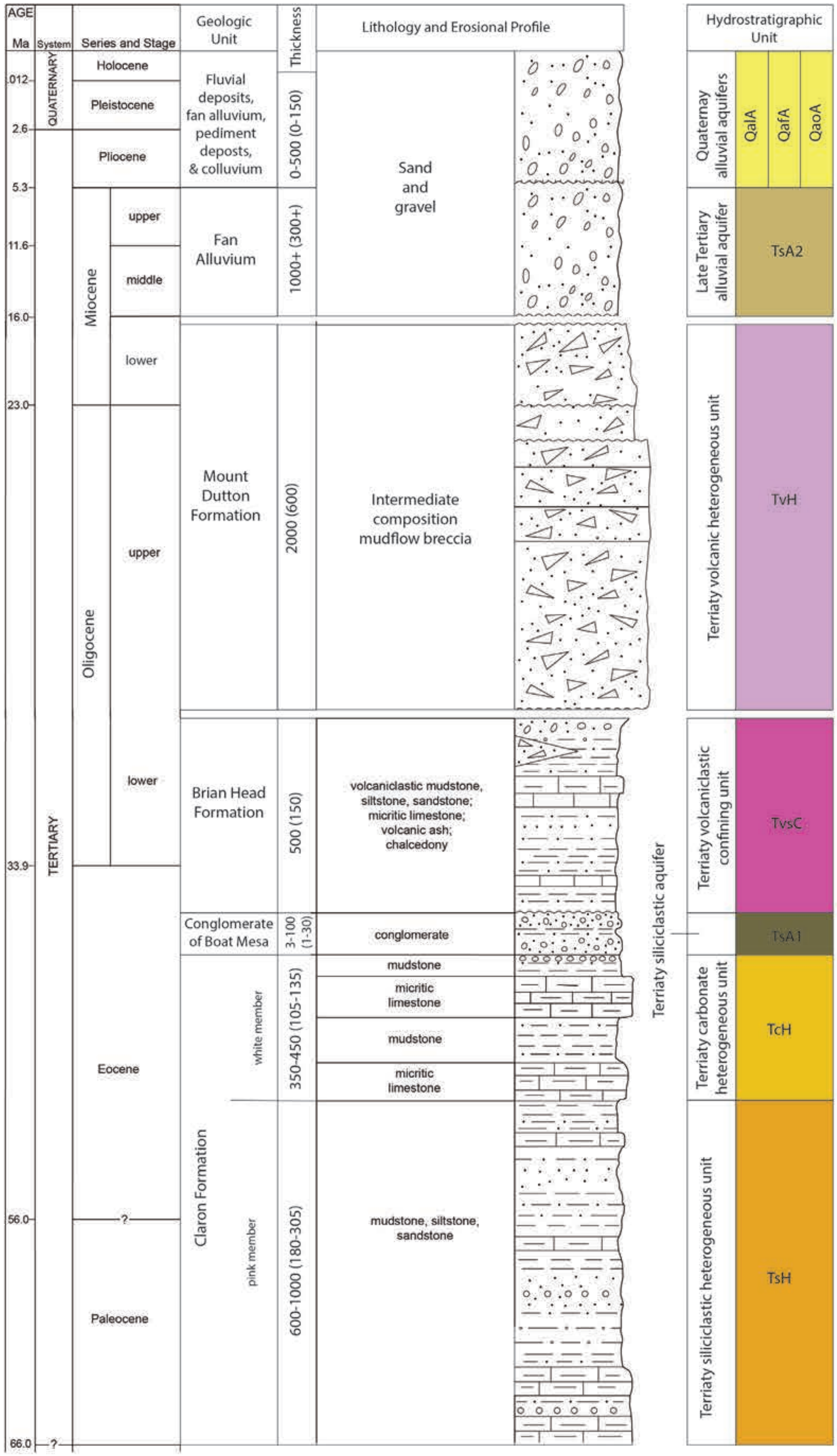

Figure 3a. *Hydrostratigraphy of Quaternary and Tertiary sedimentary deposits and rocks in the study area. Modified from Biek and others (2015).*

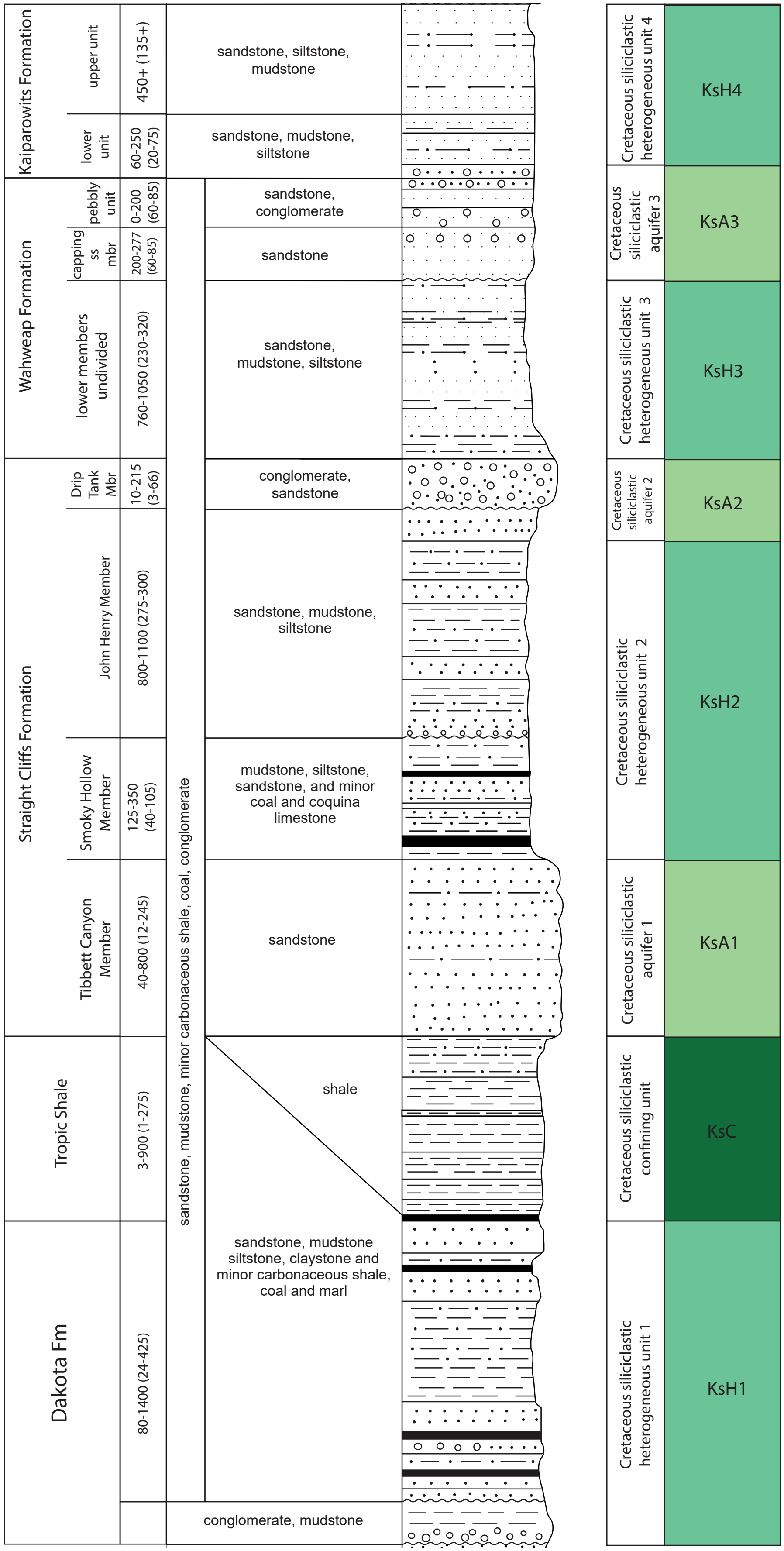

Figure 3b. *Hydrostratigraphy of Cretaceous rocks in the study area. Modified from Biek and others (2015).*

the lithology and stratigraphy of the Quaternary-Tertiary valley-fill deposits. The Mount Dutton Formation is predominantly volcaniclastic mudflow breccia and is classified as a "heterogeneous unit," due to lateral and vertical variations in texture and fracturing. This unit's water-yielding characteristics are expected to vary with location, and individual aquifers within the unit are not expected to be connected at a regional scale. The Brian Head Formation is classified as a confining unit based on its composition of volcanogenic mudstone, and localization of springs at its top in the northern part of the study area. The Claron Formation is split into two heterogeneous units; the upper unit is composed predominantly of carbonate rocks and the lower unit is composed predominantly of siliciclastic rocks (figure 3a). Both units yield water to wells. The carbonate heterogeneous unit is karstic on the Markagunt Plateau about 35 miles (56 km) to the west (Biek and others, 2015, p. 31–32). Karst features were not observed in outcrop during this study but may be present in the subsurface and control the locations of springs. Upper Cretaceous formations are composed of alternating predominantly coarse-grained and predominantly fine-grained intervals that are classified as heterogeneous units and confining units, respectively (figure 3b). The heterogeneous units are predominantly fine-grained sandstone grading to conglomerate having a coarse-grained sandy matrix and include shale interbeds. These units yield water to wells and springs.

Valley-fill Aquifer

Lithology

We entered data from drillers' well logs (appendix B) into a well management program, constructed cross sections through the valley fill, and identified laterally continuous lithologic units. We chose section lines based on the distribution of well logs within the study area. We used 38 well logs based on their proximity to section lines. The cross sections (plate 2) assist in interpreting valley-fill stratigraphy and thickness, water levels, flow paths, groundwater-surface water interactions, and constructing the conceptual flow model. The valley fill in Johns and Emery Valleys is divided into predominantly coarse (sands and gravels), predominantly fine (clay, silt, and fine sand), and mixed grain size units.

Cross section A-A′ trends northwest-southeast through central Emery Valley and includes the area of greatest groundwater development in the valley (plate 2). Within 25 to 30 feet (8–9 m) of land surface, unconsolidated deposits are predominantly coarse grained near the valley margins and predominantly mixed grain size in the valley center. In the middle to lower parts of the valley fill, predominantly fine-grained deposits exist near both ends of the cross section. The valley-fill deposits are less than 50 feet (15 m) thick and overlie Cretaceous (undivided) rocks below the valley floor and the Claron Formation (undivided). Well logs are insufficiently detailed to identify hydrostratigraphic units within the Claron Formation and Cretaceous rocks; however, several wells are completed in each suggesting they yield at least minimal groundwater. The cross section illustrates the Pine Hill thrust fault truncating the lower part of the valley-fill deposits, suggesting they are Tertiary in age and the overlapping deposits are Quaternary.

Cross section B-B′ trends east-west through Emery Valley (plate 2). Valley-fill deposits are primarily mixed grain size, are as much as 200 feet (61 m) thick and overlie Cretaceous bedrock. The John Henry Member of the Straight Cliffs Formation crops out along the north bank of a wash just south of a petroleum-exploration well. Cuttings from the petroleum-exploration well, housed in the UGS Utah Core Research Center, were examined for this study and indicated about 200 feet (61 m) of pebbly valley-fill deposits above medium-grained, well-sorted sandstone (appendix C). The pebbly deposits are the Quaternary alluvial pediment deposits (unit Qap) on the geologic map (plate 1). Well 1035 is a water-supply well for the petroleum-exploration well (plate 1), but its log indicates only bedrock. Valley-fill deposits in this area evidently vary in thickness substantially over short distances. The line of cross section B-B′ is north of a small exposure of John Henry Member of the Straight Cliffs Formation along the north wall of a modern dry wash. The valley fill-bedrock contact, therefore, rises steeply south out of the cross-section plane to intersect the land surface on the north side of the dry wash. We interpret the section to lie along an old erosional channel (now filled by the older Quaternary pediment deposits) that was bounded on the south by the rocks that now crop out on the north side of the younger wash. The modern wash channel cut a small valley south of the original one.

Cross section C-C′ trends north-south across central Emery Valley (plate 2). A bedrock ridge is shown about one-third of the distance south of the Pine Hills thrust; its subsurface geometry is unknown and is distorted by the 20-times vertical exaggeration of the section. The ridge could be erosional or related to minor Quaternary slip on the Paunsaugunt fault. North of the bedrock ridge, mixed grain-size deposits overlie coarse-grained deposits. South of the bedrock ridge, coarse-grained alluvial-fan deposits overlie mixed grain-size deposits near the mountain front, and well 1057 indicates a substantial lens of predominantly fine-grained deposits, whereas the rest of the valley fill consists of mixed-grain-size deposits.

Cross section D-D′ trends east-northeast across southern Johns Valley and includes a right-angle bend to the southeast to intersect water wells along the southeastern valley margin (plate 2). Valley-fill deposits are predominantly coarse grained in the west-southwest part of the section, and predominantly mixed grain size in the southeast part of the section. A fine-grained layer exists at about 40 to 65 feet (12–20 m) below the land surface in the central part of the section. The cross section intersects the Johns Valley thrust fault in the southwest and the Paunsaugunt normal fault in the southeast. We do not know the age of the deepest coarse-grained deposits in the central part of the section; they could be cut by either or both faults. Younger valley-fill deposits onlap the fault surfaces.

The cross sections collectively indicate that the valley-fill deposits below Emery Valley and southern Johns Valley are predominantly coarse grained to mixed grain size and are less than about 200 feet (61 m) thick in most places. Coarse-grained deposits are prevalent near the mountain fronts and are interbedded with heterogeneous deposits below the valley floor. Fine-grained layers are rare and laterally discontinuous, suggesting unconfined groundwater conditions exist in most areas. We are uncertain whether the mixed-grain-size deposits consist of poorly sorted deposits or interlayered fine- and coarse-grained deposits.

Thickness

Wells: We interpreted depth to bedrock from well drillers' logs. Locating the valley fill-bedrock contact from driller's logs can be straightforward or ambiguous, depending on the level of detail of the log and on the lithologic contrast between valley fill and bedrock. For example, cuttings from the Lion/Monsanto 1 Bryce well (plate 1; appendix C) include a wide variety of rock types having rounded edges (i.e., pebbles) in the upper 200 feet (61 m), and exclusively medium- to fine-grained sandstone angular fragments below 270 feet (82 m); the exact contact is, unfortunately, missing. The contact between multilithologic gravel and uniform sandstone would be obvious to most well drillers. Where fine-grained valley-fill deposits overlie Cretaceous shale (e.g., one of the confining hydrostratigraphic units shown on figure 3b), however, the change in lithology and drilling characteristics between valley fill and bedrock may be more difficult to detect. We subjectively chose the most reliable well logs to estimate valley-fill thickness.

Gravity study: We conducted a gravity survey in the study area to delineate valley-fill thickness and subsurface structures, acquiring 124 new gravity stations during the 2019 field season (figure 4). In gravity surveys, the working unit Gal is defined as 1 centimeter per second squared (cm/s^2) making, for example, the commonly stated acceleration due to gravity at the Earth's surface 980 Gal (9.8 m/s^2). Observed changes in the Earth's local gravity field are most sensitive to elevation (vertical changes) which makes elevation control a critical parameter in gravity surveys.

We used two Scintrex CG-5 Autogravs (precision of 1 μGal, accuracy of 5 μGal) to make field measurements of the vertical component of the gravity field, following the methods of Gettings and others (2008) and utilizing an absolute gravity base station located near the Department of Natural Resources in Salt Lake City. We established elevation control through post-processing of data collected by high-precision GPS survey equipment. When logging for a minimum of 10 minutes we observed better than 3 cm (1.18 inches) vertical precision for 114 stations, 20 cm (7.87 inches) or better for 5 stations, and the remaining 5 stations were submeter (39.37 inches). The vertical absolute accuracy depends on the local base station absolute coordinates which are within the range of 1 to 3 cm (0.39–1.18 inches). From calculations based on the vertical gravity gradient (0.3086 mGal/m), the GPS surveying procedure would result in a vertical gravity accuracy of better than 0.001 mGal (1 μGal) for 90% of the stations which is acceptable since it exceeds the gravimeter's sensor accuracy of 5 μGal. We applied terrain corrections to the processed gravity data and calculated the Complete Bouguer Gravity Anomaly (CBGA) for each station using the methods outlined in Hintze and others (2005) with a reduction density of 2.67 grams per cubic centimeter (g/cm^3). UGS gravity data were merged with 749 legacy gravity stations from PACES (Pan American Center for Earth & Environmental Studies [PACES], 2012), a national gravity and magnetics data repository, to improve data coverage in the study area.

Gravity data are tabulated in appendix D. The map of the CBGA field (figure 4) illustrates broad downward steps in a northwestward direction in the gravity anomaly signal that are on the order of 30 mGal in the southeast to 15 mGal in the northwest. These broad, sequential steps in the gravity anomaly are a result of density contrasts between the local geology bounding Emery Valley. The shape of the anomaly is elongated and shelf-like, the main axis trending south-southwest to north-northeast, situated between the towns of Panguitch and Tropic, and the steepest gradients in the gravity field are on the southeastern margins. We interpret the areas having the most widely spaced CBGA contours—central Emery Valley, southwestern Johns Valley, and northeastern Johns Valley—as the thickest parts of the valley fill.

Valley-fill isopach map: Figure 5 is a schematic isopach map of the unconsolidated valley-fill deposits in Emery and Johns Valleys based on information from drillers' well logs and the CBGA map. Uncertainty in using the driller's logs for this purpose is discussed above. The shape and gradient of the CBGA field was used to guide the location and spacing of thickness isolines;

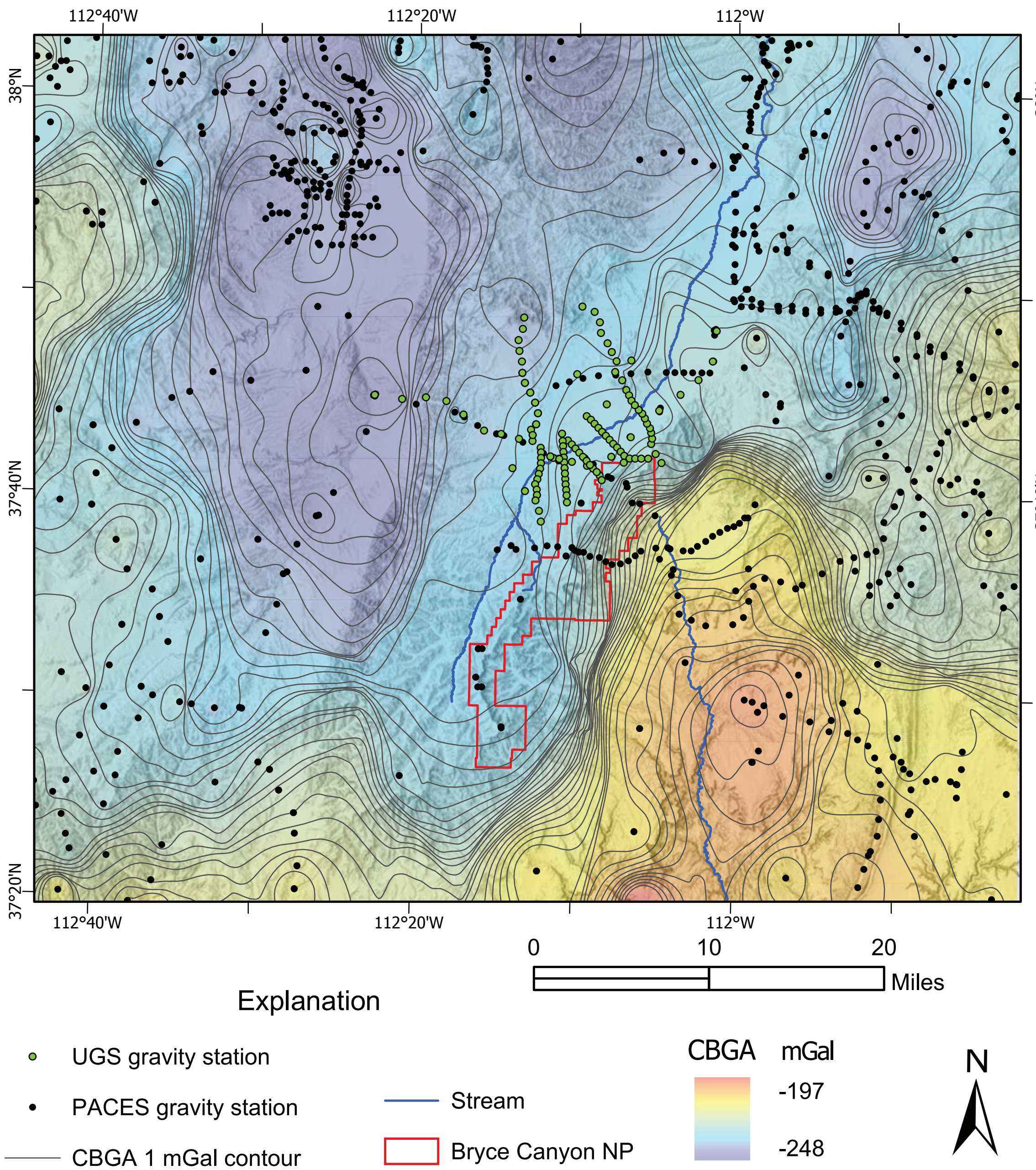

Figure 4. *Complete Bouguer Gravity Anomaly map for the study area.*

however, as discussed in the previous section the contours reflect both lateral gradients in pre-Quaternary geologic units and the thickness of the valley-fill aquifer. Our interpretations of valley-fill thickness below southwestern Johns Valley south of Flake Mountain and northeastern Johns Valley northeast of Widtsoe Junction are based solely on the CBGA anomaly and are highly speculative because no well data are available (figure 5). As drawn, the isopach contours indicate 1) mostly shallow and highly variable valley-fill thickness in western Emery Valley, 2) an elongate, northeast-trending, oval-shaped depositional center in eastern Emery Valley and southeastern Johns Valley, and 3) an oval-shaped, north-northeast-trending depositional center in northeastern Johns Valley. The isopach contours have high uncertainty and could be modified based on new well data or additional analysis of the gravity data (see following paragraph). These isopach contours should not be used to estimate depth to bedrock for potential new wells, except in a very general way, or to interpret the depositional or structural evolution of the basin.

Future work for this project may include 1) estimating the density gradient within the pre-Quaternary rocks, 2) subtracting that gradient from the CBGA values to further isolate the gravity signal due to thickness variations in the valley fill, and 3) constructing model profiles based on the revised CBGA values, where the best constrained models would include gravity stations on bedrock at either side of the valley and near wells having well constrained depth to bedrock. Models through the valley fill where wells are not present would be tied to the better constrained models.

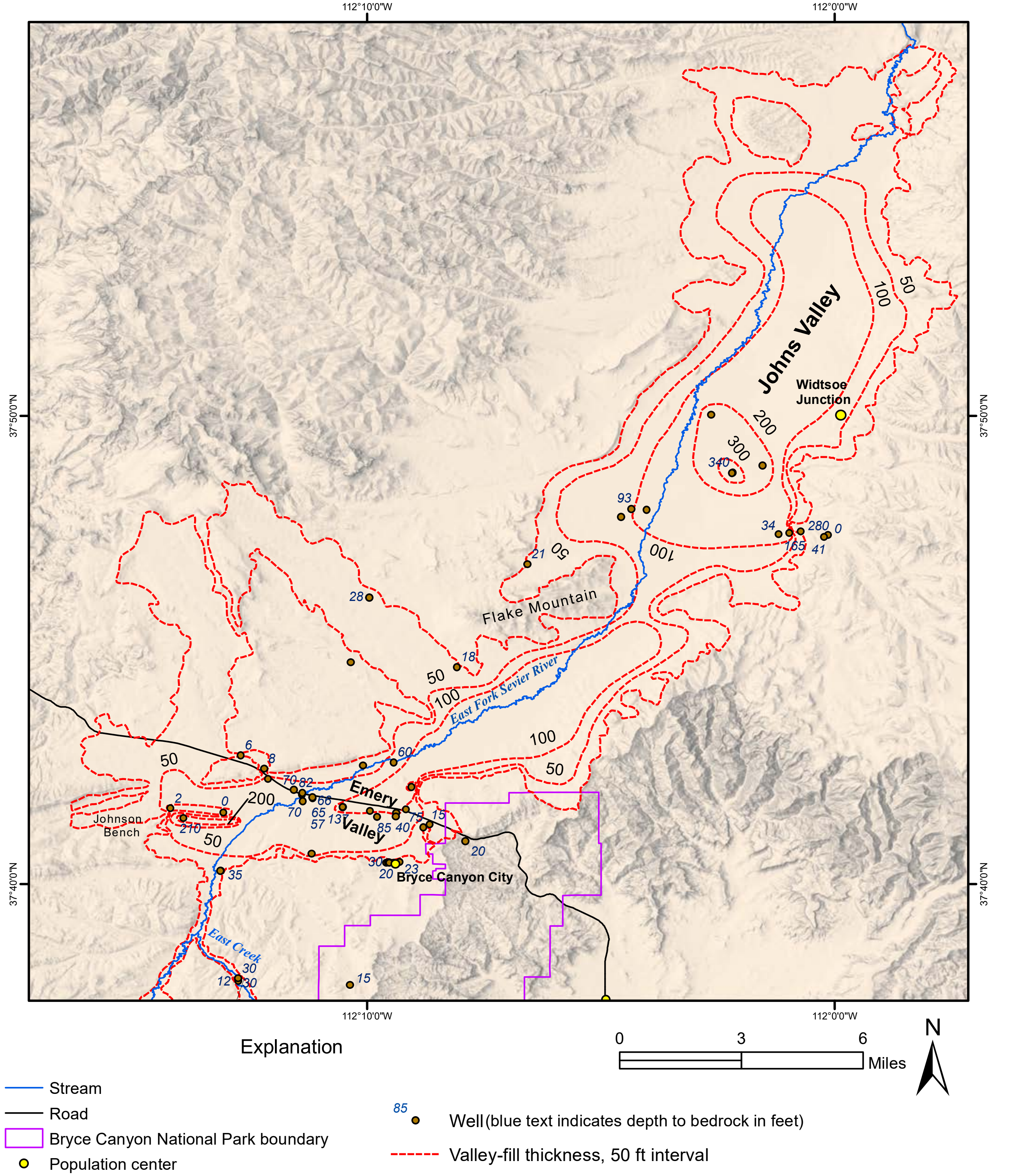

Figure 5. *Schematic isopach map for the valley fill based on drillers' well logs and gravity data.*

Aquifer Properties Estimates

Aquifer properties describe how well the aquifer will yield water to wells and springs. We compiled data from aquifer tests performed for Utah Division of Drinking Water drinking water source protection plans, which provide good estimates of aquifer properties (appendix E). Aquifer test data in the study area are scant, so we estimated aquifer properties from information obtained from drillers' water well logs (appendix E).

We estimated storativity using the equation S=Sy + (Ss*b), where S is storativity, Sy is specific yield, Ss is specific storage, and b is aquifer thickness. We based Sy and Ss on published values for aquifer materials from Johnson (1967) and Domenico (1972) and b from driller's well logs. We based specific capacity estimates from driller's well logs using draw-down data where specific capacity is the pumping rate divided by drawdown. We estimated transmissivity using specific capacity data from driller's well logs using the TGUESS algorithm of Bradbury and Rothschild (1985), which utilizes the Cooper and Jacob (1946) solution of the Theis (1935) equation. We estimated hydraulic conductivity by dividing transmissivity by saturated aquifer thickness. Aquifer thickness was assumed to be the length of the screened or perforated interval.

Six aquifer tests were conducted in the study area for public water supplies (appendix E). Four of the tests were conducted on wells in the valley-fill aquifer: three in Emery Valley and one in the East Creek drainage for a BCNP public supply well. One test each was conducted in the Claron Formation and Cretaceous bedrock. These data were not included with summary statistics of transmissivity values estimated from specific capacity data, but are shown on figure 6.

We estimated storativity and transmissivity for two general aquifers for the principal valley-fill aquifer (n=18), and the bedrock aquifers (n=15), the latter consisting of the Tertiary Claron Formation and Cretaceous sandstone (figure 6). Storativity was 0.3 for the valley-fill aquifer and ranged from 0.005 to 0.0005 for the bedrock aquifers. The valley-fill aquifer had the highest reported transmissivities, ranging from 10 to 10,680 feet squared per day (ft^2/day). The geometric mean for this aquifer was 293 ft^2/day (27 m^2/day). Transmissivities in the bedrock aquifers ranged from 8 to 1116 ft^2/day (0.7–104 m^2/day), with a geometric mean of 78 ft^2/day (7 m^2/day).

The range of transmissivity data from aquifer tests and specific capacity data is shown in figure 7. In Emery Valley, transmissivities appear to correlate with valley-fill thickness, with lower values on the valley margins and higher values toward the valley center. Transmissivities from aquifer test data generally agree with the distribution of transmissivity from specific capacity data.

GROUNDWATER LEVELS AND STREAMFLOW

Water Levels and Potentiometric Surfaces

Methods

To construct potentiometric surfaces, we measured water levels in wells at four different times: autumn 2018, spring 2019, autumn 2019, and spring 2020. We calculated the elevation at most wells using a Trimble high-precision GPS instrument having vertical accuracy of 10 centimeters. Land surface elevation for the remaining wells was derived from one-meter resolution lidar data (Utah Automated Geographic Reference Center, 2018). Water-level elevation at each well was determined by subtracting the measured depth to water from the land-surface elevation obtained from the GPS or lidar data, accounting for the height of the measuring point above land surface (table A-1 of appendix A).

We used ArcMap to create potentiometric surface maps for each season of measurement. Potentiometric surface maps were created by interpolating water-level elevations using the Topo to Raster interpolation method and converting the raster surface to polylines at 20-foot contour intervals, which were further refined manually. We created maps showing the change in water levels from autumn 2018 to spring 2019 and spring 2019 to autumn 2019 by plotting the difference in water level measured at each well. We created a saturated thickness map by subtracting the spring 2019 potentiometric surface from the valley-fill isopach map.

Potentiometric Surfaces and Saturated Thickness

Only wells completed in the valley-fill aquifer, screened in both alluvium and bedrock, or screened in bedrock with water levels consistent with nearby valley-fill wells were used to generate potentiometric surfaces (figures 8a–d). Due to the paucity of wells in the study area, we included water level data regardless of well pumping activity. Wells are differentiated by well type (public

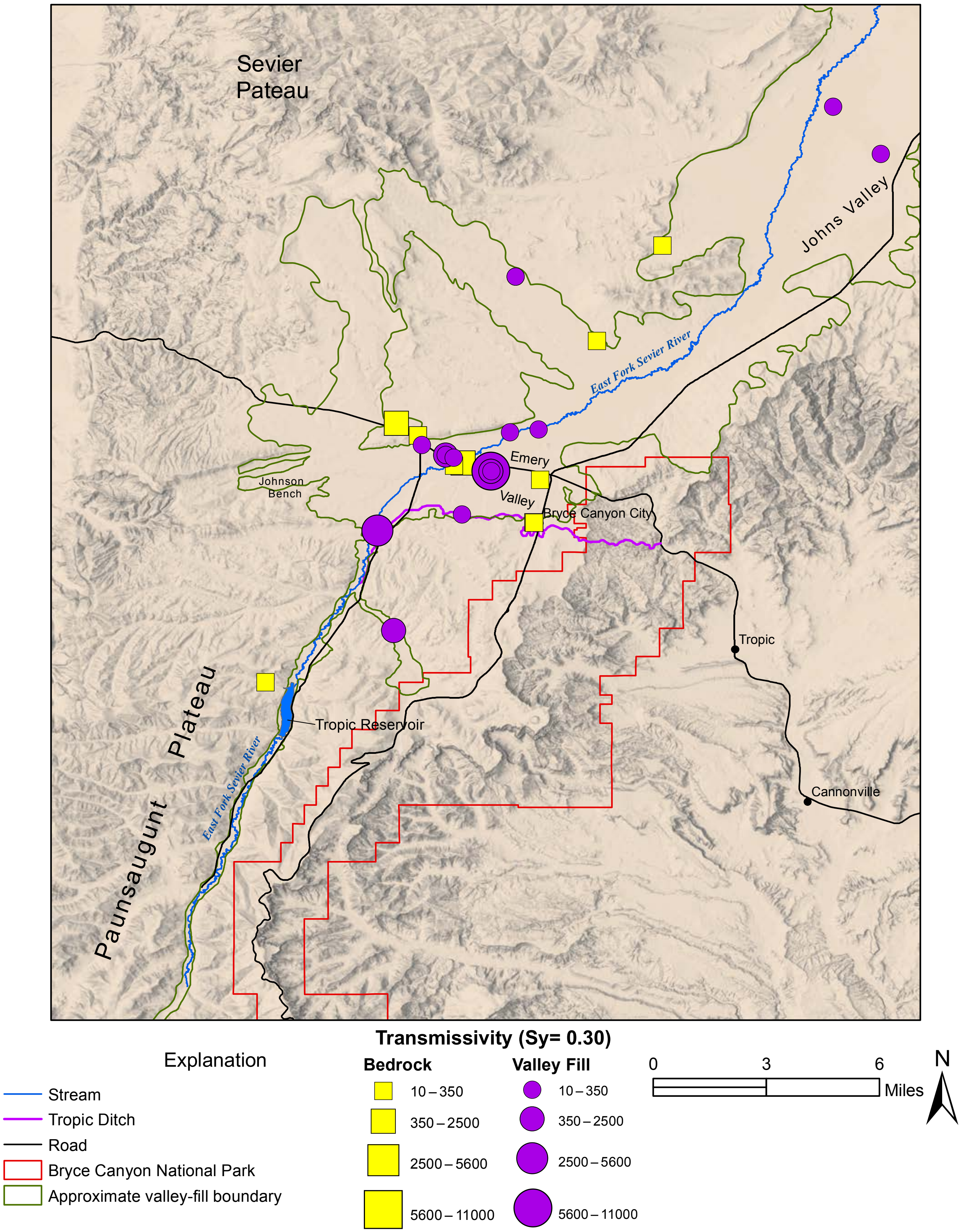

Figure 6. *Transmissivity map compiled from public supply well data and drillers' well logs.*

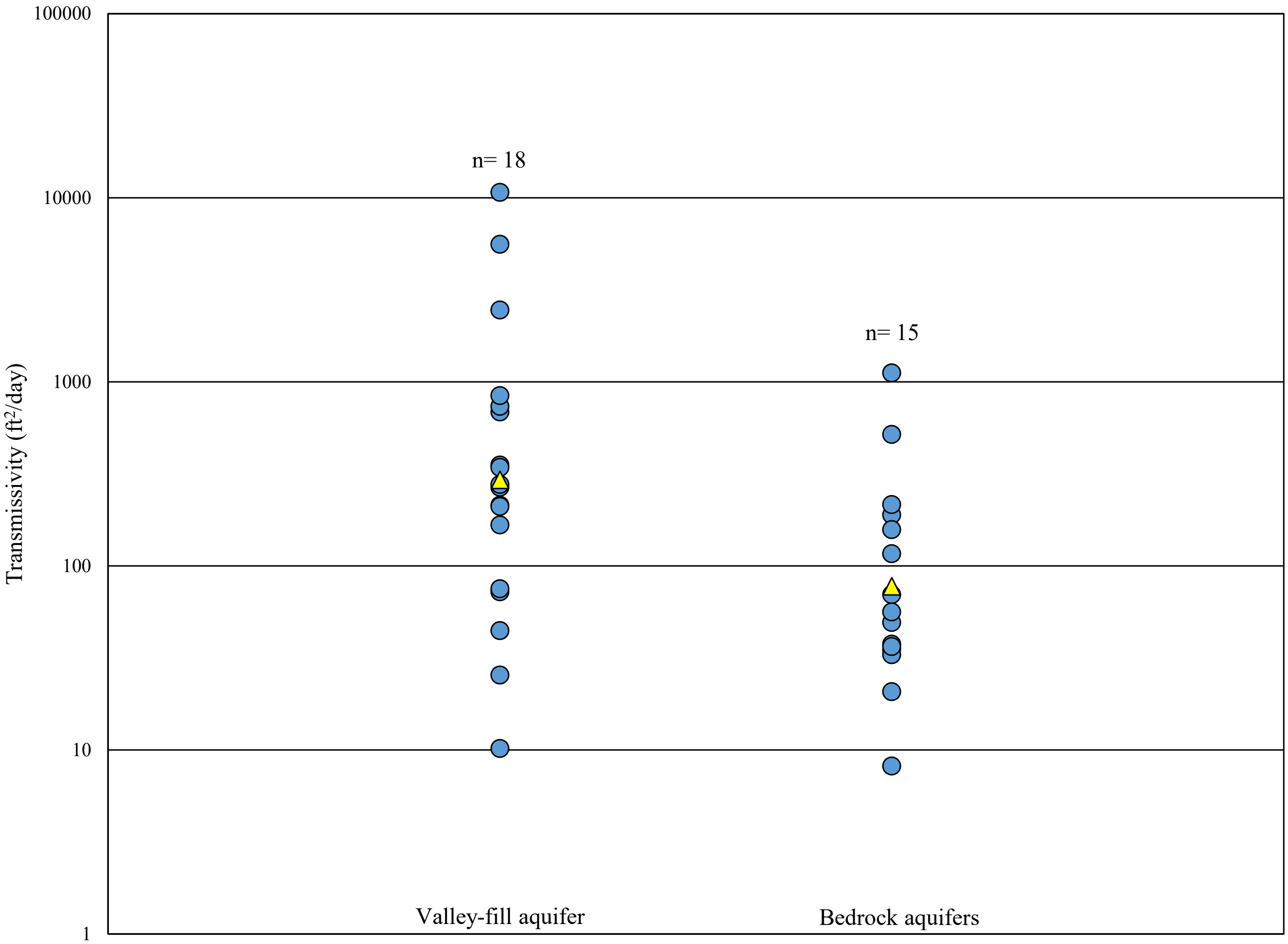

Figure 7. *Transmissivity values for study area aquifers. Yellow triangle is geometric mean.*

supply well, domestic, stock, and monitoring) on figures in this section to aid in interpreting the relative amounts of pumping activity. The potentiometric surface for the autumn 2018 season shows conditions that reflect the previous poor snowpack (85% of the 30-year median at the Agua Canyon SNOTEL site), with water levels at their lowest in most wells (figure 8a) (Natural Resources Conservation Service [NRCS], 2021). The potentiometric surface in spring 2019 had the highest water levels we observed (figure 8b), after the above-average winter snowpack (116% of the 30-year median) (appendix F). Potentiometric surfaces from all seasons show that valley-fill water-level elevations are highest in the East Creek drainage where the NPS well field is located, and lowest in both north-central Emery Valley where Highway 12 crosses the Pine Hills, and in Johns Valley northeast of Flake Mountain. Because most of the well use in Emery Valley provides water to hotels and businesses centered around high tourism season from May to September, we expect to see water level measurements reflecting pumping and localized cones of depression, evident in all four measuring campaigns (figures 8a–d). However, water level measurements in Johns Valley toward the northern boundary of the study area are from landfill monitoring wells that are pumped infrequently, if at all. Water levels in the Cretaceous bedrock aquifer fluctuate less than in the valley-fill aquifer. Hydraulic gradients are generally steeper in Emery Valley than in Johns Valley, although data are sparse in most of Johns Valley. Although the shape of groundwater contours on figures 8a–d suggest possible groundwater discharge in Emery and Johns Valley to the East Fork Sevier River, the contours are poorly constrained near the stream and groundwater levels in wells nearest to the stream are as much as 50 feet (15 m) deep. Where the streambed is permeable, streamflow may infiltrate to recharge the local valley fill, but the regional groundwater table is too deep to likely provide discharge to the stream. The spring 2019 potentiometric surface is projected onto the cross sections on plate 2.

Depth to water in valley-fill aquifer wells generally ranges from 1 to 160 feet (0.3–49 m) bgs. In the shallow drainages upgradient from Emery and Johns Valley, depth to water in valley-fill aquifer wells is generally between 1 and 15 feet (0.3–4.6 m) bgs. In northern Johns Valley, depth to water in wells near the valley margin generally ranges from 20 to 60 feet (6–18 m) bgs, whereas in the center of the valley depth to water is typically 140 to 160 feet (43–49 m) bgs. Along the

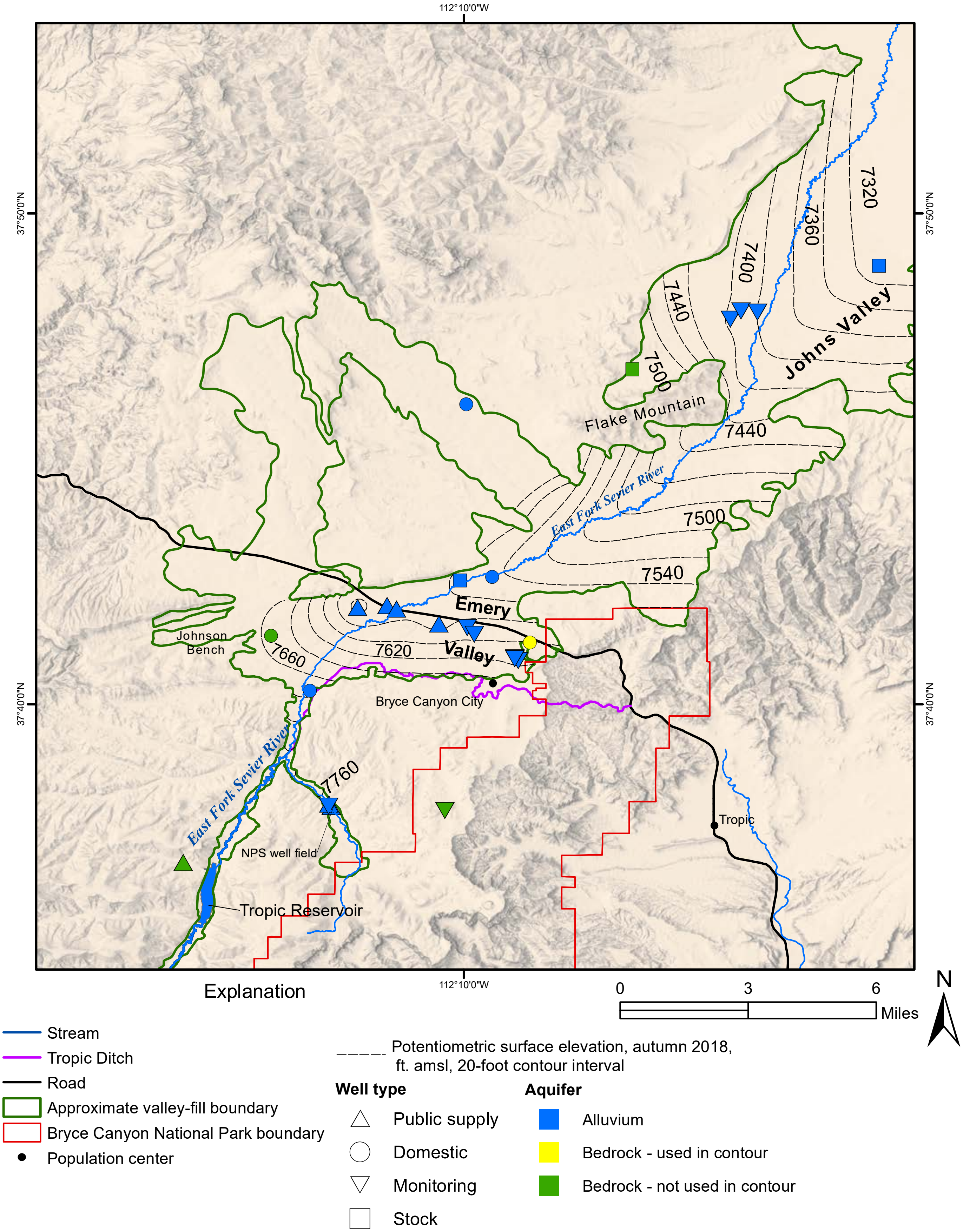

Figure 8a. *Potentiometric surface map of water wells from autumn 2018. Overall direction of groundwater flow is to the north-northeast.*

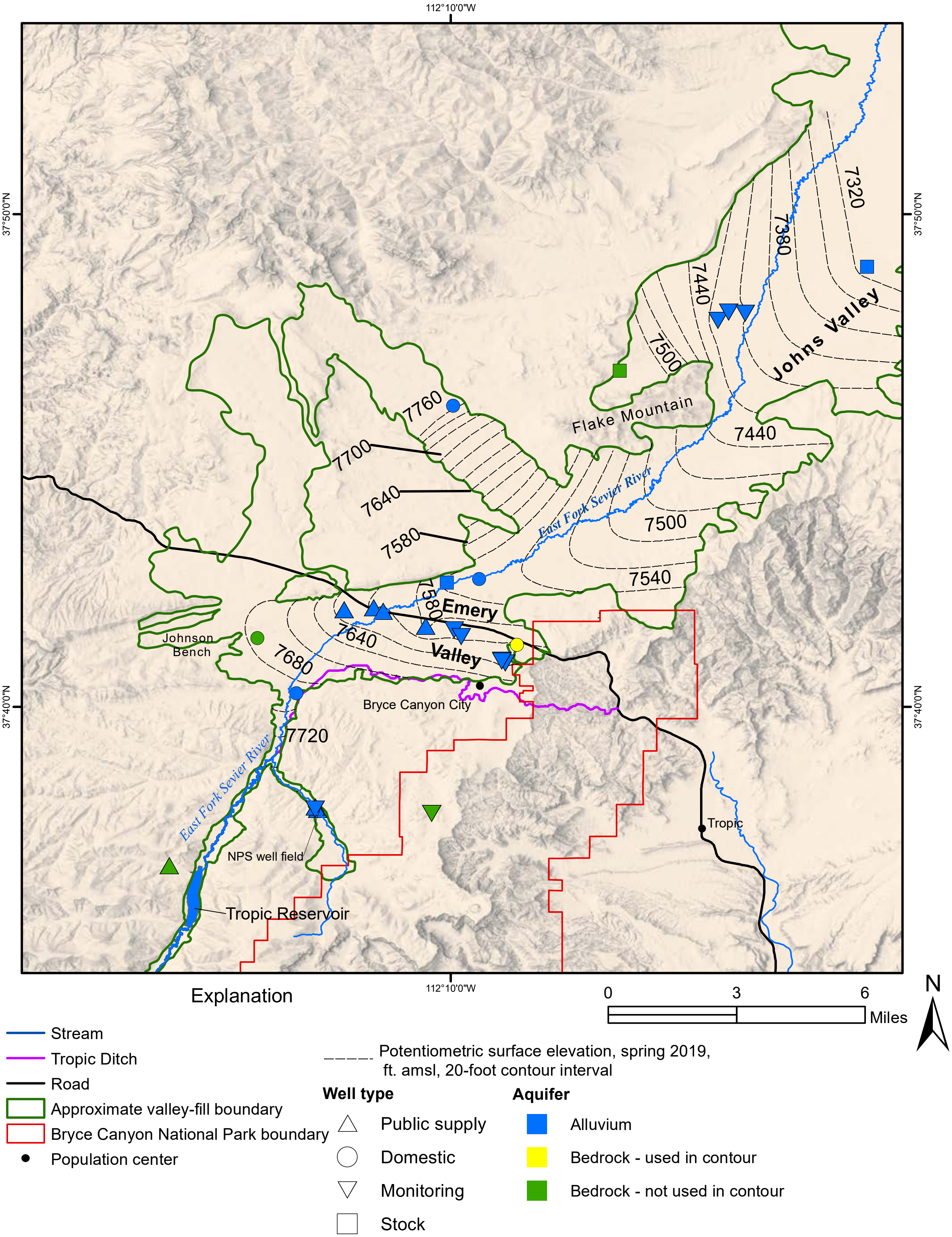

Figure 8b. *Potentiometric surface map of water wells from spring 2019. Overall direction of groundwater flow is to the north-northeast.*

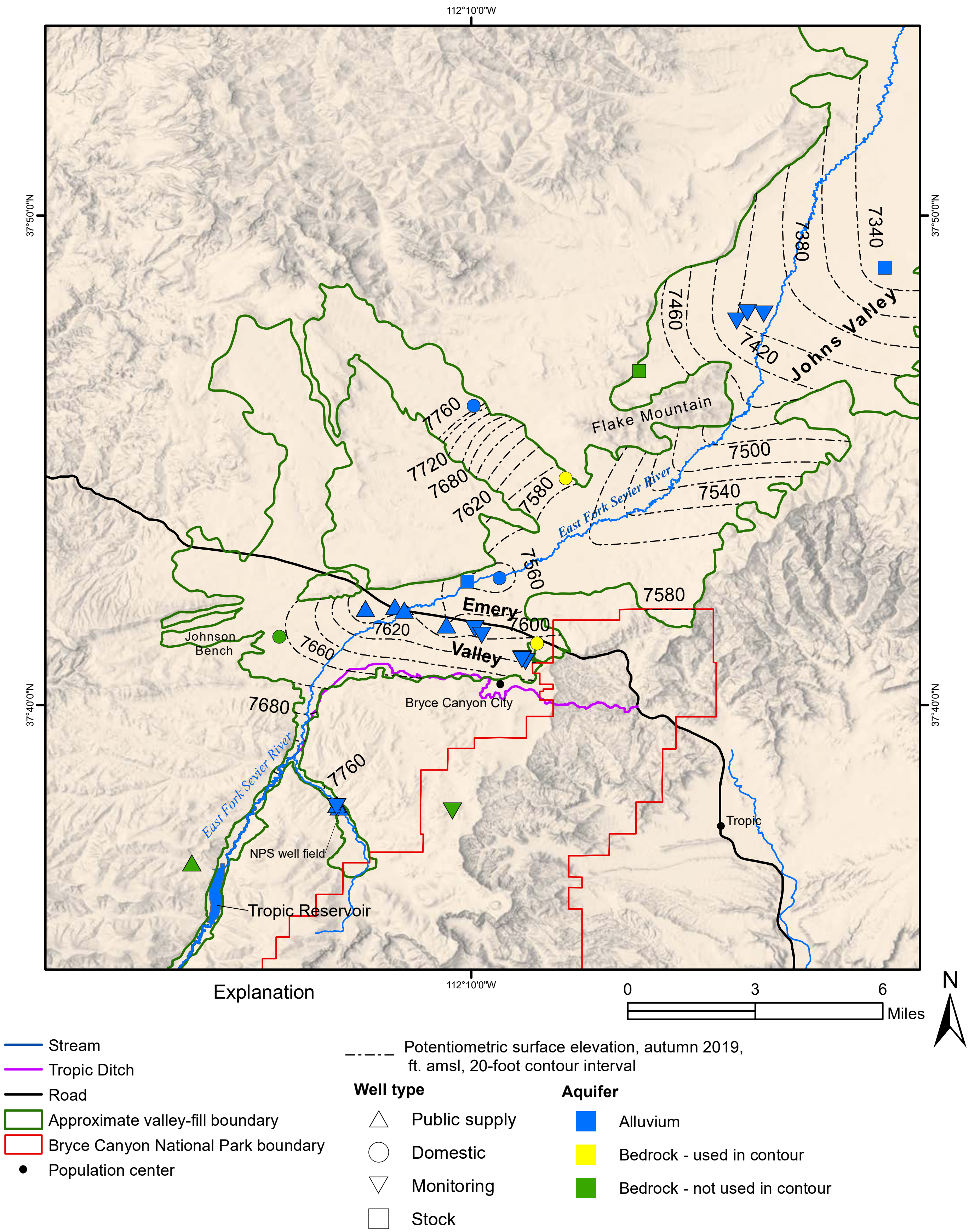

Figure 8c. *Potentiometric surface map of water wells from autumn 2019. Overall direction of groundwater flow is to the north-northeast.*

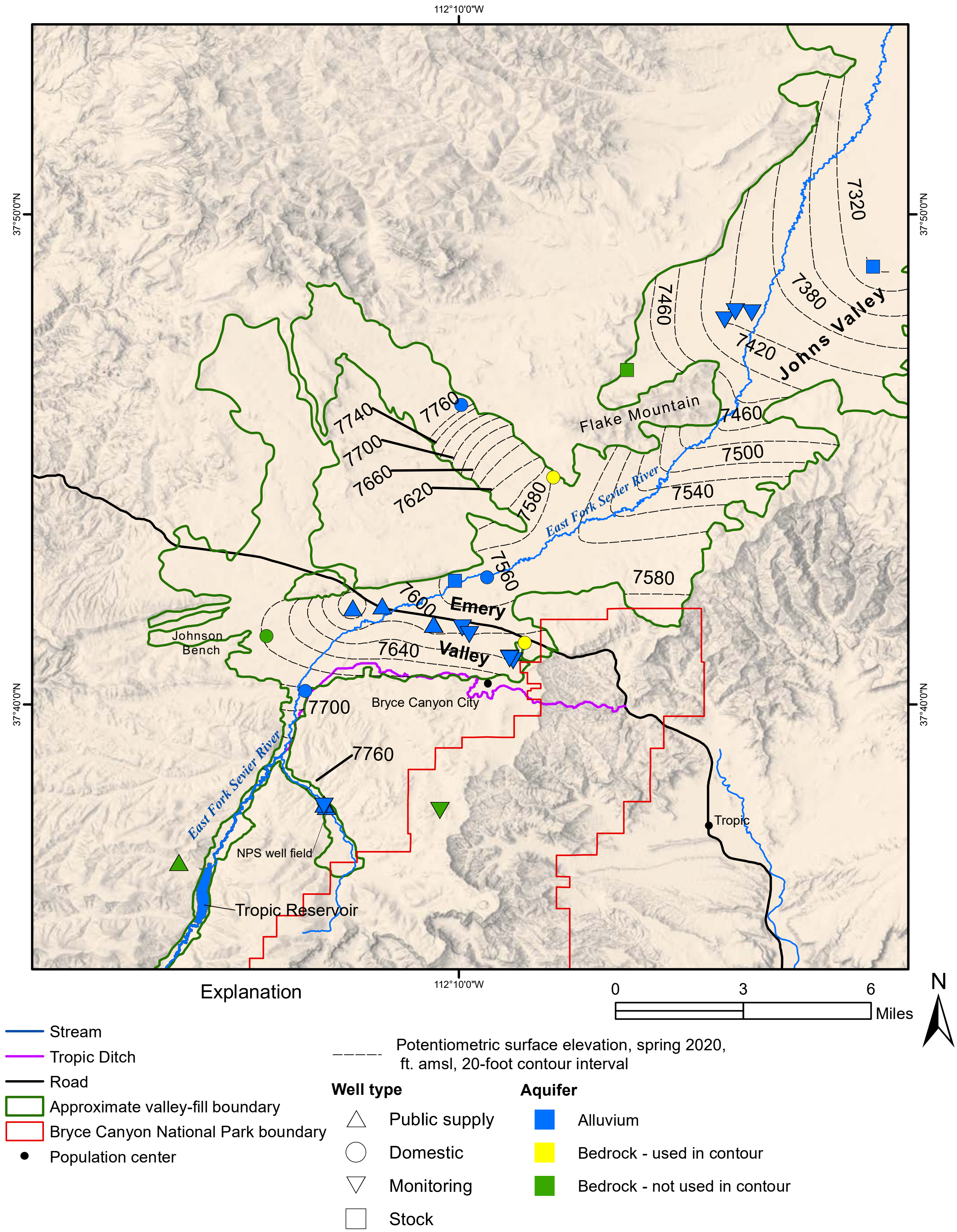

Figure 8d. *Potentiometric surface map of water wells from spring 2020. Overall direction of groundwater flow is to the north-northeast.*

Highway 12 corridor within Emery Valley, depth to water in the valley fill is typically 20 to 70 feet (6–21 m) bgs. Depth to water in the Cretaceous bedrock aquifer wells ranges from 100 to 200 feet (30–61 m) bgs, though each well fluctuated only 1to 4 feet (0.3–1.2 m).

From autumn 2018 to spring 2019, we observed changes in water levels ranging from an increase of over 60 feet (18 m) to a decrease of over 3 feet (1 m) (figure 9a). Because both times of water level measurement fell within the major tourism season, it can be difficult to tease out seasonal fluctuations from the effects of well pumping, as the well showing the largest increase (61.09 feet [18.6 m]) serves a major hotel system. The autumn 2018 measurement likely occurred during or soon after a period of pumping. However, in both Johns and Emery Valley there are several wells in the valley-fill aquifer that are not pumped extensively or at all. At the wells in Emery Valley, located east of most of the major pumping wells, water levels increased by 1.84 feet (0.56 m) (BC23W) and 2.46 feet (0.75 m) (BC24W). At the wells in Johns Valley, water level increase ranged from 12.93 to 23.29 feet (3.9–7.1 m). In contrast to the valley-fill aquifer, water levels in the Cretaceous bedrock aquifer decreased, ranging from 0.12 to 3.68 feet (0.04–1.12 m).

From spring to autumn 2019, we observed changes in water levels ranging from an increase of over 12 feet (3.6 m) to a decrease of over 30 feet (9 m) (figure 9b). As in the previous interval, it can be difficult to tease out seasonal fluctuations from the effects of well pumping, as the well that previously showed the largest increase showed the largest decrease (33.49 feet [10.2 m]). However, looking at the same wells that are pumped infrequently or not at all yields more useful data. At the wells in Emery Valley, water level change ranged from an increase of 1.56 feet (0.48 m) (BC23W) to a decrease of 0.67 feet (0.2 m) (BC24W) (figure 9b). At the wells in Johns Valley, water level decrease ranged from 5.34 to 13.84 feet (1.6–4.2 m). Water levels in the Cretaceous bedrock aquifer changed slightly, with an increase of 0.45 feet (0.14 m) at one site to a decrease of 1.6 feet (0.49 m) at another.

Water-Level Trends

Changes in water levels during different seasons show below-normal conditions during autumn 2018 with water levels lower at most wells than any other year or season measured. After a heavy snowpack in 2019 (116% of the 30-year median) and below-average snowpack in 2020 (70% of the 30-year median) (appendix F), water levels rose in alluvial wells during the spring measuring campaigns, and were lower during autumn water level measurements (figure 10a). Water levels in wells completed in bedrock were less variable (figure 10b) than alluvial wells, with some water levels declining and others rising during different seasons and years, weather independent.

Saturated Thickness

We combined the spring 2019 potentiometric surface map with the valley-fill isopach map to show saturated thickness in select areas of the study area (figure 11). Saturated thickness of the valley-fill aquifer in Emery Valley and northern Johns Valley ranges from 0 to 210 feet (0–64 m) and 0 to 330 feet (0–101 m), respectively. Due to scarcity of well data, saturated thickness was not calculated for western Emery Valley, southern Johns Valley, or the shallow drainages of the East Fork Sevier River or East Creek.

Discharge Measurements

Stream, canal, and spring discharge was measured over four time intervals: autumn 2018, spring 2019, autumn 2019, and spring 2020 (tables A-3 and A-4 of appendix A). We measured discharge to 1) determine groundwater/surface water interaction and quantify the amount of water gained or lost from streamflow, and 2) quantify the amount of groundwater discharge from springs when feasible.

We measured or estimated discharge at eight locations along the East Fork Sevier River and tributaries, three locations on the Tropic Ditch canal, and 25 springs and seeps (figure 12). We used a Hach FH950 electromagnetic current velocity meter and the 0.6 depth method to measure velocity across a stream transect and compute the cross-sectional area (figure 13). At smaller streams and culverts, we measured flow using a portable v-notch weir. For spring discharge measurement, the approach varied by spring type and size. Many of the springs within BCNP, especially in the lower parts of the drainage area, are diffuse springs that occupy wetland areas issuing from several sources that act more as seeps, but collectively discharge as standing water in wetlands. Flow from such spring systems is difficult to assess and thus was not measured. Other springs issue from one source. For these springs, we measured discharge using a portable v-notch weir or a graduated measuring device (e.g., a 5-gallon bucket, 1-gallon bucket, or a pint-size bucket) and a stop-watch (table A-3 of appendix A).

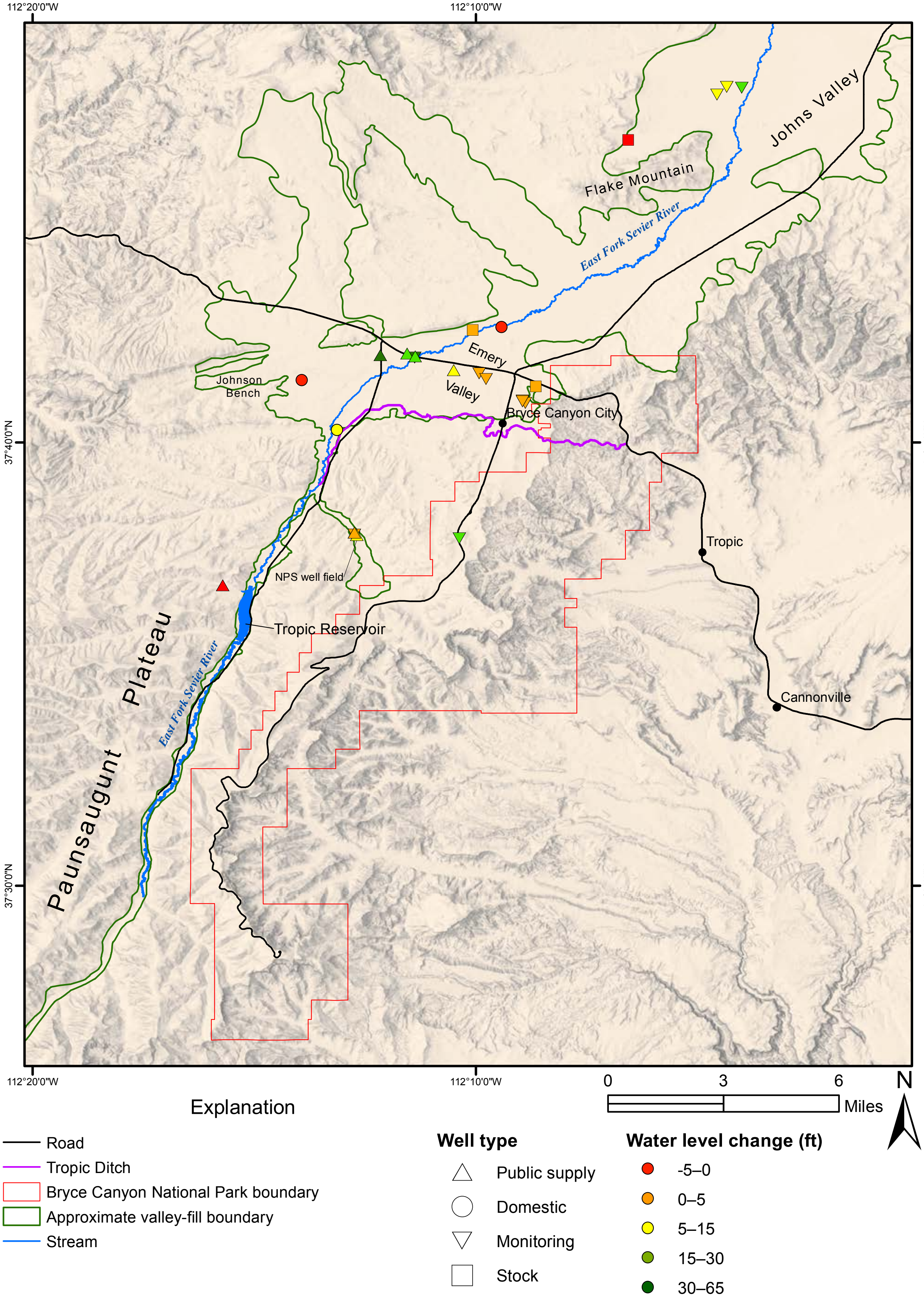

Figure 9a. *Change in water-level elevation in wells between autumn 2018 and spring 2019.*

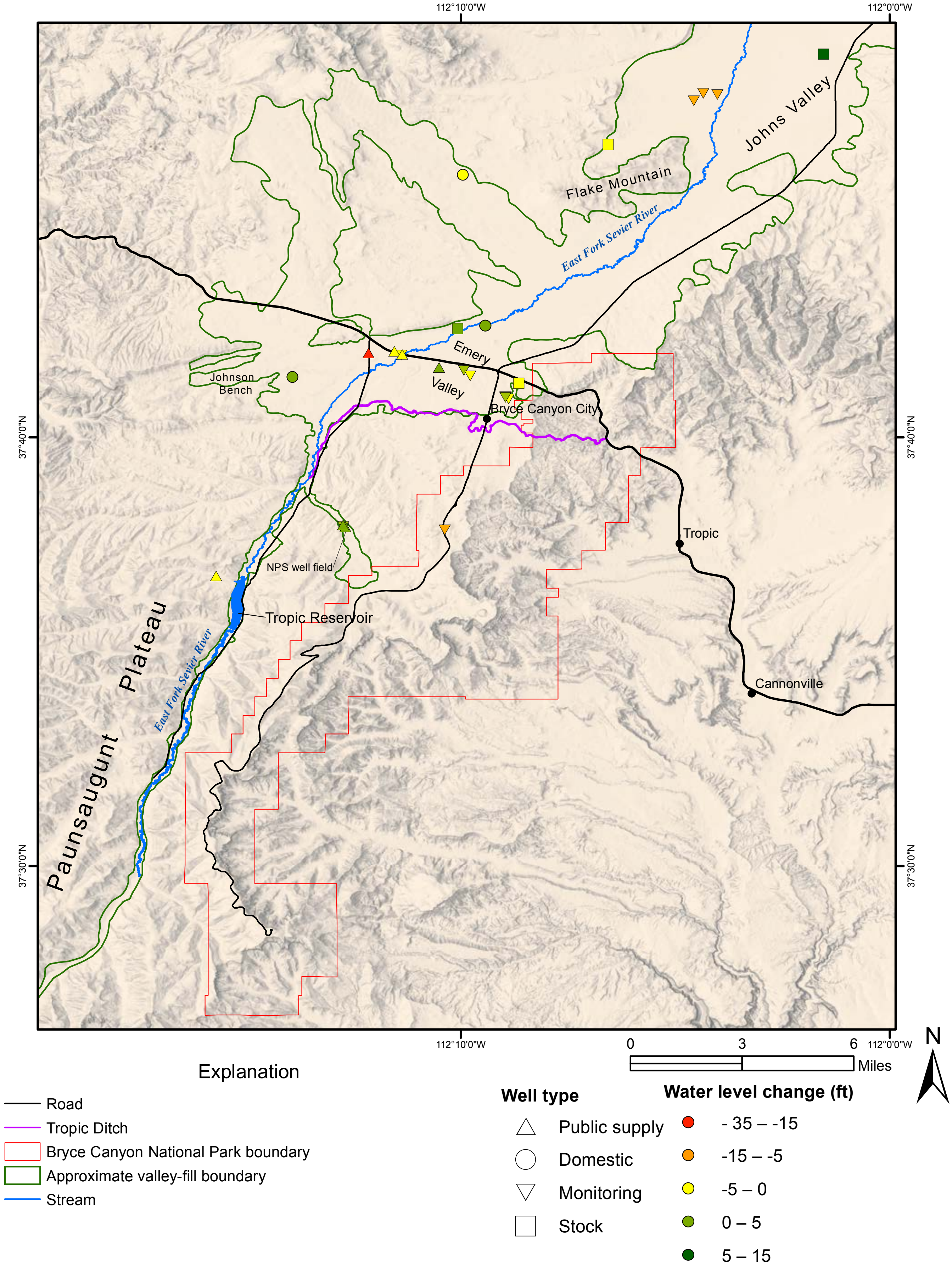

Figure 9b. *Change in water-level elevation in wells between spring and autumn 2019.*

Streams and Tropic Ditch Seepage Studies

Understanding the extent of groundwater–surface water interaction in Johns and Emery Valleys is a key goal of this study. Streams interact with groundwater in three basic ways: streams gain water from inflow of groundwater through the streambed when the water table is higher than the streambed, streams lose water to groundwater by outflow through the stream bed when the water table is below the bottom of the streambed, or they do both, gaining in some reaches and losing in other reaches (Winter and others, 1998). If the water table rises or falls through time, losing sections can become gaining sections and vice versa. A fourth option is that the stream flows over impermeable geologic materials and is unconnected with the local groundwater. Seepage studies using discharge measurements, coupled with geochemistry and environmental tracer analysis, form the basis of our understanding of the degree of interaction between surface water and groundwater. Seepage runs involve measuring streamflow on multiple sections of a watercourse, ideally in as short a time span as possible.

Methods

During 2018, 2019, and 2020, we performed a total of four seepage runs on the East Fork Sevier River and Tropic Ditch (figures 12 and 14; table A-2 of appendix A), a point 1.2 miles (1.9 km) above Tropic Reservoir dam to either the main Tropic Ditch diversion (4.4 miles [7 km] below Tropic Reservoir dam), or the northern extent of the study area depending on flow (figure 12). The East Fork Sevier River flows from its headwaters over thin stream alluvium overlying the Wahweap Formation until about 0.5 miles (0.8 km) south of Tropic Reservoir dam, where the underlying bedrock is the Claron Formation. Where the East Fork

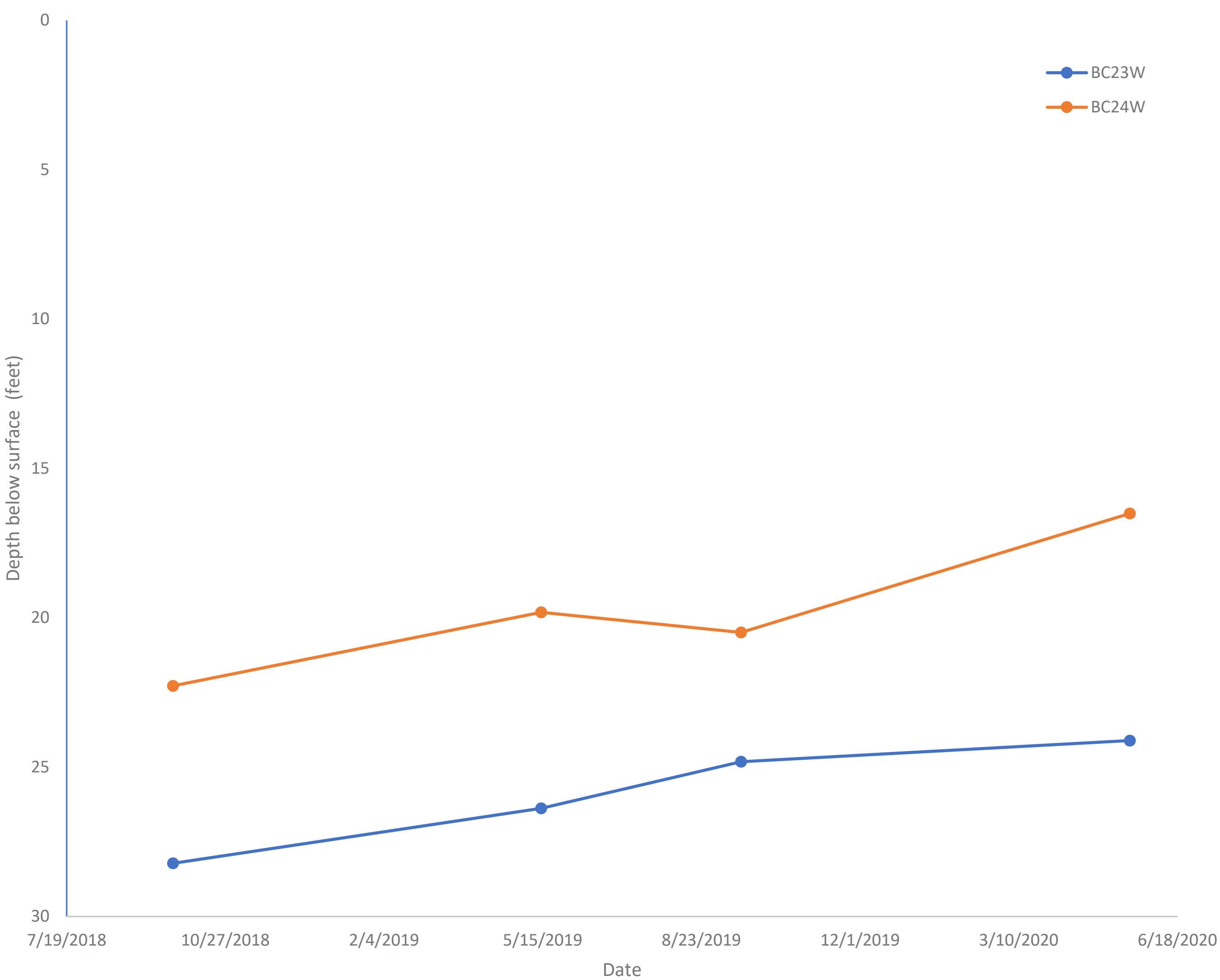

Figure 10a. *Hydrograph of two older unused wells completed in valley fill measured over four seasons; water level rise and decline are responsive to differences in snowpack totals.*

Figure 10b. *Hydrograph of two wells completed in bedrock showing water levels over four different seasons; changes in water levels in response to snowpack totals is negligible.*

Sevier River enters Emery Valley, it crosses thicker valley-fill deposits. The Tropic Ditch seepage runs were performed from the main Tropic Ditch diversion to the point where the Tropic Ditch crosses Highway 12 in BCNP. The Tropic Ditch is piped from just below the confluence of East Creek and East Fork Sevier River underground in valley-fill sediments until it daylights east of Bryce Canyon City in Water Canyon above Mossy Cave Springs before flowing across the Claron Formation within BCNP (figures 1 and 12). Only during the spring 2019 seepage run was a measurable amount of water flowing in the East Fork Sevier River past the Tropic Ditch diversion point. We inventoried major tributaries and diversions to or from the stream segments using detailed aerial imagery and ground survey before and during the seepage runs.

We conducted the autumn 2018 seepage run October 10 during a steady baseflow period but before Tropic Ditch irrigation withdrawals ceased. We measured stream and canal flow at four locations to calculate gain or loss over two stream reaches and one canal reach. The East Fork Sevier River was dry beyond the Tropic Ditch diversion point.

We conducted the spring 2019 seepage run June 18–19 after spring thaw and after irrigation season began. We measured stream and canal flow at 12 locations (figure 12) to calculate gain or loss over five stream reaches and three canal reaches. During this seepage run, the East Fork Sevier River flowed continuously past the Tropic Ditch diversion point and beyond the northern study area boundary. Notably, winter 2019 snowpack was 116% of the 30-year median (NRCS, 2021).

We conducted the autumn 2019 seepage run September 16 during a steady baseflow period but before Tropic Ditch irrigation withdrawals ceased. We measured stream and canal flow at six locations to calculate gain or loss over two stream reaches and three canal reaches. The East Fork Sevier River was dry beyond the Tropic Ditch diversion point.

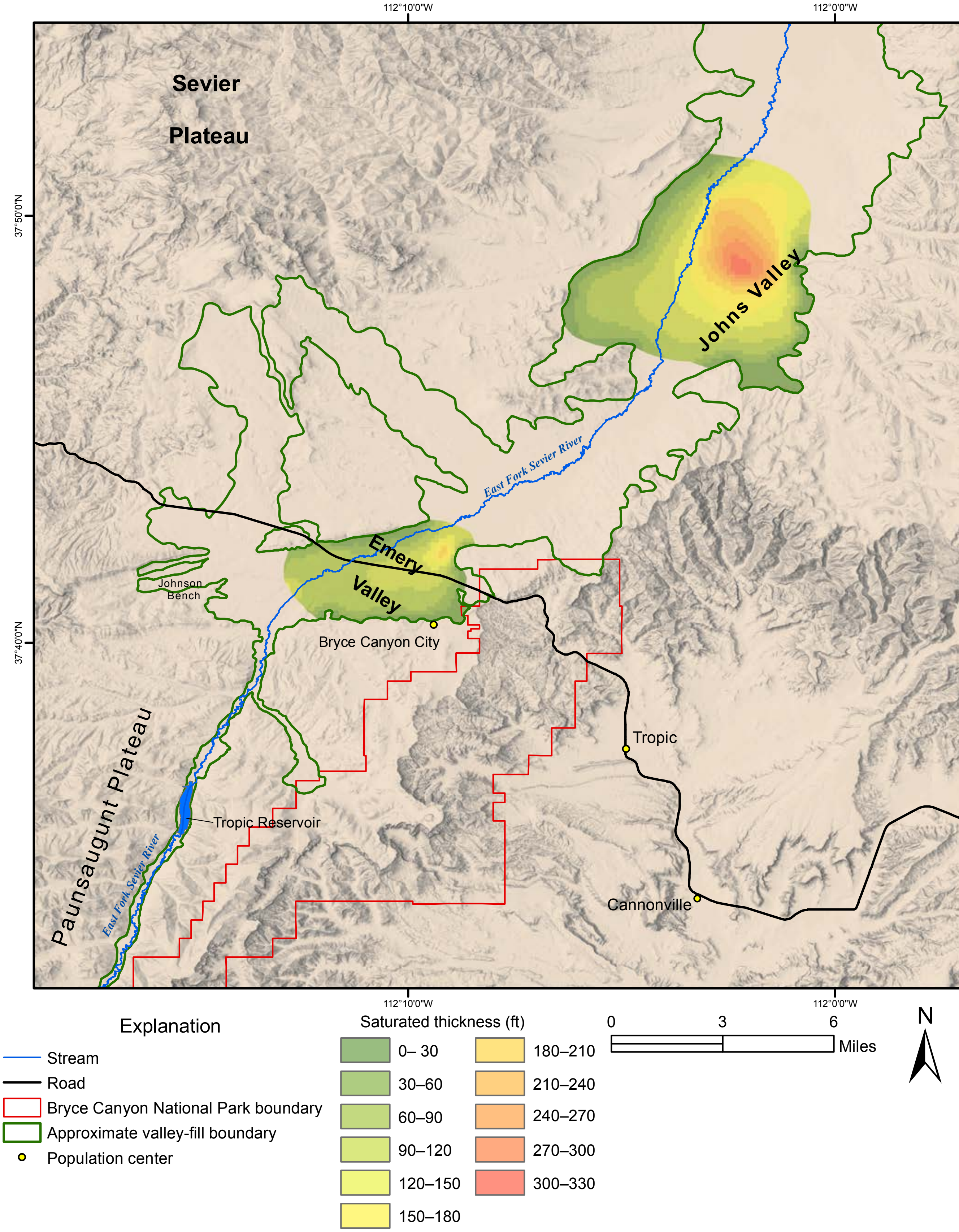

Figure 11. *Saturated thickness map of the valley-fill aquifer in Emery and central Johns Valley.*

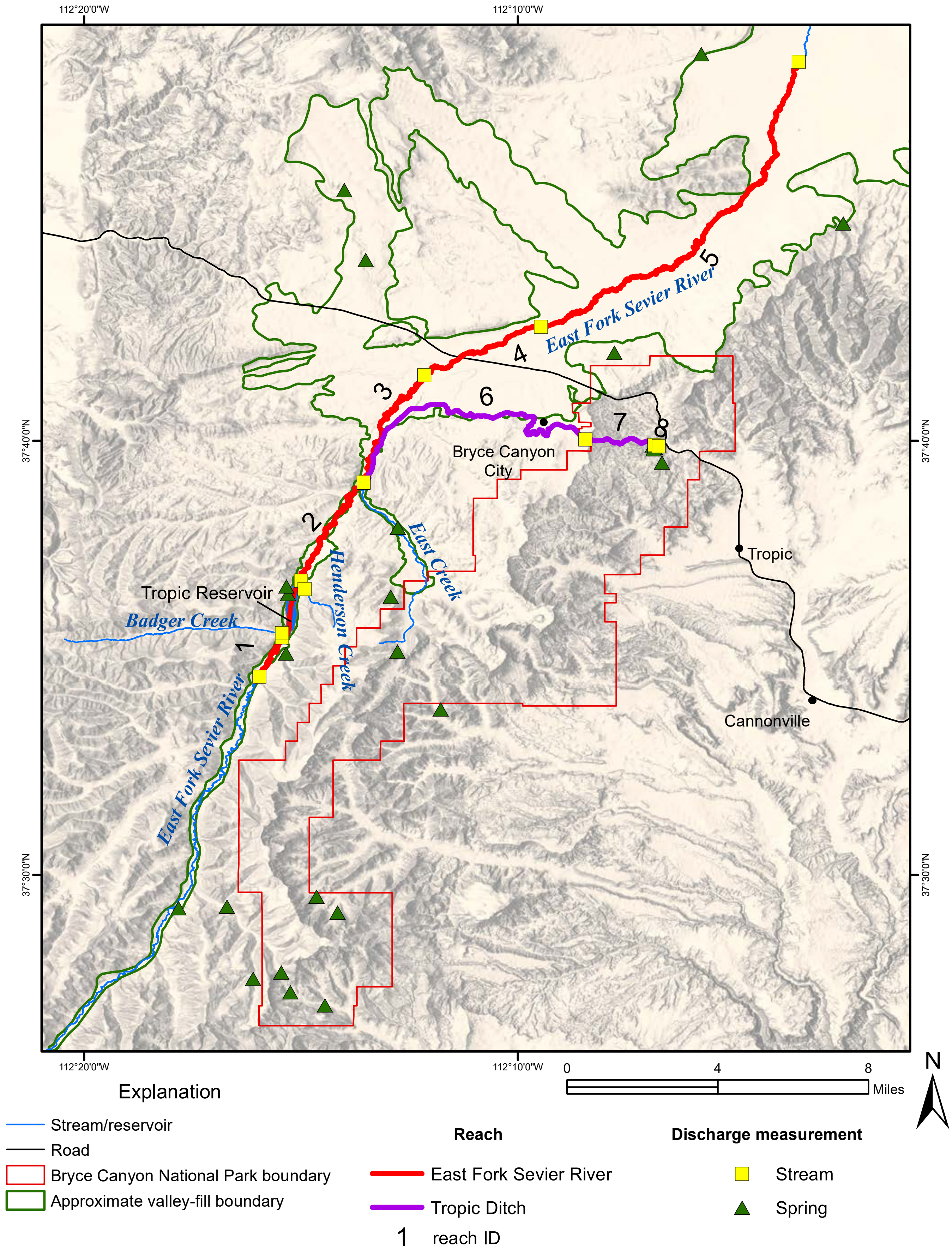

Figure 12. *Locations of seepage run reaches and stream and spring discharge measurements.*

Figure 13. *Using a current velocity meter to measure flow in the East Fork Sevier River.*

We conducted the spring 2020 seepage run May 27–28 after spring thaw and after irrigation season began. We measured stream and canal flow at six locations to calculate gain or loss over two stream reaches and three canal reaches. The East Fork Sevier River was dry beyond the Tropic Ditch diversion point.

We calculated gains and losses for discrete reaches of the East Fork Sevier River and Tropic Ditch as the difference between the flow at each measurement point location and the measurement point immediately upstream, plus any tributary flow and minus any diversions (equation 1).

$$\text{Gain or loss} = \text{downstream flow} - (\text{upstream flow} + \text{tributary} - \text{diversion}) \tag{1}$$

Negative values indicate the stream channel lost flow between the upstream and downstream locations and positive values indicate the stream gained water from its banks between the locations.

Seepage Study Results

During the autumn 2018 seepage run, we observed flows on the East Fork Sevier River and Tropic Ditch ranging from 0 cfs (0 m^3/s) on the East Fork Sevier River at E Fork Rd to 9.1 cfs (0.26 m^3/s) above Tropic Reservoir. Two stream segments were losing, three stream segments were dry, and one canal segment was gaining (figure 14a, table 1). Two canal segments were measured in later seepage runs. The stream segments above the Tropic Ditch diversion were both losing, though reservoir release rate was likely the greatest control on the upper segment. The Tropic Ditch diversion captured all flow from the East Fork

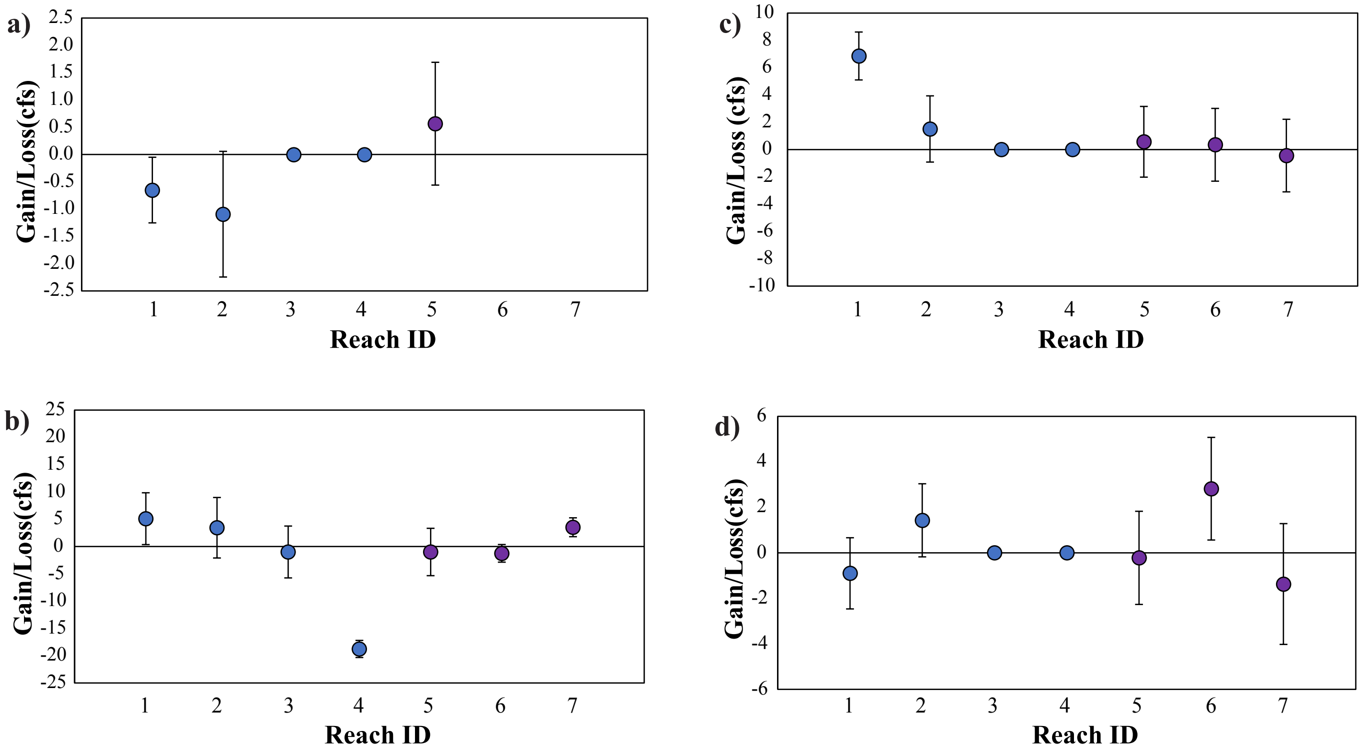

Figure 14. *Gaining and losing reaches of the East Fork Sevier River (blue symbols) and Tropic Ditch (purple symbols) from **a)** autumn 2018, **b)** spring 2019, **c)** autumn 2019, **d)** spring 2020. See table 1 for reach IDs.*

Sevier River—segments beyond the diversion were dry. The canal segment was measured as gaining, but within measurement error. The Tropic Ditch is piped immediately after the main diversion and does not surface until it flows over the rim of BCNP into Water Canyon, so we were unable to observe any diversions or return flows.

During the spring 2019 seepage run, we observed flows on the East Fork Sevier River and Tropic Ditch ranging from 6.3 cfs (0.18 m3/s) on the East Fork Sevier River at Tom Best Spring Road to 43.8 cfs (1.24 m^3/s) on the East Fork Sevier River at the Tropic Ditch diversion point. Two stream segments were gaining, three stream segments were losing, two canal segments were losing, and one canal segment was gaining (figure 14b, table 1). The upper segments had notable gains, as the thin alluvium was likely saturated during runoff season. The Tropic Ditch is permitted to divert up to 20 cfs (0.57 m^3/s) from April 1 to June 1 and up to 15 cfs (0.42 m^3/s) from June 1 to October 15. Due to the above-average snowpack, up to 60% of the East Fork Sevier River flow continued past the diversion point. As the river flowed over deep permeable valley-fill deposits, approximately 75% of the flow was lost to groundwater by the time it reached the farthest downstream measurement point, 30 stream miles (48 km) away (figure 14b). As water from the Tropic Ditch flows through Water Canyon within BCNP, it receives notable gains in the vicinity of Mossy Cave, both from visible spring tributaries and subsurface gains. A previous study by Doremus and Kreamer (2000) also reported that this reach in Water Canyon was a gaining stream.

During the autumn 2019 seepage run, we observed flows on the East Fork Sevier River and Tropic Ditch ranging from 0 cfs (0 m^3/s) on the East Fork Sevier River at E Fork Rd to 16.8 cfs (0.48 m^3/s) on the Tropic Ditch below Tropic Ditch Falls in Water Canyon. Two stream segments were gaining, three stream segments were dry, two canal segments were gaining, and one canal segment was losing (figure 14c, table 1). The two stream segments above the Tropic Ditch diversion were both gaining. As in autumn 2018, the Tropic Ditch diversion captured all flow from the East Fork Sevier River—segments beyond the diversion were dry. All Tropic Ditch segments were within measurement error. The gaining reach in Water Canyon observed during the spring 2019 seepage run transitioned to losing, although this may be an artifact of higher measurement error associated with these flow measurements.

During the spring 2020 seepage run, we observed flows on the East Fork Sevier River and Tropic Ditch ranging from 0 cfs (0 m^3/s) on the East Fork Sevier River at E Fork Rd to 15.5 cfs (0.44 m^3/s) on the Tropic Ditch below Tropic Ditch Falls in Water Canyon). One stream segment was gaining, one stream segment was losing, three stream segments were dry, two canal segments were losing, and one canal segment was gaining (figure 14d; table 1). The upper segment encompassing Tropic Reservoir was losing, likely due to the Tropic Reservoir dam releasing less than inflow. However, the downstream reach was gaining as it was during the previous runoff season. Unlike in the spring 2019 seepage run, the Tropic Ditch diversion captured all flow

Table 1. *Gains and losses and reach status for seepage runs on the East Fork Sevier River and Tropic Ditch.*

		October 2018 Seepage Run				June 2019 Seepage Run				September 2019 Seepage Run				May 2020 Seepage Run			
Reach ID	Reach Description	Gain/loss (cfs)	Cumulative measurement error (cfs)	% of flow gained/lost	Reach status	Gain/loss (cfs)	Cumulative measurement error (cfs)	% of flow gained/lost	Reach status	Gain/loss (cfs)	Cumulative measurement error (cfs)	% of flow gained/lost	Reach status	Gain/loss (cfs)	Cumulative measurement error (cfs)	% of flow gained/lost	Reach status
1	East Fork above Tropic Reservoir to below Tropic Reservoir dam	-0.65	0.60	-7	losing	5.1	4.75	15	gaining	6.86	1.76	91	gaining	-0.9	1.56	-7	losing (within error)
2	East Fork below Tropic Reservoir Dam to Tropic Ditch diversion	-1.09	1.15	-13	losing (within error)	3.4	5.54	9	gaining (within error)	1.51	2.42	10	gaining (within error)	1.43	1.61	12	gaining (within error)
3	East Fork above Tropic Ditch diversion to E Fork Rd bridge	0	0	0	dry	-1.0	4.75	-2	losing (within error)	0	0	0	dry	0	0	0	dry
4	East Fork at E Fork Rd bridge to airport bridge	0	0	0	dry	-3.1	2.35	-12	losing	0	0	0	dry	0	0	0	dry
5	East Fork at airport bridge to Tom Best Spring Rd	0	0	0	dry	-15.7	1.41	-72	losing	0	0	0	dry	0	0	0	dry
6	East Fork Tropic Ditch diversion to Tropic Ditch above Bryce Canyon rim	0.56	1.12	8	gaining (within error)	-1.0	4.34	-2	losing (within error)	0.57	2.59	4	gaining (within error)	-0.22	2.05	-2	losing (within error)
7	Tropic Ditch above Bryce Canyon rim to below Tropic Ditch falls	-	-	-	-	1.3	1.61	-7	losing (within error)	0.35	2.66	2	gaining (within error)	2.82	2.26	22	gaining
8	Tropic Ditch below falls to below Mossy Cave outflow	-	-	-	-	3.5	1.73	23	gaining	-0.44	2.66	-3	gaining (within error)	-1.37	-2.65	-9	losing (within error)

from the East Fork Sevier River, leaving the downstream reaches dry. We calculated a losing reach (within error) in the Tropic Ditch in the vicinity of the Mossy Cave spring complex. However, the reach between the BCNP and Tropic Ditch Falls showed a notable gain, supporting the presence of groundwater contribution from the Claron Formation in this reach. We also note that in December 2020, despite the Tropic Ditch not flowing, we observed flow in Water Canyon upstream of the visible Mossy Cave spring complex, showing that this reach gains groundwater from the Claron Formation.

Bryce Canyon National Park Springs, Seeps, Wells, and Surface Water

Most springs and seeps within the boundaries of BCNP contribute flow toward the Paria River drainage rather than toward the East Fork Sevier River except those situated along the westernmost boundaries of the park. Spring discharge measurements are shown in table 2. Springs that issue along the higher elevation trail systems along the Pink Cliffs are mostly within the Claron Formation (figure 15a), whereas those at the lower elevation accessed from the eastern BCNP boundary are within the Cretaceous formations, mostly sandstone and siltstone of the Wahweap and Straight Cliffs Formations (figure 15b). Westernmost springs are mostly within the Wahweap Formation except one spring located within the East Creek drainage, where the main NPS well field is located. There, the alluvial spring complex feeds into East Creek, a tributary of the East Fork Sevier River.

Discharge from springs varies throughout BCNP, some of which are measurable having flow from a channel (figure 16) or issuing from a single source, others are diffuse seeps and exist within expansive wet meadows (figure 15b) that are not easily measured without specialized instrumentation. A 2017 water right agreement between BCNP and the State of Utah identifies four springs having State appropriative water rights for administrative uses: Hopkins, Trough, Shaker, and Yovimpa springs. Only Yovimpa spring was measured during this study (table 2). The other three were not flowing.

Most wells in BCNP are in the East Creek drainage, which is a tributary to the East Fork Sevier River. Three wells are completed in valley-fill alluvium, two of which serve as public supply wells; the third is no longer in use. A newly drilled well completed in Cretaceous bedrock is also located in this well field but does not produce enough yield to augment the existing public-supply wells. An older 30-foot (9 m) hand-dug well completed in 1949 and deepened to 80 feet (24 m) in 1955 once supplied water to a 5000-gallon tank used as a municipal source for the nearby Bryce Canyon Lodge.

During our autumn and spring campaigns, the ephemeral streams (East, Podunk, and Daves Hollow) were mostly low except during spring 2019 runoff, with the exception of Daves Hollow, where we witnessed no flow conditions during our visits. Intermittent creeks within the park including Campbell, Sheep, Swamp, and Yellow Creeks were mostly not flowing during our visits, except for Yellow Creek (after a monsoon summer rainstorm) at the lower reaches of the creek near the easternmost park boundary.

Table 2. *Discharge data from springs within Bryce Canyon National Park and headwaters of East Fork Sevier River.*

SAMPLE ID	LATITUDE	LONGITUDE	SITE NAME	SAMPLE DATE	AQUIFER	DISCHARGE (CFS)	NOTES
BC8S	37.5859545	-112.2129966	Swamp ck trail	9/17/19	Claron/alluvium	0.02	V-notch weir measurement
BC11s	37.63347798	-112.2127794	NPS 4	10/10/18	alluvium	0.0025	bucket and stopwatch
BC35S	37.66357729	-112.1146533	Mossy Cave	6/18/19	Claron	0.098	V-notch weir measurement
BC68S	37.46275289	-112.2575568	Yovimpa	6/18/19	Claron	0.136	bucket and stopwatch
BC62S	37.6069991	-112.2155197	Whiteman	6/19/19	Claron	0.0027	V-notch weir measurement
BC69S	37.48562437	-112.2359886	Birch	7/14/19	Straight Cliffs	-	diffuse - unable to quantify
BC70S	37.49173437	-112.2439886	Iron	7/14/19	Straight Cliffs	0.008	bucket and stopwatch
BC71S	37.44999974	-112.2409189	Riggs	7/16/19	Straight Cliffs	0.0004	diffuse - estimated
BC81S	37.58901435	-112.1642886	Yellow	8/28/19	alluvium/fault contact	0.0045	diffuse - estimated
BC83S	37.56368436	-112.1963486	Sheep Ck	8/28/19	Straight Cliffs/alluvium	-	diffuse - unable to quantify
BC85S	37.45505438	-112.2541786	Trail spring	8/20/19	Straight Cliffs/alluvium	-	diffuse - unable to quantify
BC86S	37.46024438	-112.2684886	Cougar Hollow spring	8/20/20	alluvium	0.01	V-notch weir measurement
BC88S	37.54387	-112.2735	Boundary Spring	10/3/20	alluvium	0.11	V-notch weir measurement
BC89S	37.42609	-112.33659	Mill Creek Meadow	10/3/20	alluvium	0.0045	V-notch weir measurement
BC90S	37.41758	-112.36143	E Fork headwaters	10/3/20	alluvium	0.03	V-notch weir measurement
BCJH	37.658349	-112.1113501	Jolly Hollow	9/18/19	Claron	0.0094	bucket and stopwatch

a)

b)

Figure 15. a) *Spring issuing from the Claron Formation near Mossy Cave within BCNP.* ***b)*** *Yellow Spring issuing as a diffuse spring/wetland area from alluvium near contact with the Wahweap Formation within BCNP.*

Figure 16. *Measuring spring discharge with a 90-degree V-notch weir for an unnamed alluvial spring located on the westernmost boundary of BCNP.*

GROUNDWATER QUALITY

We collected water samples from wells, springs, surface water, and precipitation. During 2018, sample collection focused on characterizing the valley-wide major solute chemistry and stable-isotope composition of water from wells, springs, and streams, as well as limited sampling of radiogenic isotopes and possible seasonal variations in stable isotopes. Stable and radiogenic isotopes are discussed in the next section. During 2019, we resampled the same wells and added a few more wells and springs that were previously inaccessible. A third sampling event in 2020 included a subset of wells sampled for water quality and stable isotopes. The water was analyzed for major cations and anions and nutrients (nitrate plus nitrite, ammonia, and phosphate). A subset of wells was analyzed for iron. Table A-4 of appendix A summarizes the general chemistry, nutrients, and metals data.

Most sampled wells are completed in valley-fill material, three wells are completed in bedrock only, and four wells are completed in bedrock and screened in both bedrock and valley-fill material. Springs issue from alluvium, the Claron Formation (mostly within BCNP), and Cretaceous sandstone (Kaiparowits, Wahweap, and Straight Cliffs Formations). Data show most groundwater is of excellent quality, having less than 500 mg/L total-dissolved-solids (TDS) concentration, and better quality water comes from alluvium and the Claron Formation compared to the Cretaceous aquifers.

Methods

We collected water samples using standard field sampling practices (Utah Division of Water Quality, 2014). At or very near each flow location, we measured field chemistry parameters: pH, specific electrical conductance (conductivity), and temperature. Most wells had been in use on the day of sampling and the well was run at least 15 minutes to allow stabilization while measuring pH, temperature, and specific conductance within 0.1 pH, 0.1 degrees C, and 5 µs/cm for conductance. Dissolved metals samples were field filtered within 15 minutes of collection time. Water was filled in state-lab provided bottles and stored on ice until proper delivery within holding times for chemical constituents.

Results

Overall, water is of uniform quality from streams, springs, and wells with a few exceptions (table A-4 in appendix A). Total-dissolved-solids concentrations are low and no water contains elevated primary or secondary water quality constituents that exceed Utah State or U.S. EPA primary or secondary drinking water-quality standards.

Groundwater General Chemistry Composition

Trilinear Piper diagrams show the most recent general chemistry data for each site (figure 17a–c). The diagrams indicate that groundwater chemistry is dominantly calcium-magnesium bicarbonate type (figure 17a). Wells and springs are plotted on separate Piper diagrams (figure 17b and17c) and divided by aquifer source, but despite the disparate sources, the water type compositions show considerable overlap. Uniform chemical signatures from most samples study-area wide may indicate relatively short travel distances where water does not have sufficient time to incorporate additional ions, or the aquifers through which water flows have similar geologic chemical composition, yielding indistinguishable soluble constituents.

Total-Dissolved-Solids Concentrations

Measured TDS concentrations range from 192 to 716 mg/L (figure 18; table A-4 in appendix A); the average TDS concentration from the valley fill is 304 mg/L. Total-dissolved-solids concentrations for groundwater samples from all but two wells tested for general chemistry are below 500 mg/L. In addition to TDS, we measured specific conductance for every site visited (figure 19). The range of specific conductance for 70 wells and springs is from 297 to 1152 µS/cm. We computed TDS concentrations from specific conductance measurements using a conversion factor of 0.63. This conversion factor was calculated by comparing TDS and specific conductance data collected in this study (figure 20). Using this conversion factor, we calculated TDS values for 3 wells and 26 springs sampled for this study. The converted TDS values range from 195 to 726 mg/L. Lower quality water, in terms of higher measured TDS, occurs within the Cretaceous sandstone aquifer. The higher quality water in the valley-fill material is likely due to recharge directly from precipitation in the higher elevations and from surface infiltration. The lower quality water in the bedrock aquifer may be from water discharging from the higher quality valley-fill aquifer and mixing locally with connate water or from longer residence time of groundwater reaching the bedrock aquifer.

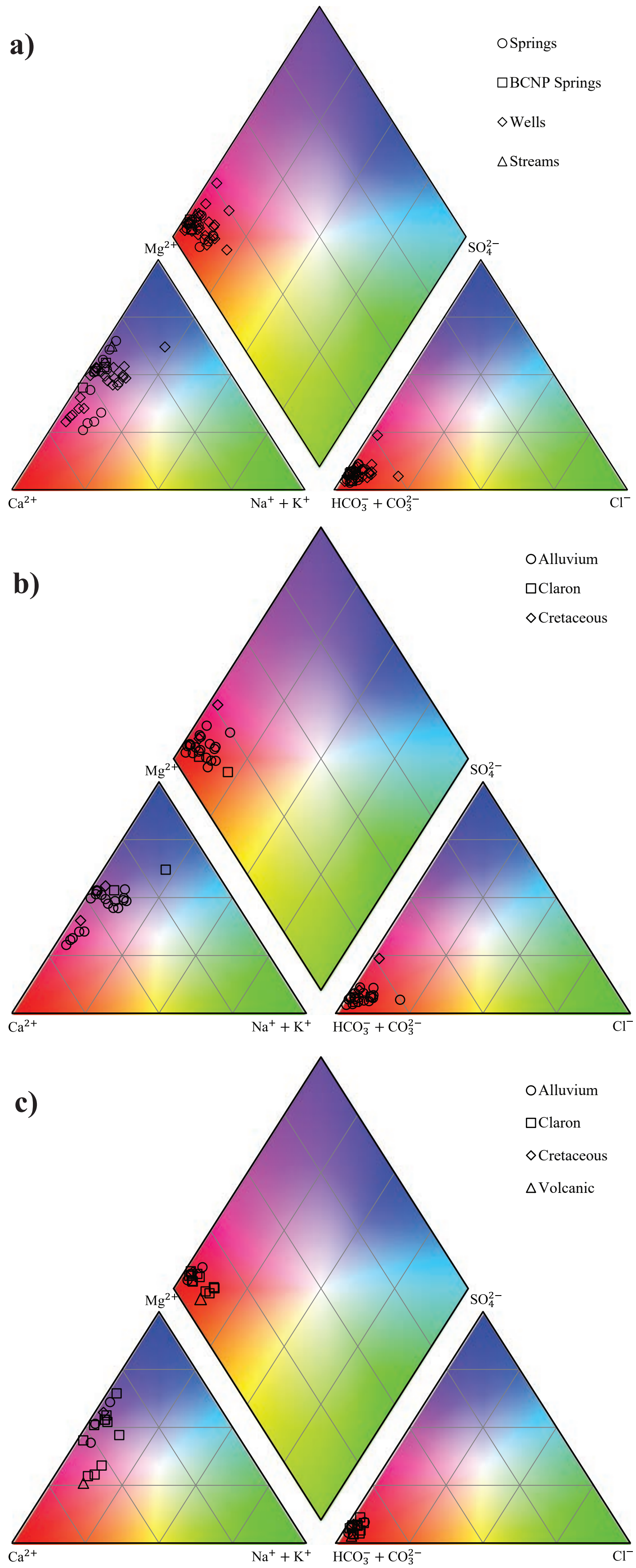

***Figure 17.** General chemistry, characterized by an overall calcium-magnesium bicarbonate type for **a)** all sample sites in the study area; **b)** all wells in the study area sub-divided by aquifer; **c)** all springs in the study area sub-divided by aquifer.*

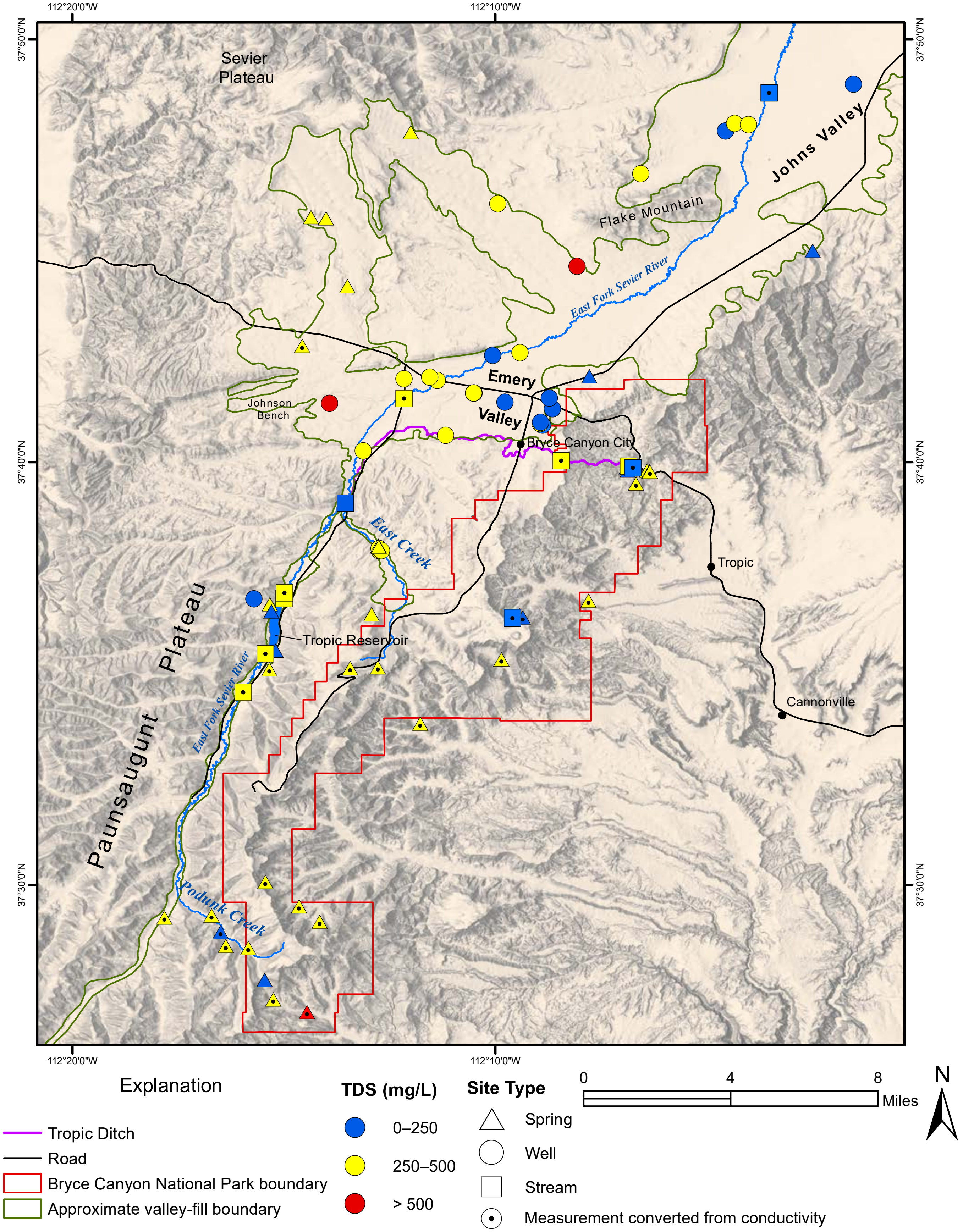

Figure 18. *Total-dissolved-solids concentration map for wells, springs, and streams within Johns and Emery Valleys.*

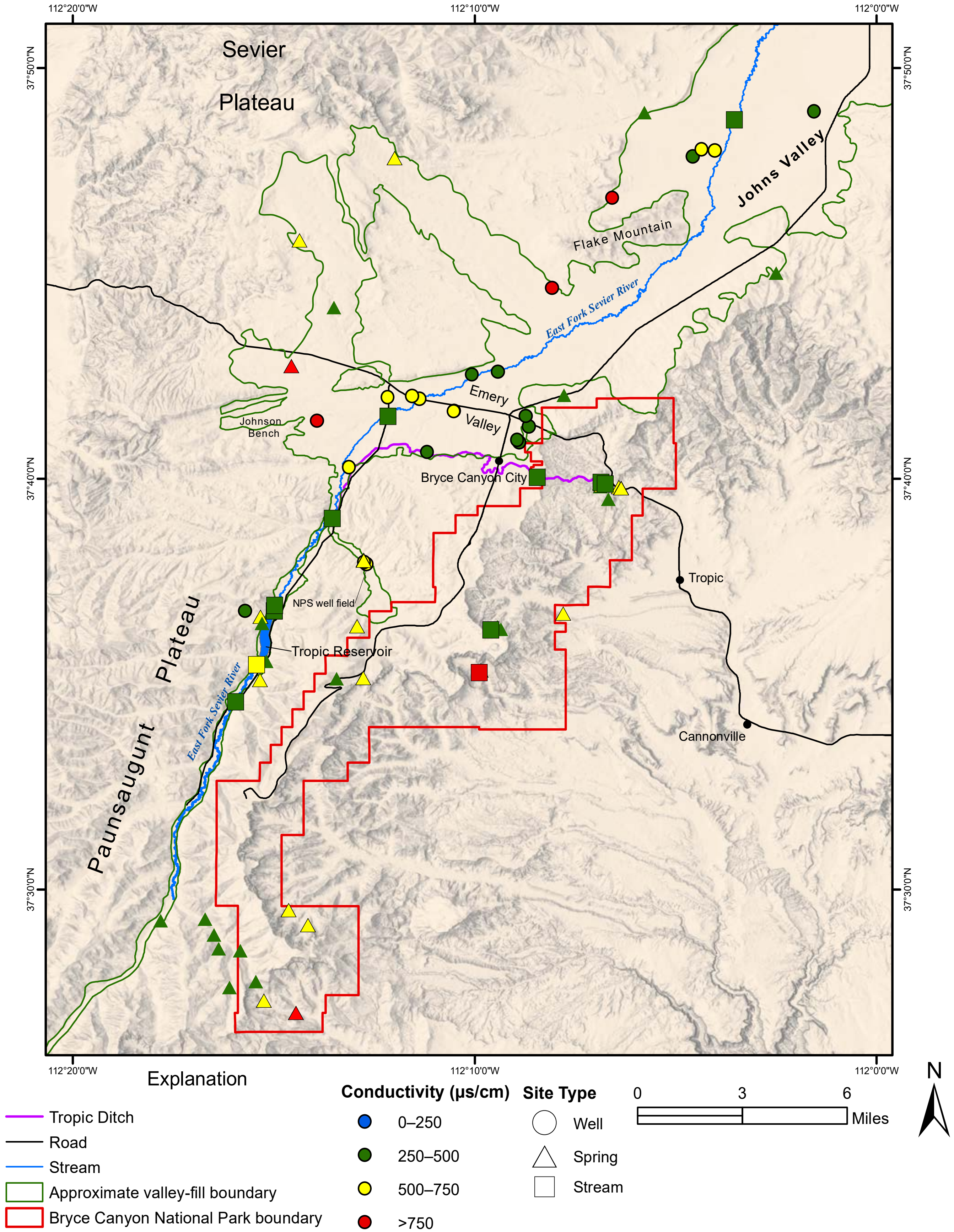

Figure 19. Specific conductance data for all sites visited including wells, springs, and streams within Bryce Canyon National Park and Johns and Emery Valleys.

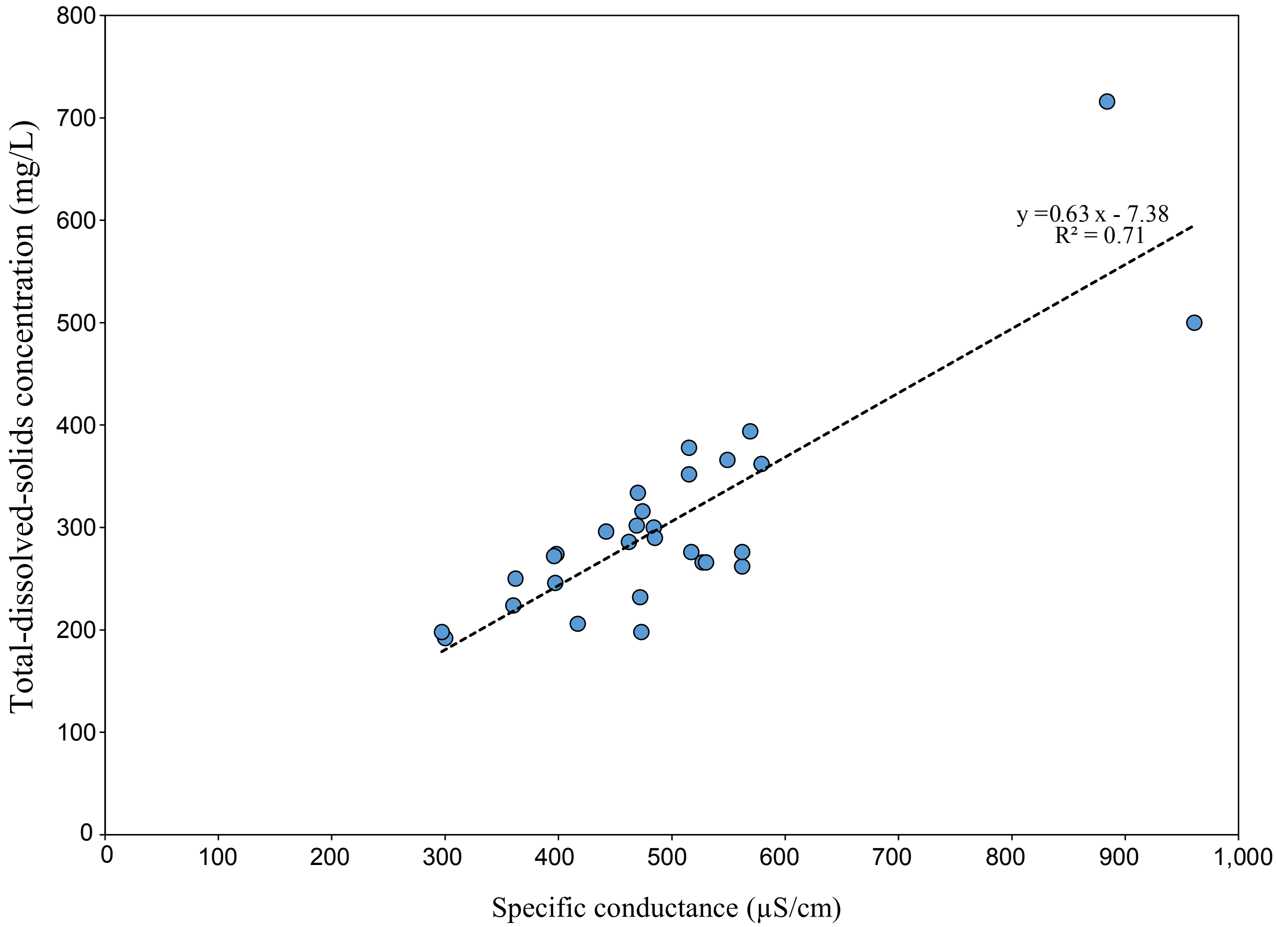

Figure 20. *Specific conductance versus total-dissolved-solids concentration data for 29 wells in Johns and Emery Valleys. R-squared is 0.71. Based on Hem's (1985) equation for estimating TDS from specific conductance: KA=S, where K=specific conductance, S=TDS, A ranges from 0.4 to 0.8 with an average A=0.63 (slope) used as the conversion factor to compute TDS in the study area.*

Nutrients

We sampled about 47 wells and springs for nutrients (nitrate plus nitrite, ammonia, and phosphate) (figure 21). Nitrate plus nitrite concentrations ranged from <0.1 mg/L to 1.47 mg/L, the latter is from water on an elk preserve, and could be related to waste associated with the animals. All sampled sites had ammonia concentrations of <0.05. Total phosphate ranged from no detect to 0.157 mg/L.

Other Constituents

No samples had water with dissolved metals that exceeded groundwater-quality standards. Many other rural and urban Utah valleys have elevated concentrations of chloride and sodium in groundwater; water from wells in the study area has low concentrations of these constituents, even below detectable levels in some samples. Iron concentrations were analyzed in 13 wells with a range of <30 to 192 µg/L, the majority below detection levels (table A-4 in appendix A).

ENVIRONMENTAL TRACERS

Environmental tracers are naturally occurring or anthropogenic chemicals or isotopes that can indicate water sources and flow processes such as recharge, flow rate, geologic subsurface interactions, residence times, and mixing between sources (Kendall and Caldwell, 1998). Ideal tracers have well-defined input sources and input histories, are inert (no reactions) or geochemically conservative (limited reactions), have transport mechanisms identical to water, and are detected precisely and economically. The use of multiple tracers provides a more comprehensive understanding of the groundwater system. We analyzed water samples from wells and springs for tritium and radiocarbon concentrations, and from precipitation, streams, wells, and springs for stable isotope composition.

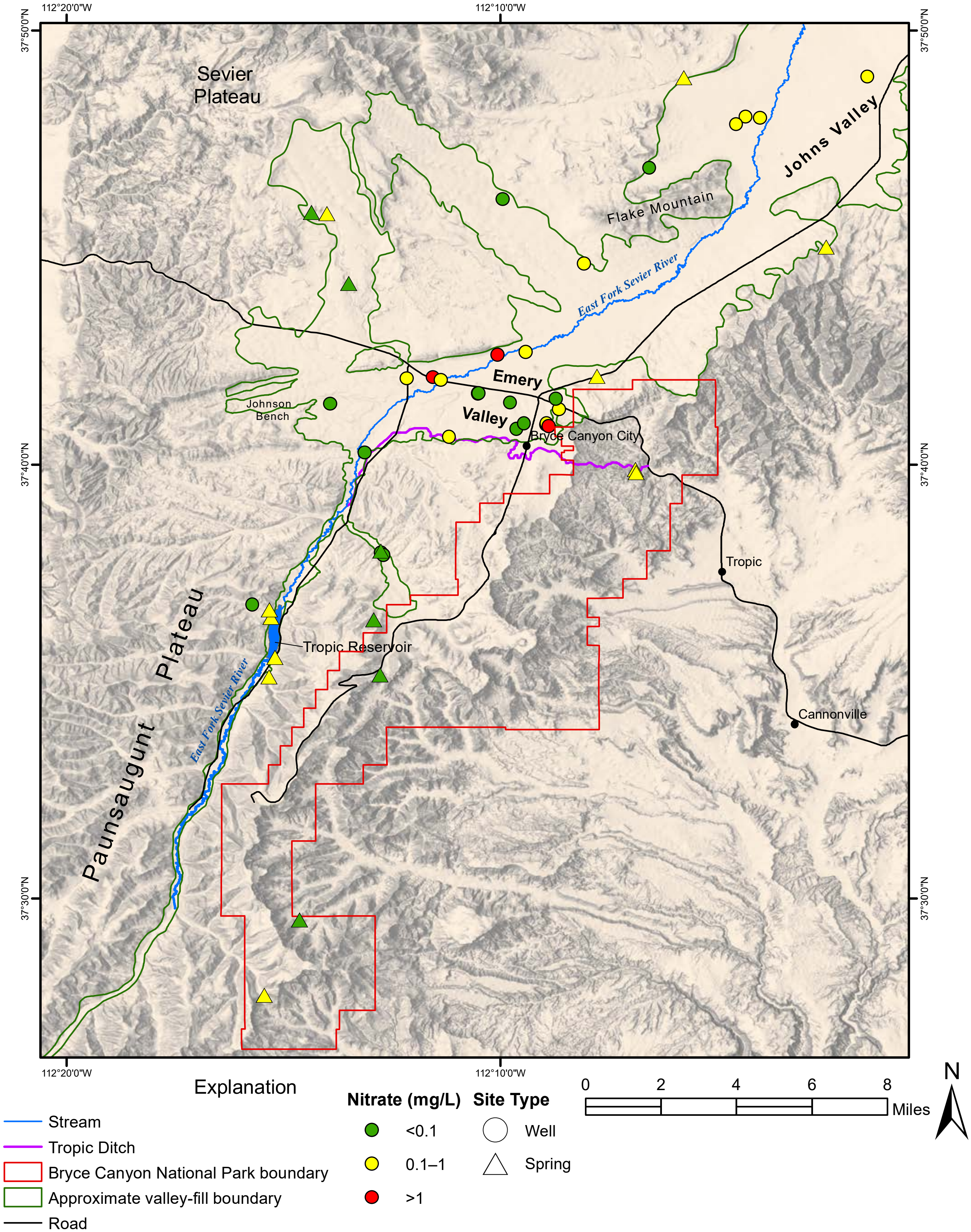

Figure 21. *Nitrate concentration map for wells and springs in the Bryce Canyon study area in Johns and Emery Valleys.*

Methods and Theory

Stable Isotopes of Water

Oxygen-18 (^{18}O) and deuterium (^{2}H) are naturally occurring stable isotopes of oxygen and hydrogen. Water molecules containing the lighter isotopes (i.e., $^{1}H_2{}^{16}O$) and heavier isotopes (i.e., $^{2}H^{1}HO$ and $H_2{}^{18}O$) fractionate preferentially during phase changes such as evaporation and condensation. Values for ^{18}O and ^{2}H are expressed as ratios in delta notation (δ) as per mill (‰) relative to a reference standard:

$$\delta_x = (R_x/R_{standard} - 1) \times 1000 \qquad (2)$$

where:

δ_x = delta notation of the sample x (in per mill, ‰)

R_x = isotopic ratio of $^{2}H/^{1}H$ or $^{18}O/^{16}O$ in the sample (no units)

$R_{standard}$ = isotopic ratio of $^{2}H/^{1}H$ or $^{18}O/^{16}O$ in the standard (no units)

The reference standard for ^{18}O and ^{2}H is Vienna Standard Mean Ocean Water (VSMOW) (Gonfiantini, 1978). The global meteoric water line (GMWL) represents approximate isotopic composition for $\delta^{18}O$ and $\delta^{2}H$ of precipitation (Craig, 1961; Rozanski and others, 1993; Clark and Fritz, 1997) (figure 22):

$$\delta^{2}H = 8(\delta^{18}O) + 10 \qquad (3)$$

Higher fractions of heavier isotopes are considered "enriched" (less negative) and lower fractions of heavier isotopes are considered "depleted" (more negative) (figure 22). Precipitation can be enriched or depleted depending on origin, distance inland, elevation, form of precipitation, and event intensity. Precipitation at high elevation, inland areas, and snow is more depleted relative to precipitation at low elevation, coastal areas, and rain (Clark and Fritz, 1997). Regionally, precipitation generally plots along a local meteoric water line (LMWL), which often differs slightly from the GMWL (Clark and Fritz, 1997). During evaporation of groundwater or surface water, $\delta^{18}O$ is enriched more than $\delta^{2}H$, so samples that have been partially evaporated deviate from the LWML (figure 22).

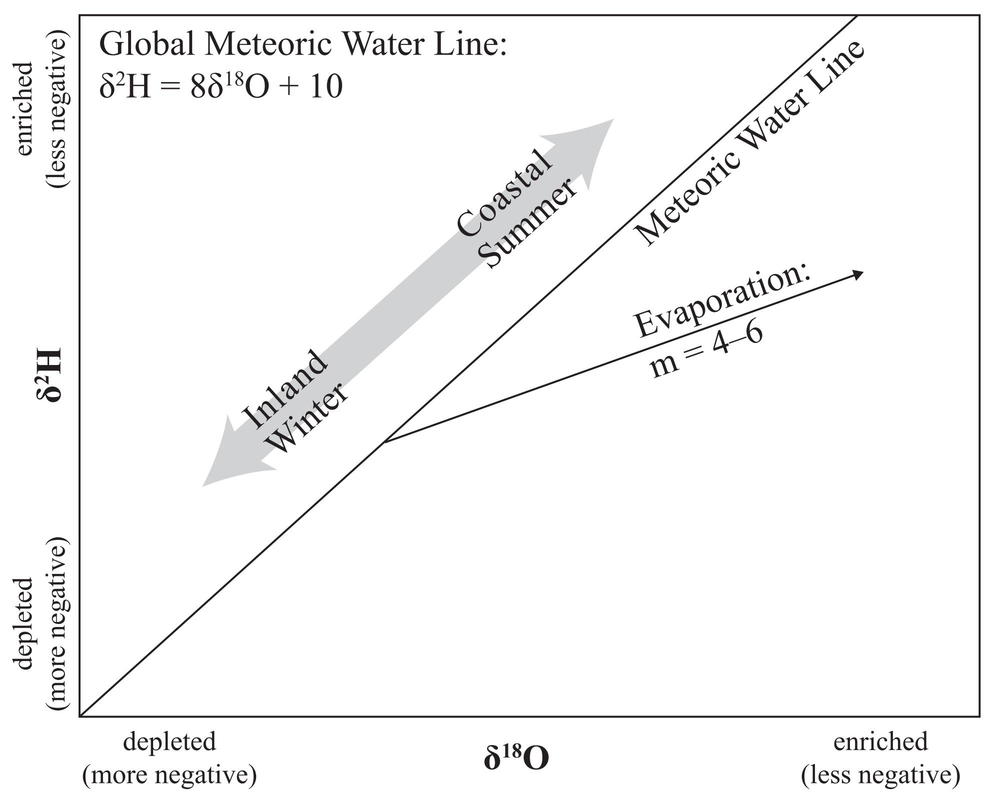

Figure 22. *Relation of oxygen-18 to deuterium in waters, including some factors that affect depletion and enrichment.*

We collected stable isotope samples of precipitation, streams, wells, and springs (figure 1). Precipitation samples were collected approximately every six to eight weeks for a total of eight samples. The precipitation collection site was chosen for its central location within the study area and accessibility. Our precipitation sampler consists of a 2.5-gallon HDPE carboy containing approximately 16 ounces of mineral oil to prevent evaporation connected to a funnel, housed in a 30-gallon garbage can with the lid inverted to aid in the collection of rain and snow (modified from those described by Ingraham and Taylor [1991] and Scholl and others [1996]) (figure 23). Precipitation collection began December 2018 and is ongoing.

Stream samples were collected from 11 sites along the East Fork Sevier River and Tropic Ditch, as well as from Yellow Creek at the south end of BCNP (figure 1). Sampling occurred in October 2018, June 2019, and September 2019. Four sites were sampled more than once.

Groundwater samples were collected from 27 wells and 37 springs. Repeat sampling was performed at 22 wells and 12 springs. Sampling occurred between September 2018 and May 2020.

All stable isotope samples were field-filtered with disposable 0.45-µm disc filters into 10 mL snap-cap or crimp-cap vials with no head space. Isotopic analysis of $\delta^{18}O$ and $\delta^{2}H$ was performed by cavity ring-down spectrometry at the University of Utah Stable Isotope Ratio Facility for Environmental Research (SIRFER).

Figure 23. *Precipitation collector for the study area.*

Tritium

Tritium (^3H) provides a qualitative age of groundwater for determining the relative time when water entered the groundwater system (Clark and Fritz, 1997). Tritium is an unstable isotope of hydrogen with a half-life of 12.32 years; tritium concentration in groundwater isolated from other water will decrease by one-half after 12.32 years. Tritium is produced naturally in the upper atmosphere in small quantities, but above-ground thermonuclear testing from 1952 to the late-1970s added tritium to the atmosphere in amounts that far exceed the natural production rates, and, as a result, tritium concentrations in precipitation also increased. The amount of tritium in the atmosphere from weapons testing peaked in the early to mid-1960s and has been declining since atmospheric nuclear testing ceased. Tritium concentrations in water are reported in tritium units (TU). One TU represents one tritiated water molecule per 10^{18} non-tritiated water molecules (Clark and Fritz, 1997). In Utah, concentrations in precipitation measured since 1953 ranged from background levels of 3 to 13 TU to over 8000 TU in 1963 (Lindsey and others, 2019). Tritium in the atmosphere is incorporated into water molecules and enters the groundwater system as recharge from precipitation. Because tritium is part of the water molecule, it is not affected by chemical reactions other than radioactive decay, and thus can be used as a tracer of groundwater on a time scale of less than 10 to about 67 years before present. Water that entered the groundwater system before 1952 and has remained isolated from younger water contains negligible tritium. Therefore, tritium can be used to distinguish between water that entered an aquifer before 1952 and water that entered the aquifer after 1952. Location-specific thresholds for a groundwater sample can be calculated for defining modern and premodern groundwater, using measured or estimated time-series records of tritium for a given location (Lindsey and others, 2019). Using the tritium record in precipitation for a grid cell defined by 37–39° N. latitude and 110–115° W. longitude and a groundwater sample collected in 2019, we define a premodern threshold of 0.19 TU and a modern threshold of 1.7 TU. Samples falling within this range are considered mixed. A mixture of water having different tritium ages complicates interpretation. We sampled nine wells and four springs for tritium analysis (table 3). Samples were collected in two 0.5 L HDPE bottles and sealed with minimal head space. Tritium concentration was measured at the University of Utah Department of Geology and Geophysics Dissolved and Noble Gas Laboratory in Salt Lake City, Utah, via the tritium-^3He ingrowth method (Solomon and Cook, 2000), which measures the concentration of ^3He, a radioactive decay product of tritium.

Radiocarbon

Carbon-14 (^{14}C) is a naturally occurring radioactive isotope of carbon that has a half-life of about 5730 years, which allows the determination of groundwater residence times of up to 40,000 years (Kalin, 2000). ^{14}C data are expressed as percent modern carbon (pmC) relative to A.D. 1950 levels, based on the National Bureau of Standards oxalic acid standard. Carbon-13 (^{13}C) is a naturally occurring stable isotope of carbon that is used to evaluate chemical reactions involving carbon (Clark and Fritz, 1997). ^{13}C is expressed as an isotopic ratio ($^{13}C/^{12}C$), reported as delta (δ) values in units of parts per thousand (per mil or ‰) relative to the Vienna Pee Dee Belemnite (VPDB) standard. The $\delta^{13}C$ ratio in groundwater depends upon numerous factors, which include the type of vegetation in the recharge area, whether carbonate (and the $\delta^{13}C$ compositions of those minerals) is dissolved or precipitated during recharge, and whether the system is open or closed. We sampled nine wells and four springs for carbon isotope analysis (table 3). Samples were collected in 1 L HDPE bottles sealed with minimal head space and processed to solid concentrate at the Brigham Young University Hydrogeochemistry Lab in Provo, Utah, and analyzed by accelerator mass spectrometer at the University of Georgia Center for Applied Isotope Studies in Athens, Georgia.

^{14}C is produced naturally in the upper atmosphere by a cosmic ray reaction with nitrogen. Atmospheric testing of nuclear weapons also produced elevated ^{14}C concentrations, so in some instances values greater than 100 pmC can occur in groundwater. ^{14}C is not part of the water molecule, so ^{14}C activities are affected by chemical reactions between the aquifer material and the dissolved constituents in the water. Chemical reactions can either add or remove carbon; therefore, knowledge of chemical reactions that occur during recharge and transport through the aquifer are necessary for estimating the initial activity (A_0) of ^{14}C. Age calculations require estimates of some chemical parameters during recharge and model calculations of reactions during groundwater transport.

A_0 is the initial, non-decayed ^{14}C composition of the groundwater and must be determined to calculate ^{14}C ages. In the absence of subsurface reactions, A_0 is assumed to be 100 pmC. However, this assumption is rarely valid due to the common presence of carbonate minerals and elevated CO_2 concentrations in the soil. Many models account for geochemical reactions and gas exchanges to determine A_0 (Ingerson and Pearson, 1964; Mook, 1972; Tamers, 1975; Fontes and Garnier, 1979; Han and Plummer, 2013). We calculated A_0 using the revised Fontes and Garnier model of Han and Plummer (2013), which models isotopic exchange controlled by soil gas CO_2 in the unsaturated zone and carbonate minerals in the saturated zone. We assumed end members of radiocarbon activity and $\delta^{13}C$ ratios to be 100 pmC and -21.8 ± 1.4‰ for soil gas CO_2 (Hart, 2009), and 0 pmC and 0‰ for carbonate minerals, respectively.

Table 3. *Tritium and radiocarbon concentrations, carbon isotope ratios, and radiocarbon model age results for Johns and Emery Valleys.*

					TRITIUM	CARBON-14				
SAMPLE ID	SITE NAME	SITE TYPE	SAMPLE DATE	AQUIFER	CONCENTRATION (TU)	CONCENTRATION (pmC)	d^{13}C (‰)	UNCORRECTED AGE (yr B.P.)	FONTES AND GARNIER CORRECTION AGE (yr B.P.)	MODIFIED FONTES AND GARNIER CORRECTION AGE (yr B.P.)
BC6S	Dripping Vat	Spring	5/15/19	Claron	1.56	73.346	-9.38	2563	--	--
BC35S	Mossy Cave	Spring	6/11/19	Claron	1.951	55.087	-7.87	4929	--	--
BC31S	Tom Best	Spring	6/11/19	Claron	5.595	85.684	-11.21	1277	--	--
BC68S	Yovimpa	Spring	6/18/19	Claron	3.789	100.320	-10.58	--*	--	--
BC142W	Dave's Hollow	Well	5/15/19	Alluvium		96.350	-10.81	307	--	--
BC40W	Elk Preserve	Well	5/16/19	Alluvium	0.4040	80.000	-8.17	1845	--	--
BC21W	Ruby 2	Well	5/14/19	Alluvium	2.8000	98.027	-10.49	165	--	--
BC44W	NPS 1	Well	5/15/19	Alluvium	3.5000	96.503	-11.52	294	--	--
BC66W	Smith	Well	6/12/19	Alluvium	2.8840	99.048	-9.19	79	--	--
BC28W	Landfill 1	Well	6/11/19	Alluvium	1.3930	73.458	-10.13	2550	--	--
BC30W	Landfill 3	Well	6/11/19	Alluvium	2.8300	--	--	--	--	--
BC48W	SITLA 1	Well	5/15/19	Claron	3.7104	105.573	-12.02	--	--	--
BC13W	Poe	Well	5/13/19	Cretaceous	0.0059	16.223	-6.88	15,036	6734	4821
BC19W	King's Creek CG	Well	6/10/19	Cretaceous	0.1190	12.030	-7.96	17,508	10,170	8567

* Null value indicates a given model resulted in a negative age

Groundwater age is calculated by:

$$t = \tau \ln (A_0/A) \tag{4}$$

where:

t = groundwater age (years)

τ = 8267, a constant equal to ^{14}C half-life (5730 yrs) ÷ ln 2

A_0 = calculated initial ^{14}C activity (pmC)

A = measured ^{14}C activity (pmC)

The sample likely contains ^{14}C produced from nuclear testing if A is greater than A_0. This indicates a sample has at least some component of modern water and can be verified using tritium data.

Results

Stable Isotopes of Water

Stable isotope ratios from precipitation, surface water, and groundwater range from -126‰ to -24.7‰ for δ^2H and -16.7‰ to -3.4‰ for $\delta^{18}O$ (table A-5 in appendix A). Ninety-five percent of samples fall within the range of -110‰ to -85‰ for δ^2H and -15‰ to -10‰ for $\delta^{18}O$. Differences in sample ratios are apparent when divided by sample type (figure 24).

Precipitation: The mean δ^2H and $\delta^{18}O$ ratios in precipitation are -90.4 ± 35.6‰ and -12.3 ± 4.8‰, respectively (figure 25). Winter precipitation is much more depleted than summer precipitation. Precipitation origin is likely the cause of this difference. During winter, the polar jet stream brings storm systems from the Pacific Ocean, whereas during summer, monsoonal flow brings limited amounts of precipitation originating from the Gulf of California, Gulf of Mexico, and Pacific Ocean (Gillies and Ramsey, 2009).

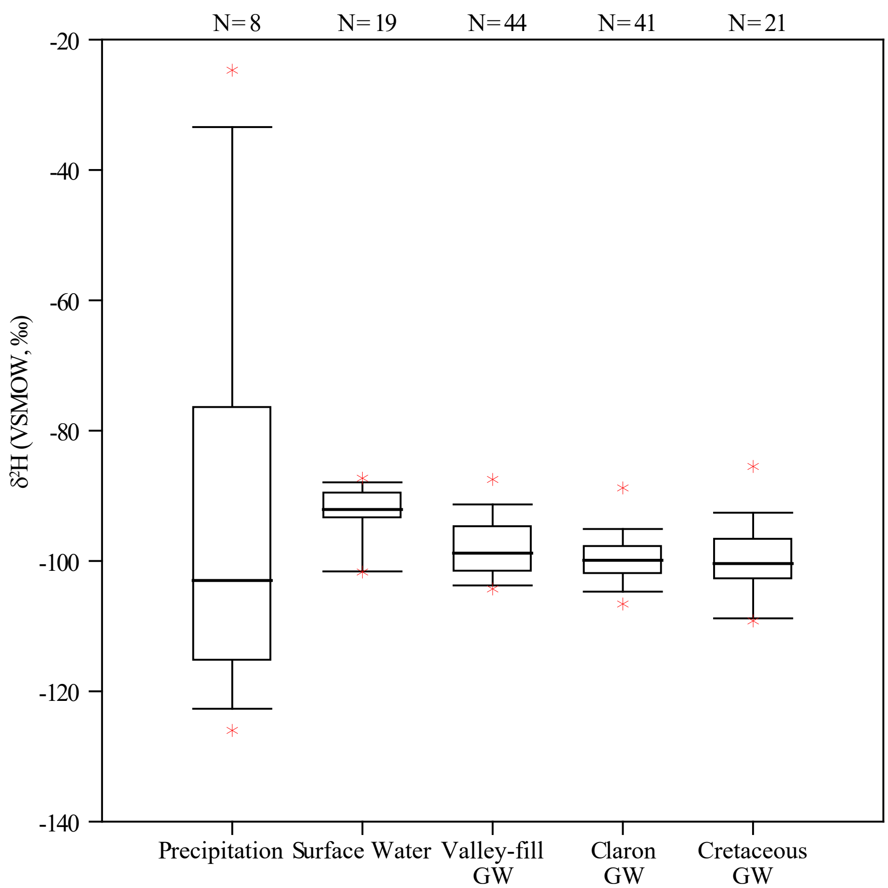

Figure 24. *Statistical comparison of δ^2H in study area waters.*

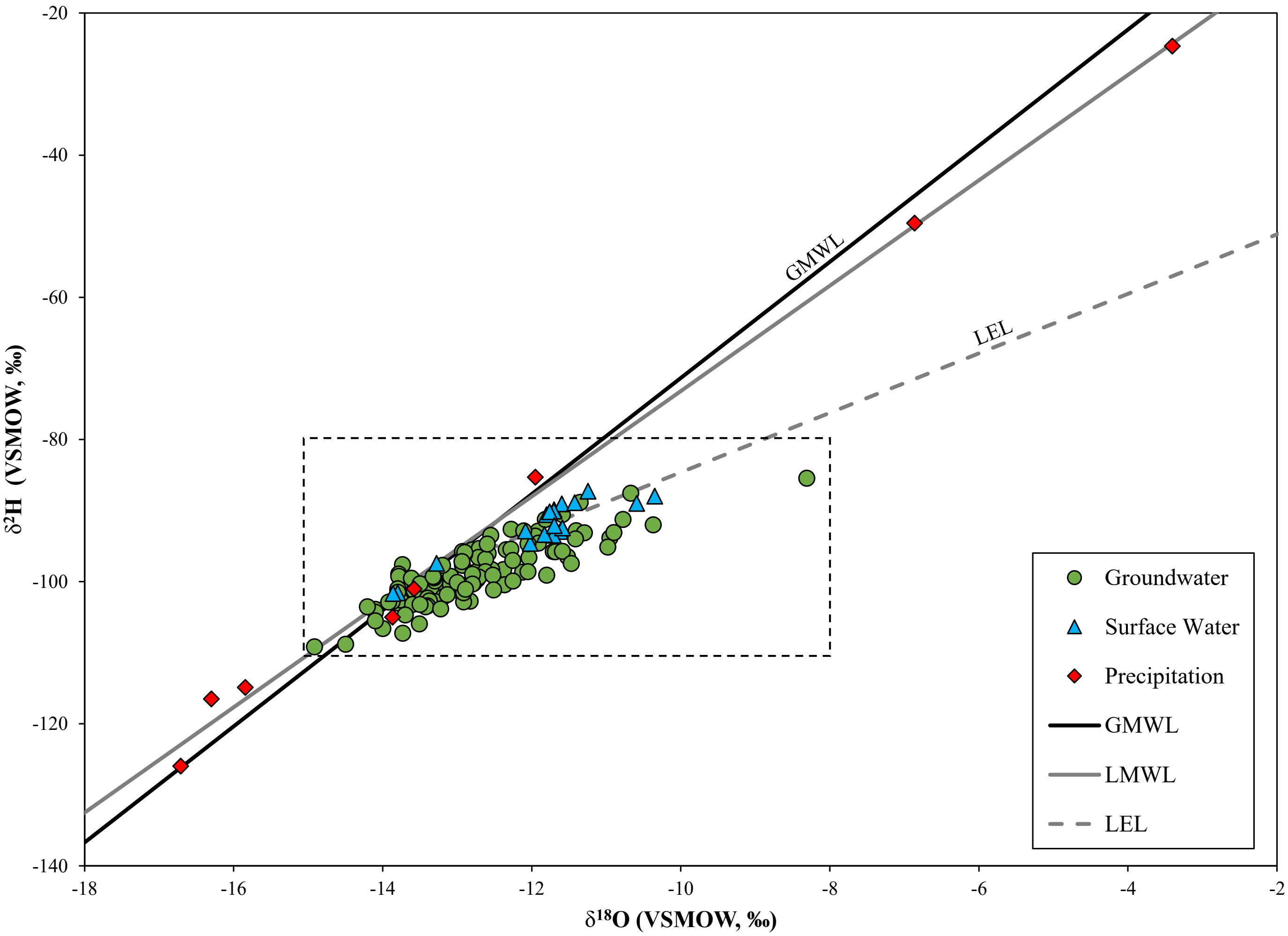

Figure 25. *Stable isotope ratios in precipitation, groundwater, and surface water. The dashed box shows the extent of figure 29, which gives a detailed plot of groundwater and surface water ratios. GMWL = global meteoric water line, LEL = local evaporation line.*

The slope of a linear regression line using all precipitation is 7.4. Global and local meteoric water lines typically have slopes near 8 (Clark and Fritz, 1997). Due to what is likely evaporation of summer precipitation, either during rainfall or within the precipitation collector, the slope of a LMWL based on our samples is underestimated.

Surface water: Surface water samples consist exclusively of East Fork Sevier River and Tropic Ditch samples, except for one sample from Yellow Creek (BC82R), an ephemeral stream on the east side of BCNP. The mean ratios of δ^2H and $\delta^{18}O$ in surface water are -92.4 ± 4.1‰ and -11.9 ± 0.9‰, respectively (figure 25). The data fall along a local evaporation line (LEL) based on a linear regression ($R^2 = 0.85$) of surface water data with a slope of 4.2, which is consistent with evaporative fractionation of surface water found elsewhere (Clark and Fritz, 1997). The most enriched surface water sample was ST-EF7, the East Fork Sevier River at the furthest point downstream within the study area (figure 26).

We assessed temporal and along-reach trends for the spring (June 2019) and autumn (September 2019) sampling events along the East Fork Sevier River and Tropic Ditch. In both spring and autumn we observed isotopic enrichment due to evaporation from upstream to downstream of Tropic Reservoir, followed by isotopic depletion, likely from small tributaries or groundwater input, until the Tropic Ditch diversion (figure 27). In spring 2019, after the heavy snowpack, the East Fork Sevier River was still flowing beyond the Tropic Ditch diversion point. The stable isotope composition remained constant until the river fully entered Emery Valley, at which point it became a losing reach and we observed evaporative enrichment. In spring 2019, the river composition was within or near the range of valley-fill aquifer compositions until the enrichment over the losing reach. However, the autumn 2019 river composition starts closer to the mean valley-fill aquifer composition but is then enriched heavily via evaporation across Tropic Reservoir.

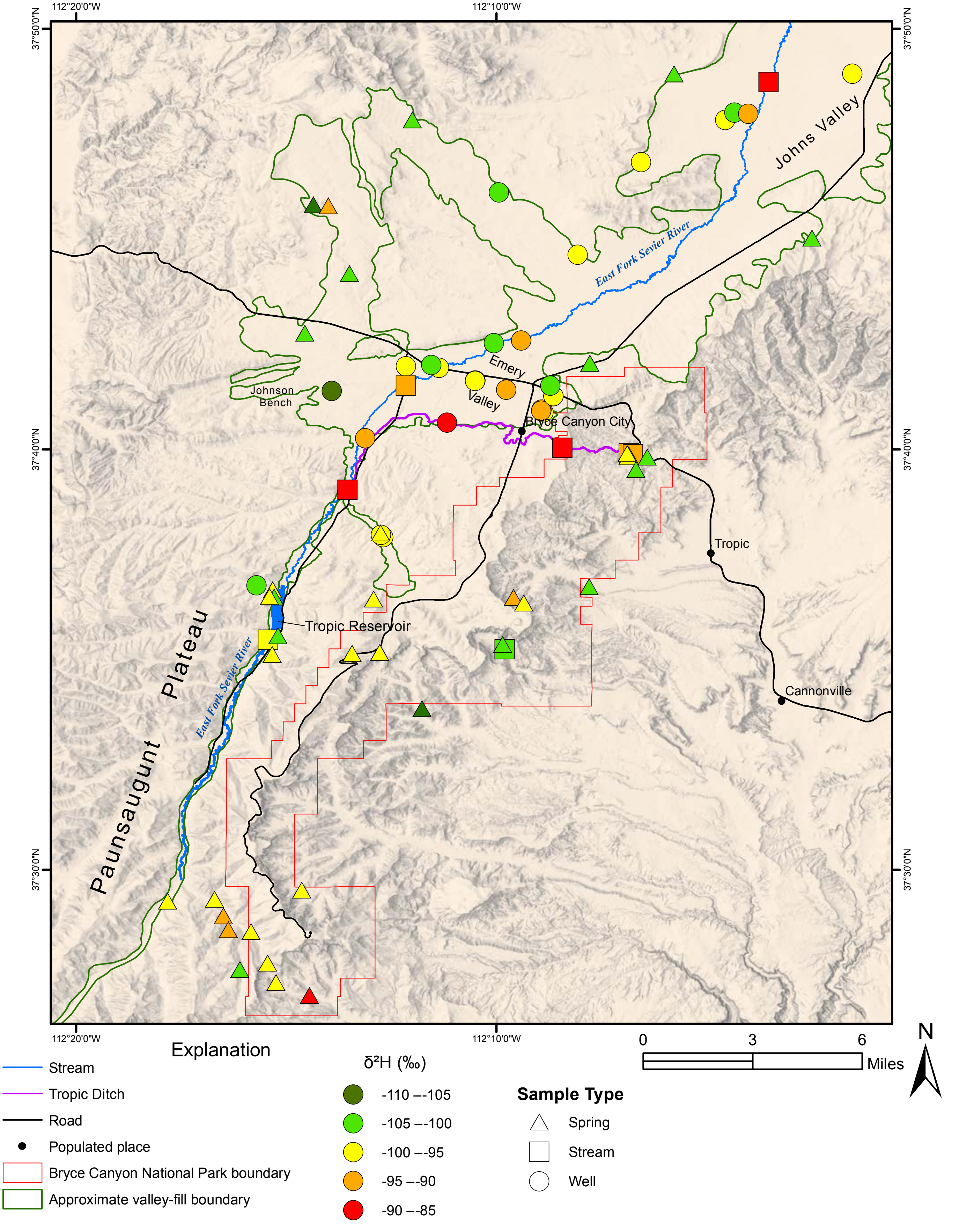

Figure 26. *Map of δ^2H in study area wells, springs, and streams.*

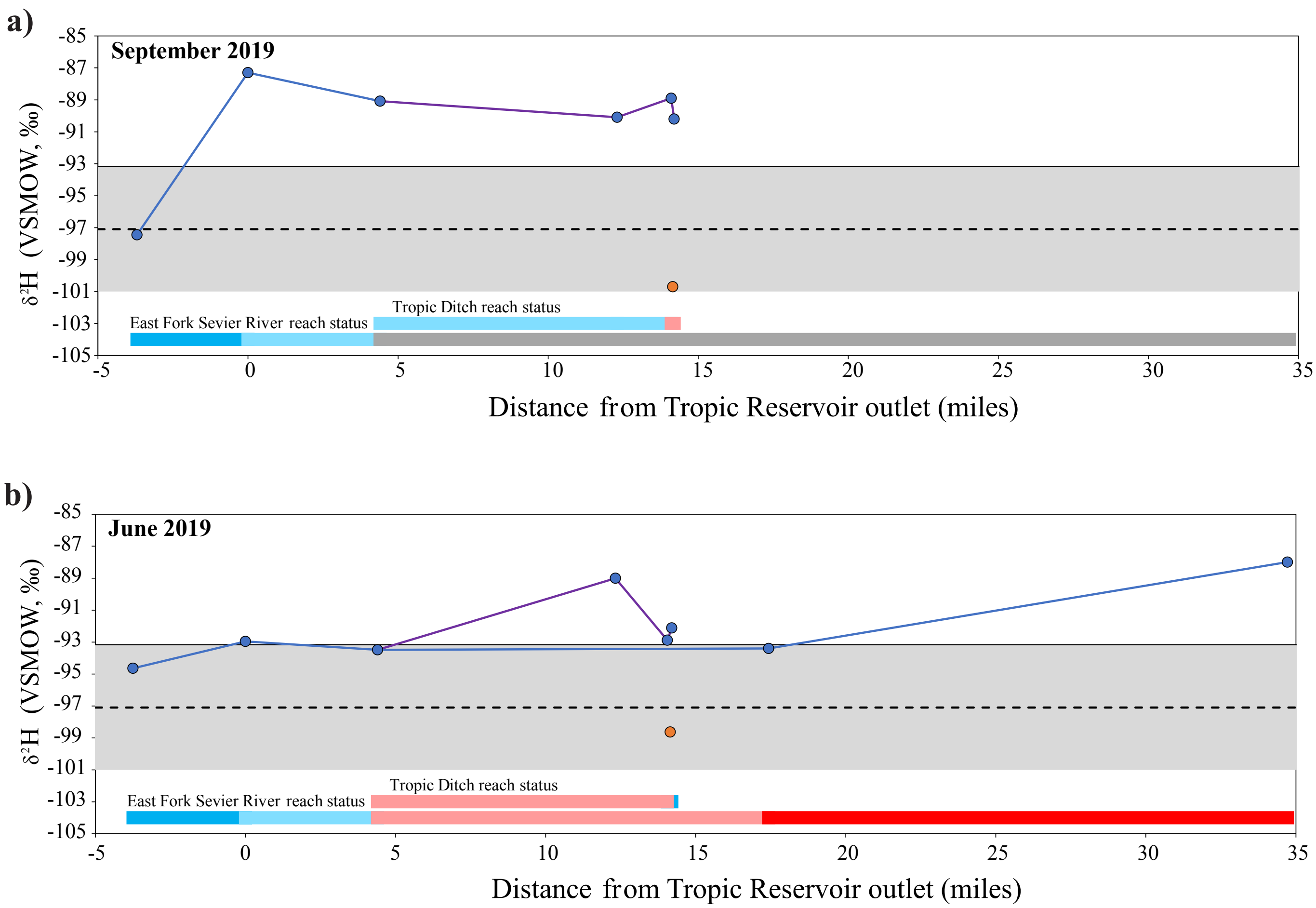

Figure 27. *δ^2H and gaining or losing status in stream reaches versus distance from Tropic Reservoir:* ***a)*** *δ^2H and reach status in June 2019,* ***b)*** *δ^2H and reach status in September 2019. Blue line is East Fork Sevier River, purple line is Tropic Ditch; orange circle is Mossy Cave spring; black dashed line and gray box are valley-fill aquifer average and standard deviation, respectively. Reach status: red = losing, light red = losing within measurement error, blue = gaining, light blue = gaining within measurement error.*

The isotopic composition of the Tropic Ditch was enriched in spring 2019 from the diversion point to the rim of Water Canyon, despite being piped below ground. We observed depletion as the Tropic Ditch flows through Water Canyon, possibly due to groundwater input from the springs and seeps of the Claron Formation. However, the composition enriched slightly beyond the input from Mossy Cave springs (figure 27a). In autumn 2019, we observed completely opposite changes in isotope composition in the Tropic Ditch: depletion from the diversion point to the start of Water Canyon, followed by enrichment within Water Canyon. This change may reflect increased evaporation and a seasonal decrease in groundwater input, although the composition depletes with the addition of Mossy Cave springs outflow (figure 27b). The dominant factor controlling autumn isotope composition of the East Fork Sevier River and Tropic Ditch appears to be residence time within Tropic Reservoir, allowing heavy evaporative enrichment.

Springs and wells: The mean ratio of δ^2H in wells is -98.5 ± 4.4‰. Enrichment of heavier isotopes (less negative isotopic signatures) in groundwater in the western United States has been attributed to paleoclimate effects (White and Chuma, 1987) such as arid conditions, and to extensive evaporation prior to recharge. Evaporation prior to recharge occurs in both surface water and soil water and can yield evaporation line slopes ranging from 2.5 in soils to above 6 in large water bodies (Gibson and others, 2008). Evaporative enrichment is evident in wells screened in all three aquifers, most notably in the valley-fill and Claron aquifers (figure 28). The mean ratio of δ^2H in springs is -99.4 ± 4.4‰. Evaporative enrichment is also apparent in spring samples, most notably from springs issuing from the Claron Formation. Evaporative enrichment in the Claron Formation may be from evaporation during direct recharge, or from evaporation-influenced alluvial groundwater seeping into the Claron. Some of these samples may have experienced evaporation from the time of discharge to sample collection. One spring sample issuing from the Cretaceous aquifer (BC71S) is more highly enriched than any surface water sample, suggesting a slow flow path or ponding prior to sample collection (figure 29). Generally, well and spring samples from the Cretaceous bedrock aquifer include the most depleted ratios, excluding precipitation. Stable isotope ratios of groundwater throughout the study area indicate that recharge is a mixture of winter and summer precipitation, predominantly weighted toward winter precipitation (figure 29).

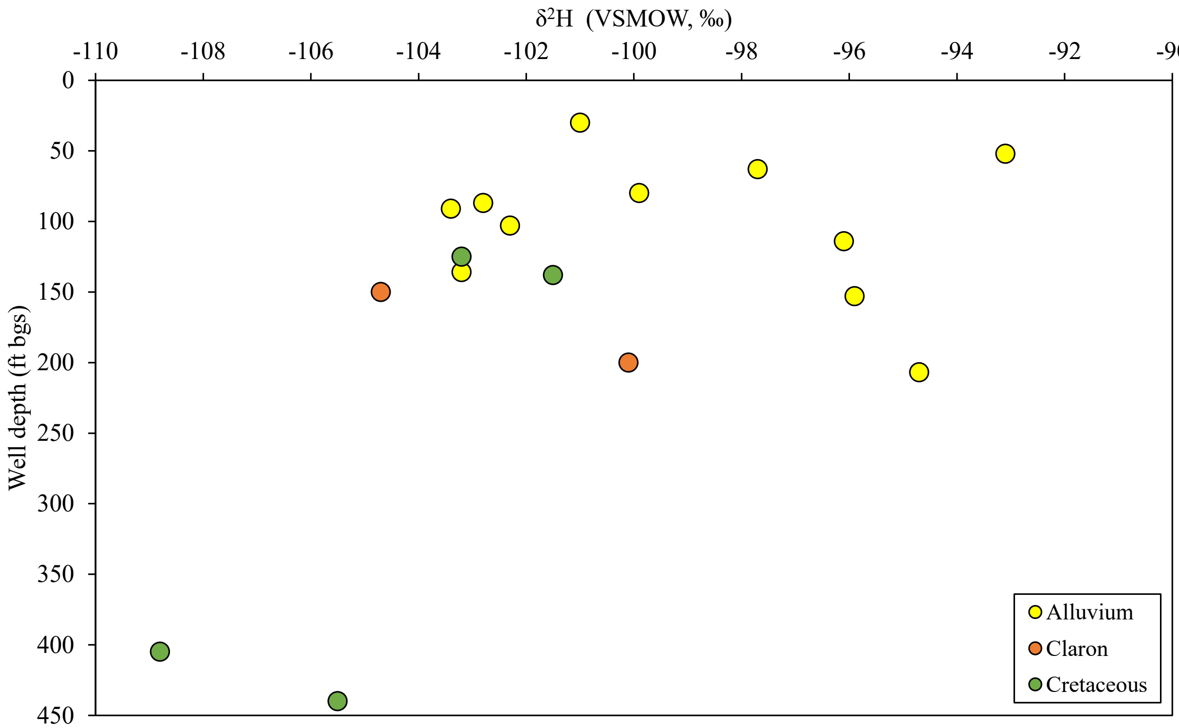

Figure 28. *δ²H in valley-fill and bedrock aquifers relative to well depth.*

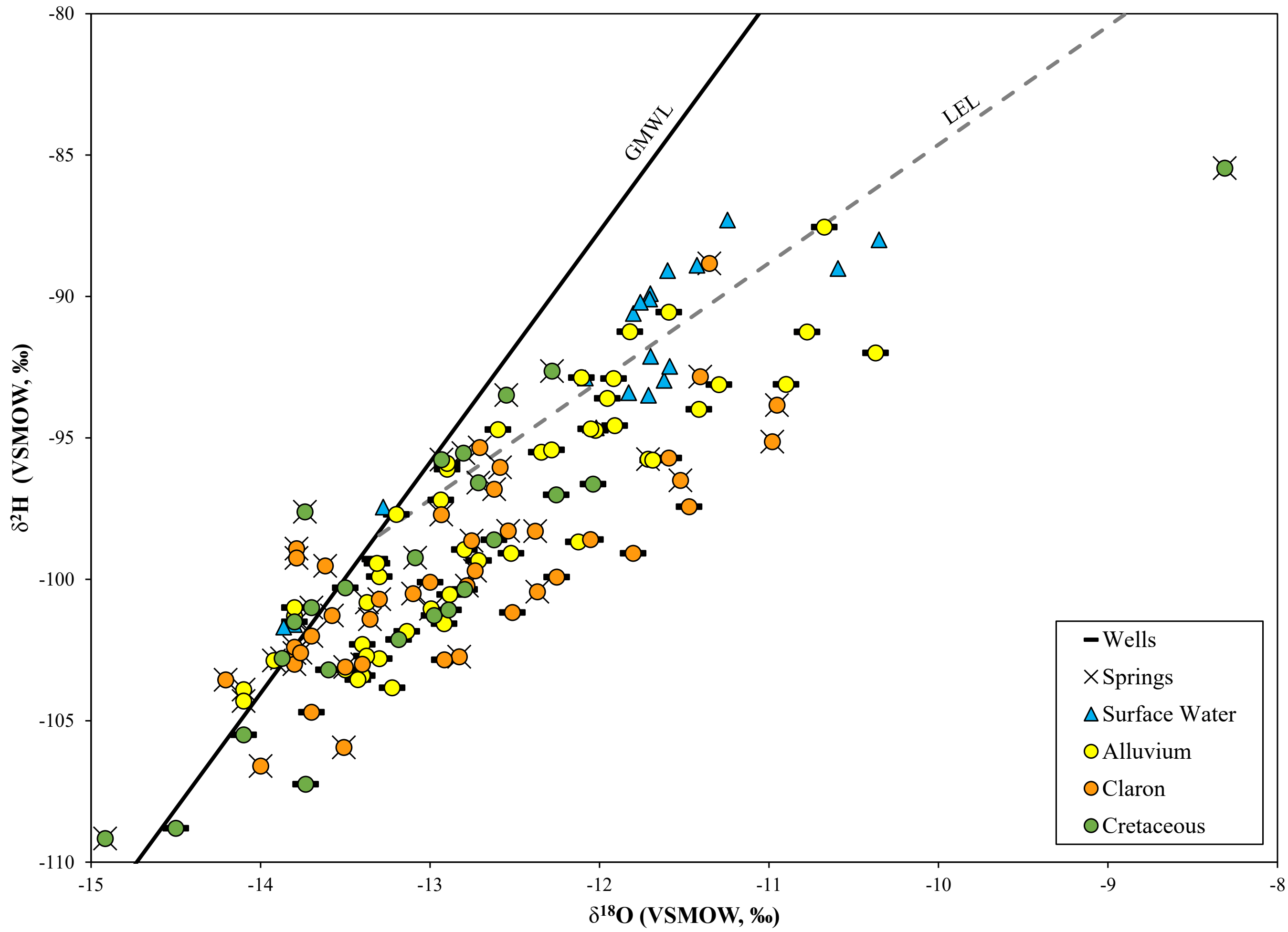

Figure 29. *Stable isotope ratios in groundwater and surface water. GMWL = global meteoric water line, LEL = local evaporation line.*

We assessed stable isotope composition versus well depth and aquifer (figure 28). Generally, deeper wells and wells screened in bedrock aquifers have more depleted compositions. Shallow wells, typically screened in the valley-fill aquifer, tend to have more enriched compositions closer to the average surface water composition.

Groundwater data for $\delta^{18}O$ and $\delta^{2}H$ collected from springs and wells in the BCNP area plot similarly to samples from the rest of the study area, along both the GMWL and evaporation lines (figure 29). The enrichment of heavier isotopes in the groundwater shown on figure 29 indicates the presence of evaporation of surface runoff or soil water or sublimation of the snow prior to recharge. The most depleted isotope compositions are from the two lower-elevation springs located within diffuse seep/spring complexes (figure 15b) on the BCNP eastern boundary, at or near contacts with the Cretaceous sandstone aquifer. The depleted nature of these isotopes suggests that recharge to the Cretaceous aquifer is less susceptible to evaporative processes.

Tritium

We collected water samples for tritium analysis from nine wells and four springs in the study area (figure 30, table 3). Tritium concentrations measured in groundwater range from 0.01 to 5.60 TU with a mean of 2.35 TU and a mean measurement uncertainty of 0.26 TU. Samples BC13W and BC19W have tritium concentrations less than 0.19 TU and are considered premodern. Eight samples have tritium concentrations greater than 1.7 TU and are considered modern, while the remaining three samples have concentrations between 0.19 and 1.7 TU and are considered mixed (table 3). The two premodern samples are from wells screened in the Cretaceous bedrock aquifer. The remaining samples are from the alluvial aquifer or Claron bedrock aquifer.

Radiocarbon

We collected water samples for radiocarbon analysis from nine wells and four springs in the study area (figure 31, table 3). ^{14}C values ranged from 12.0 to 105.6 pmC (table 3). The mean measurement uncertainty is 0.22 pmC, excluding samples from BC13W and BC19W, which had uncertainties of 0.064 and 0.066 pmC, respectively. $\delta^{13}C$ ratios ranged from -12.0‰ to -6.9‰ (table 3). Bomb-peak ^{14}C is present in most of the samples, as indicated by a measured ^{14}C activity greater than the A_0 value calculated using the revised Fontes and Garnier model (Han and Plummer, 2013). Bomb-peak ^{14}C is also evident by comparing $\delta^{13}C$ ratios to ^{14}C activities. Samples with bomb-peak ^{14}C plot above and right of the mixing line between soil gas and carbonate minerals on figure 31.

We calculated ^{14}C ages using the revised Fontes and Garnier model (Han and Plummer, 2013) for the two samples with measured ^{14}C activities less than the calculated A_0 values. The ^{14}C ages for samples BC13W and BC19W are 4800 ±500 and 8600 ±500 ^{14}C yr B.P., respectively. The age uncertainty is derived from the uncertainty in soil gas CO_2 $\delta^{13}C$ ratios (Hart, 2009).

DISCUSSION

Conceptual Model of Groundwater Flow

We derived a conceptual model for the local and regional groundwater flow systems in the study area, including valley-fill and bedrock aquifers and groundwater-surface water interactions, based on our flow measurements, cross sections, potentiometric surface maps, and geochemical analyses of water from wells, springs, and streams. We conceptualized groundwater interactions by evaluating the hydraulic properties, flow systems, and hydraulic connectivity between the shallow unconsolidated aquifer and the East Fork Sevier River and from Tropic Reservoir through Emery Valley and Bryce Canyon City to Johns Valley.

The study area boundary, most of which is the surface drainage divide for the East Fork Sevier River, provides a good approximation of the limits of the groundwater basin. We recognize, however, that some localized sections of the study area boundary may not represent the true groundwater divide. The underlying Cretaceous aquifer, part of the regionally extensive Mesaverde aquifer group, extends northward below the surface drainage divide.

Valley-Fill Aquifer

The valley-fill aquifer receives recharge from in situ infiltration of snowmelt on the valley floor and seepage from streams, primarily the East Fork Sevier River, as they enter the valley. Septic-tank leachate also provides local recharge to the valley-fill aquifer. Subsurface inflow from adjacent bedrock aquifers is unknown. Our ongoing work will attempt to quantify the relative

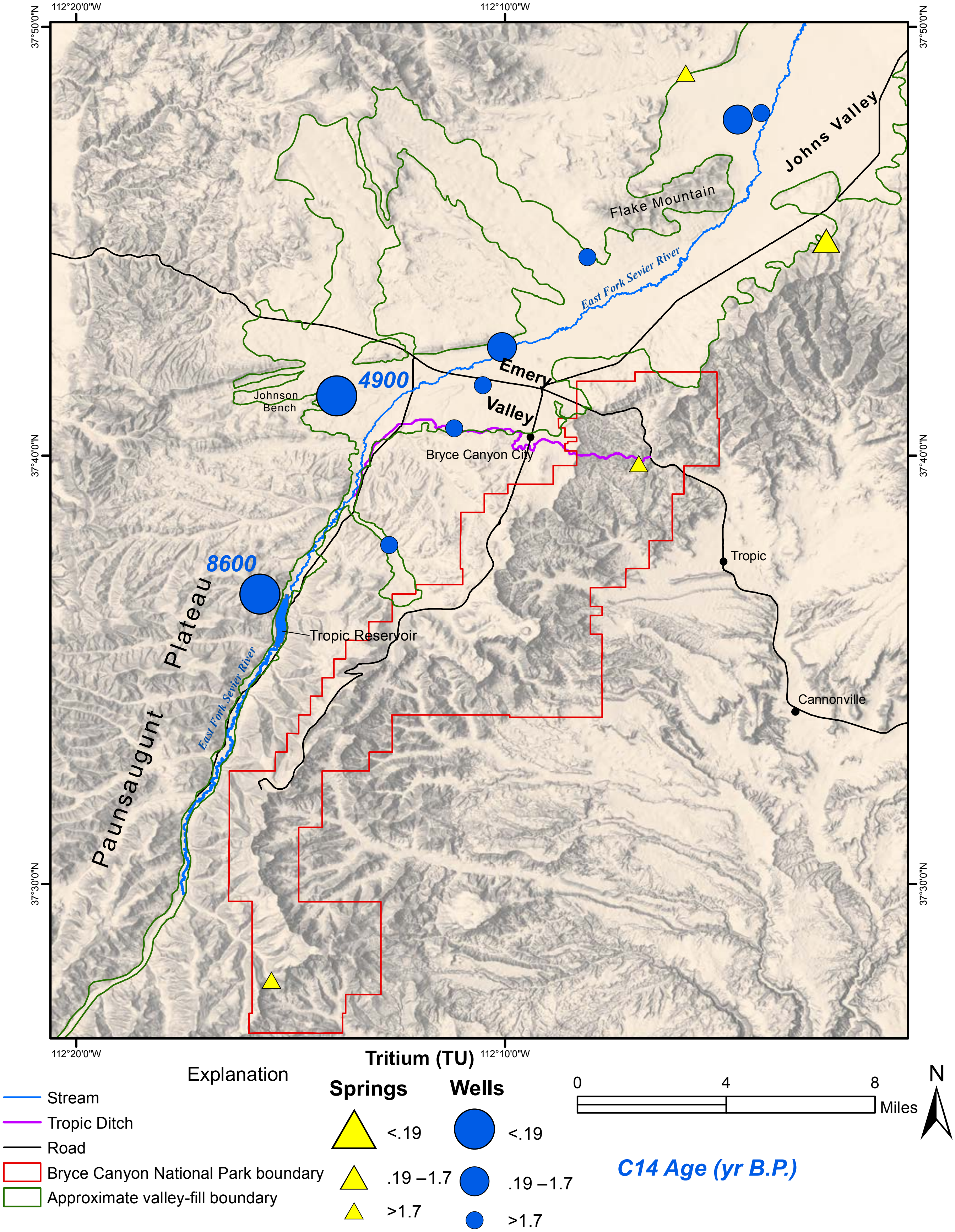

Figure 30. Environmental tracer map for Johns and Emery Valleys showing tritium concentrations and select radiocarbon ages.

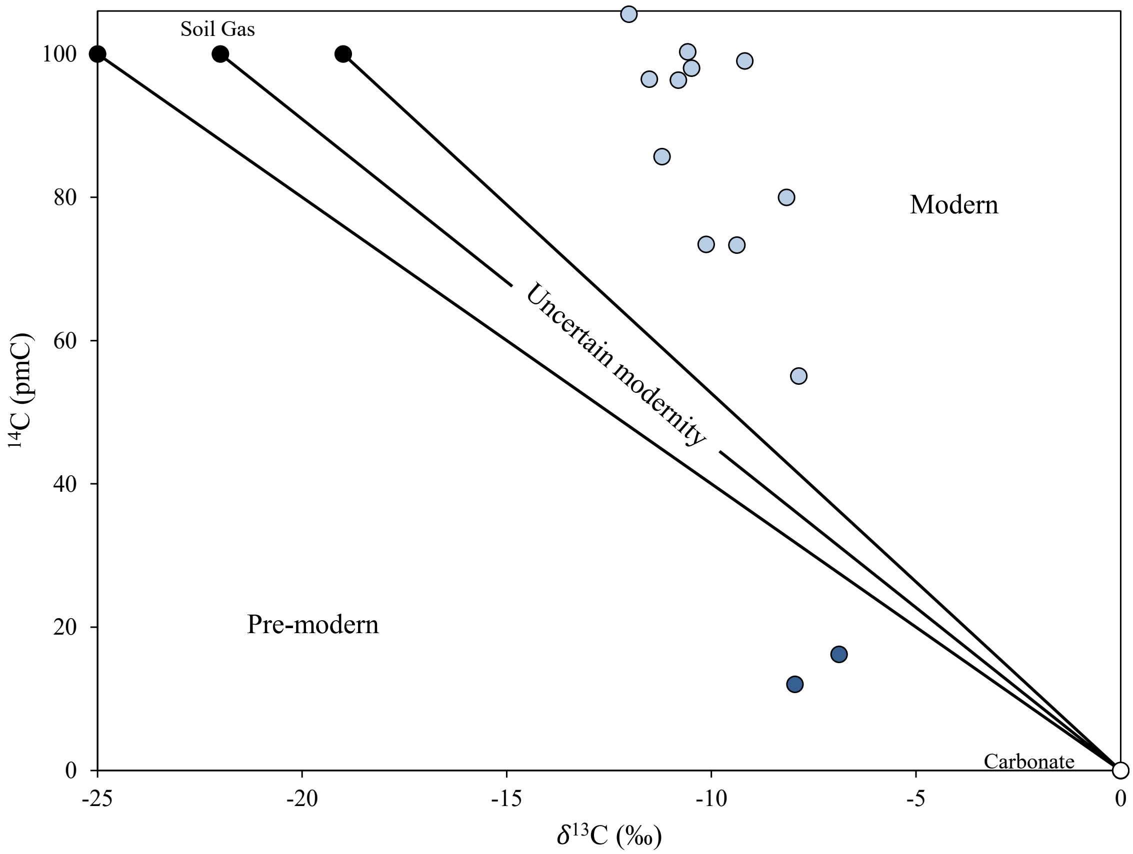

Figure 31. *Carbon isotopes in groundwater samples and simple mixing lines.*

importance of these recharge sources. Groundwater in the valley-fill aquifer flows from the valley margins toward Tropic Reservoir and the East Fork Sevier River, approximately perpendicular to potentiometric contours assuming no major anisotropy in the horizontal component of hydraulic conductivity. Valley-fill groundwater discharges to wells in Emery and southwestern Johns Valleys, and to the East Fork Sevier River near the northeast boundary of the study area.

Valley-fill aquifer thickness varies from less than 50 to 350 feet (<15–107 m) (figure 5). Valley-fill deposits along the valley margins are less than 50 feet (<15 m) thick, and well logs provide no evidence of thickening adjacent to valley-bounding faults. The spatial distribution of valley-fill thickness is poorly constrained but is highly variable in eastern Emery Valley; valley fill is as much as 200 feet (61 m) thick in central Emery Valley and tentatively as much as 350 feet (107 m) thick in southwestern Johns Valley. Additional analyses of the gravity data during the continuation of this study may improve our understanding of the valley-fill aquifer thickness. These sediments are the principal reservoir for groundwater; however, groundwater storage in the valley fill is relatively limited based on its thickness.

Water levels in most valley-fill wells fluctuate depending on winter precipitation, having relatively short-term increases and declines depending on snowfall amounts, indicating storage is limited. The potentiometric surface in the valley-fill aquifer generally increases in the spring and declines in the fall; the greatest rise was post-heavy snowfall during winter 2019. The heavy 2019 snowpack, followed by a below-normal snowpack in 2020 (appendix F), resulted in increased water levels in many valley-fill aquifer wells. Over half the valley-fill wells had water-level increases of at least 10 feet (3 m). Water levels in wells completed in bedrock aquifers were less variable than wells completed in valley fill, with some water levels declining and others rising during different seasons and years, weather independent. Water-level increases in valley-fill wells after heavier winter snowpack indicates the valley-fill aquifer is more sensitive to precipitation via surface water runoff and direct infiltration than the bedrock aquifers. Groundwater pumping also likely contributes to water-level fluctuations in the valley-fill aquifer, particularly along the more densely developed Highway 12 corridor. Future studies will attempt to quantify the impact on groundwater levels and the overall valley water budget of well pumping, reduced irrigation recharge, winter demand for potable water, and evapotranspiration.

Surface water plays a key role in the groundwater system of Johns and Emery Valleys. Losing streams and tributaries recharge the valley-fill aquifer when and where the water table is below the bottom of the streambed, especially during low-flow conditions. Conversely, streams are gaining in areas having shallow water tables, especially during runoff season when the aquifer is receiving in-place recharge on the valley floor. This interchange of groundwater and surface water is apparent in the environmental isotope data. Our results show an evaporative signal in the alluvial aquifer, and considerable overlap between the isotopic signatures of surface water and the valley-fill aquifer, suggesting recharge from streams.

Bedrock Aquifers

Recharge from precipitation to the bedrock aquifers flows either toward springs and streams to become surface flow, or through the bedrock below Johns and Emery Valleys. The Claron Formation is the highest stratigraphic layer of the Pink Cliffs within BCNP; springs situated along the rim likely receive recharge directly from precipitation in the higher elevation areas of the rim on the escarpment of the Paunsaugunt Plateau. The lower elevation springs that emanate from the Cretaceous formations may receive recharge from the overlying stratigraphy or directly from precipitation on Cretaceous bedrock outcrop exposures, though no measurements were made in this study to validate this.

The hydraulic properties of the Rubys Inn thrust fault and the Paunsaugunt fault may influence regional groundwater flow patterns and potential capture of spring flow and groundwater by future groundwater development in Emery Valley and southwest Johns Valley. Without pump-test data, we can only provide qualitative evaluations. The Rubys Inn thrust fault is a type area for deformation bands where it cuts Cretaceous sandstones (Davis, 1999, p. 73–78). Deformation bands are roughly planar zones of grain crushing due to small displacements near a fault, and typically form dense networks adjacent to faults having more than a few meters of slip (Antonellini and Aydin, 1994; Davis, 1999). Grain-size reduction and chemical reactions reduce the permeability of individual deformation bands by several orders of magnitude compared to the undeformed rock (Antonellini and Aydin, 1994). Connected networks of deformation bands substantially reduce cross-fault fluid flow (Caine and others, 1996). For the Rubys Inn thrust, shale smears derived from fine-grained deposits common in the Cretaceous rocks (figure 3b) may also substantially limit cross-fault fluid flow. Along the northeastern 1.4 miles (2.25 km) of its surface trace before intersecting the Paunsaugunt fault, the Rubys Inn thrust fault juxtaposes Claron Formation Pink Member against itself (plate 1). The Pink Member is composed of sandstone, limestone, and conglomerate, all having variable clay content (Biek and others, 2015), and fault-zone structures are likely heterogeneous.

Whereas fault-zone structures such as deformation bands and shale smears dramatically reduce cross-fault fluid flow, development of these features along fault zones is heterogeneous in three dimensions (Caine and others, 1996; Kattenhorn and Pollard, 2001; Lindanger and others, 2007). Fault zones typically consist of braided, anastomosing strands that show lateral displacement gradients and subsidiary faults at high angle to the main displacement zone (Kattenhorn and Pollard, 2001). At a scale of kilometers, fault zones include segment boundaries composed of complex networks of smaller faults having a wide variety of orientations near a change in strike or offset of the fault plane. In summary, fault-zone heterogeneity results in complex permeability distribution that may allow local cross-fault fluid flow (Caine and others, 1996; Caine and Forster, 1999).

The Rubys Inn thrust shows several potential segment boundaries along strike, particularly along the eastern part of its trace where it bifurcates and is cut by the Paunsaugunt fault, which has several anastomosing strands (Biek and others, 2015; plate 1). The Paunsaugunt fault cuts through the southern part of Johns Valley into the bedrock in the main part of BCNP (plate 1) and may provide a conduit for along-strike (i.e., north-south) groundwater flow from the bedrock to the valley fill.

Together with the heterogeneous nature of fault-zone structures, these along-strike complexities and fault intersections suggest that there is some potential for south-to-north groundwater flow from bedrock aquifers south of Emery and Johns Valleys to bedrock aquifers below the valley and to the valley-fill aquifer. Increased groundwater pumping in the valley-fill aquifer would result in steeper hydraulic gradients along the subsurface part of the Rubys Inn thrust, potentially inducing flow from the bedrock aquifers. It is unclear whether and where this cross-fault groundwater flow would actually occur and whether springs and water levels in wells south of the Rubys Inn thrust would be measurably impacted. This question deserves more focused work (currently a paucity of wells exist south of the thrust fault). The potential for south-to-north groundwater flow along the complex Paunsaugunt fault trace seems greater. However, the fault trace is east of the likely recharge area of the main springs within BCNP.

Most groundwater in the valley-fill aquifer has experienced some evaporation and contains some tritium, consistent with our interpretation that groundwater in the valley-fill aquifer that originated as recharge into the bedrock aquifers discharged to surface water before infiltrating into the valley-fill aquifer. Conversely, the isotopic signature of water from the Cretaceous aquifer shows little evidence of evaporation or connection to surface water. Radiometric dating using carbon and tritium isotopes indicates that groundwater in the Cretaceous-age bedrock aquifer below the valley fill is much older— radiocarbon ages range from approximately 4800 to 8600 years before present—than groundwater in the valley-fill aquifer.

Groundwater–Surface-Water Interaction

We used hydrogeologic, seepage, geochemistry, and environmental tracer data to delineate areas of groundwater–surface-water interaction. Our chemistry and streamflow analyses show that surface water in streams, precipitation falling on the valley floor, and groundwater in the valley-fill aquifer and Claron aquifer are a highly connected system. Stable isotopes of water provide important constraints on the location and amount of surface water and groundwater interaction. The similarity of stable isotope composition of surface water and valley-fill groundwater, as well as the predominance of an evaporative signature in the valley-fill aquifer, suggest both a high degree of surface-water–groundwater connectivity and the presence of in situ recharge of snowmelt in the valley floor.

The interchange between surface water and the shallow valley-fill aquifer between Tropic Reservoir and Emery Valley is net losing from groundwater during spring and generally transitions to net gaining to groundwater by autumn, unless the area experienced above-average snowpack the winter prior. Based on our observations from spring 2019, the valley-fill aquifer in Johns and Emery Valleys is net gaining to groundwater when surface water is actively flowing through the valleys (figure 27b).

Potential for Impacts of Climate Variability and Development

The water supply for BCNP and Bryce Canyon City is modern groundwater from the valley-fill aquifer. The widespread presence of modern groundwater in the valley-fill and Claron Formation aquifers suggests these aquifers are actively recharged with relatively short flow paths and thus sensitive to fluctuations in snowpack levels and climate change and are susceptible to surface-based contamination sources.

Shallow groundwater systems such as the Johns and Emery Valleys valley-fill aquifer that are dominated by modern water suggest active in situ recharge and are typically highly responsive to climate variability on short time scales (Kundzewicz and Doell, 2009). If, in the future, climate change results in reduced snow water equivalent and soil moisture and increased extreme precipitation events and consumptive water use due to higher potential evapotranspiration as predicted for central Utah (National Climate Assessment, 2018a, 2018b), in situ recharge to the valley-fill aquifer may decline.

Shallow, young groundwater systems lacking major areas of valley-floor discharge (i.e., upward vertical hydraulic gradient) and laterally continuous confining layers above the aquifer are highly susceptible to contamination from nearby sources. The most likely new sources of potential groundwater contamination will come from tourism-related development (Wallace and others, 2021; Wallace and Schlossnagle, in preparation).

Bryce Canyon National Park straddles the surface and groundwater divide between the East Fork Sevier River (Great Basin) and the Paria River (Colorado River) drainages. Many springs in or just below the Pink Cliffs in BCNP discharge into the Paria River drainage; however, others discharge into the East Fork Sevier River drainage. Increased groundwater development in Emery and southwestern Johns Valleys would reduce groundwater levels in the valley-fill aquifer, increasing the south-to-north hydraulic gradient between bedrock aquifers that supply springs in western BCNP and the East Fork Sevier River headwaters, and bedrock and valley-fill aquifers below Emery and southwestern Johns Valleys. The Rubys Inn thrust would likely form an overall low-flow structure between the area of pumping and the springs' recharge area; however, local cross-fault groundwater flow and flow parallel to the Paunsaugunt fault is possible. The magnitude of potential capture of spring flow within and west of BCNP by groundwater pumping in Emery and southwestern Johns Valleys would depend on many additional factors including the springs' recharge areas, groundwater levels, hydraulic connectivity within the bedrock aquifers on either side of the Rubys Inn thrust, and hydraulic connectivity between the valley-fill aquifer, where the majority of groundwater development is expected to occur, and the bedrock aquifers. More detailed study of the springs and the Claron aquifer may help address these questions.

SUMMARY

Groundwater resource development and the threat of future drought in Garfield County in the Bryce Canyon National Park and Bryce Canyon City areas in Johns and Emery Valleys prompted this study. Water quality and quantity and the potential for water-quality degradation are critical elements determining the extent and nature of future development in the valley. Because of the potential increase in growth from tourism-related development and an increased demand on drinking water, this study was warranted to aid with careful land-use planning and resource management to preserve Johns and Emery Valleys' surface and groundwater resources. To shed light on the groundwater–surface-water relationship, we measured flow in streams and canals, including a water diversion known as the Tropic Ditch, and measured water levels in wells to generate seasonal potentiometric surface maps. We collected geochemistry and stable isotope data from wells, springs, and streams in the area to characterize water quality and to determine how groundwater and surface water interact. We used radiogenic isotope data to determine how long the water has been in the groundwater system.

We evaluated water quantity and water quality during a 2.5 year study. We measured water levels bi-annually in about 30 wells over two seasons. We measured seasonal discharge in the East Fork Sevier River, tributaries, and springs. We evaluated water quality and environmental tracers in streams, wells, and springs based on three different sampling seasons: autumn 2018, spring 2019, and autumn 2019.

Water levels were measured in wells across four seasons from 2018 to 2020. Winter snowpack was below average in 2018, far above average in 2019, and below average in 2020. The heavy 2019 snowpack, followed by a below-average snowpack in 2020, resulted in increased water levels in many valley-fill aquifer wells. More than half of the valley-fill wells had water-level increases of at least ten 10 feet (3 m). Water levels in wells completed in bedrock aquifers were less variable than wells completed in valley fill, with some water levels declining and others rising during different seasons and years, weather independent. Increase in water levels in valley-fill wells from springtime measurements after heavier winter snowpack indicates the valley-fill aquifer is more sensitive to precipitation via surface water runoff and in situ recharge than bedrock wells.

Seepage runs consist of measuring flow at multiple points along streams and canals to determine where water seeps from the stream into the ground or from the ground into the stream. The difference between flow at the upstream and downstream ends of a stream reach is assumed to be due to seepage. During most irrigation seasons, the entirety of the East Fork Sevier River is diverted into the Tropic Ditch, which for about a century has transported water through Water Canyon within BCNP to irrigate crops in the nearby town of Tropic. During one of the seepage runs after the heavy snowpack of winter 2019, we measured over half the total flow of the East Fork Sevier River continuing past the Tropic Ditch diversion point during irrigation season. By the time the East Fork Sevier River reached the downstream boundary of the study area, 75% of its flow was lost to groundwater, recharging the valley-fill aquifer.

The region has three primary aquifers: a shallow valley-fill aquifer, the limestone of the Eocene Claron Formation, and a Cretaceous sandstone aquifer(s). Water quality in the valley-fill aquifer is excellent and very good in the bedrock aquifers. Environmental tracer data indicate that groundwater in the study area aquifers is a mixture of modern (recharged since 1952) and old (recharged several thousand years ago) components. Water from the valley-fill aquifer, including the NPS well field, as well as water from the four springs sampled, which all discharge from the Claron Formation, consists of modern groundwater recharged since or just prior to 1952. By contrast, water from wells completed in the Cretaceous aquifers consists of old groundwater, recharged at least several thousand years ago. Groundwater from the valley fill and Claron Formation generally has lower TDS concentrations than groundwater from the Cretaceous aquifers. The presence of modern groundwater in most wells and springs suggests these aquifers are actively recharged and thus sensitive to climate change, as well as susceptible to surface-based contamination sources. Water quality, quantity, and the potential for water-quality degradation are critical elements that may determine the extent and nature of future development in Johns and Emery Valleys.

Our data show a connection between surface water and groundwater in the valley-fill aquifer based on shared geochemical characteristics, isotopic tracer signatures, increases in water levels in wells in direct response to heavy precipitation seasons, and seepage run measurements showing streams with distinct gaining and losing reaches. Because of the potential increase in growth from tourism-related development, an increased demand on drinking water warrants continued research that will assist land-use planning and resource management to preserve local water resources. Over the next two years, the UGS will continue to study the interaction between groundwater and surface water in the study area by constraining recharge and discharge to develop a water budget.

ACKNOWLEDGMENTS

This study was funded by the Utah Division of Water Rights, the National Park Service, the Utah Division of Water Quality, and the Utah Geological Survey. We thank William Sawyer, Wayne Jones, and Moyle Johnson (NPS) for accompanying us in the field at BCNP. We thank Fred Syrett for showing us additional monitor wells to sample and allowing access to Ruby’s Inn water supply wells. We thank Kaden Figgins of Garfield County for providing critical county-wide comment and insight. We thank the landowners for allowing us to access their property and sample their wells. We thank Will Hurlbut (UGS) and Emily McDermott (formerly of UGS) for valuable contributions to fieldwork for this study. We thank Stephanie Carney and Mike Hylland (UGS); Jim Reeves, James Greer, and David Jones (UDWRi); and Jeff Hughes (NPS) for providing comments to the report.

REFERENCES

Antonellini, M., and Aydin, A., 1994, Effect of faulting on fluid flow in porous sandstones— petrophysical properties: American Association of petroleum Geologists Bulletin, v. 78, p. 355–377.

Biek, B., Rowley, P.D., Anderson, J.J., Maldanado, F., Moore, D.W., Hacker, D.B., Eaton, J.G., Hereford, R., Sable, E.G., Filkhorn, H.F., and Matyjasik, B., 2015, Geologic map of the Panguitch 30 x 60 quadrangle, Garfield, Iron, and Kane Counties, Utah: Utah Geological Survey Map M-270dm, 112 p., 3 plates, 1 appendix, scale 1:62,500, https://doi.org/10.34191/m-270dm.

Bowers, W.E., 1991, Geologic map of Bryce Canyon National Park and vicinity, southwestern Utah: U.S. Geological Survey Miscellaneous Investigations Series Map I-2108, 15 p., 1 plate, scale 1:24,000.

Bown, T.M., Hasiotis, S.T., Genise, J.F., Maldonado, F., and Bowers, E.M., 1997, Trace fossils of Hymenoptera and other insects, and paleoenvironments of the Claron Formation (Paleocene and Eocene), southwestern Utah, *in* Maldonado, F., and Nealey, L.D., editors, Geologic studies in the Basin and Range-Colorado Plateau transition in southeastern Nevada, southwestern Utah, and northwestern Arizona, 1995: U.S. Geological Survey Bulletin 2153, p. 43–58.

Bradbury, K.R., and Rothschild, E.R., 1985, A computerized technique for estimating the hydraulic conductivity of aquifers from specific capacity data: Groundwater, v. 23, no. 2, p. 240–246.

Caine, J.S., Evans, J.P., and Forster, C.B., 1996, Fault zone architecture and permeability structure: Geology, v. 24, p. 1025–1028.

Caine, J.S., and Forster, C.B., 1999, Fault zone architecture and fluid flow—Insights from field data and numerical modeling, *in* Haneberg, W.C., Mozley, P.S., Moore, J.C., and Goodwin, L.B., editors, Faults and subsurface fluid flow in the shallow crust: American Geophysical Union Geophysical Monograph 113, p. 101–127.

Clark, I., and Fritz, P., 1997, Environmental isotopes in hydrogeology: CRC Press, Boca Raton, 328 p.

Cooper, H.H., and Jacob, C.E., 1946, A generalized graphical method for evaluating formation constants and summarizing well-field history: Eos, Transactions American Geophysical Union, v. 27, no. 4, p. 526–534.

Craig, H., 1961, Isotopic variations in meteoric waters: Science, v. 133, no. 3465, p. 1702–1703.

Davis, G.H., 1999, Structural geology of the Colorado Plateau region of southern Utah, with special emphasis on deformation bands: Geological Society of America Special Paper 342, 157 p.

Davis, G.H., and Pollock, G.L., 2010, Geology of Bryce Canyon National Park, Utah, *in* Anderson, P.B., Chidsey, T.C., Jr., and Sprinkel, D.A., editors, Geology of Utah's Parks and Monuments: Utah Geological Association Publication 28, p. 37–59.

Domenico, P.A., 1972, Concepts and models in groundwater hydrology: New York, McGraw Hill, 416 p.

Doremus, L., and Kreamer, D., 2000, Groundwater movement and water chemistry at Bryce Canyon National Park: Water Resources in Arizona and the Southwest—Proceedings of the 2000 Meetings of the Hydrology Section Arizona-Nevada Academy of Science, p. 81–94.

Fontes, J.C., and Garnier, J.M., 1979, Determination of the initial ^{14}C activity of the total dissolved carbon—A review of the existing models and a new approach: Water Resources Research, v. 15, p. 399–413.

Garfield County Economic Development Plan, 2019, Online, accessed August 18, 2020: https://www.garfield.utah.gov/home/showdocument?id=788.

Gettings, P., Chapman, D.S., and Allis, R., 2008, Techniques, analysis, and noise in a Salt Lake Valley 4D Gravity experiment: Geophysics, v. 73, no. 6, p. WA71–WA82.

Gibson, J.J., Birks, S.J., and Edwards, T.W.D., 2008, Global prediction of δ_A and δ^2H-$\delta^{18}O$ evaporation slopes for lakes and soil water accounting for seasonality: Global Biogeochemical Cycles, v. 22, no. 2, p. GB2031.

Gillies, R.R., and Ramsey, R.D., 2009, Climate of Utah, *in* McGinty, E.I.L., editor, Rangeland resources of Utah: Logan, Utah State University Cooperative Extension Service, p. 39–45.

Gonfiantini, R., 1978, Standards for stable isotope measurements in natural compounds: Nature, v. 271, no. 5645, p. 534–536.

Goldstrand, P.M., 1994, Tectonic development of Upper Cretaceous to Eocene strata of southwestern Utah: Geological Society of America Bulletin, v. 106, p. 145–154.

Han, L.F., and Plummer, L.N., 2013, Revision of Fontes & Garnier's model for the initial ^{14}C content of dissolved inorganic carbon used in groundwater dating: Chemical Geology, v. 351, p. 105–114.

Hart, R., 2009, Isotopic evaluation of carbon dioxide in soil gas in Utah for a more accurate input variable in groundwater age models: Provo, Utah, Brigham Young University, M.S. thesis, 62 p.

Hem, J.D., 1985, Study and interpretation of the chemical characteristics of natural water: U.S. Geological Survey Water-Supply Paper 2254, 263 p.

Hintze, W.J., Aiken, C., Brozena, J., Coakley, B., Dater, D., Flanagan, G., Forsberg, R., Hildenbrand, T., Keller, G.R., Kellogg, J., Kucks, R., Li, X., Mainville, A., Morin, R., Pilkington, M., Plouff, D., Ravat, D., Roman, D., Urrutia-Fucugauchi, J., Veronneau, M., Webring, M., and Winester, D., 2005, New standards for reducing gravity data—The North American gravity database: Geophysics, v. 70, no. 4, p. J25–J32.

Ingerson, E., and Pearson, F.J., 1964, Estimation of age and rate of motion of ground water by the ^{14}C method, *in* Miyake, Y. and Koyama, T., editors, Recent researches in the fields of hydrosphere, atmosphere and nuclear chemistry: Editorial Committee for Sugawara Volume, Water Research Laboratory, Nagoya University, Tokyo, p. 263–283.

Ingraham, N.L., and Taylor, B.E., 1991, Light stable isotope systematics of large-scale hydrologic regimes in California and Nevada: Water Resources Research, v. 27, no. 1, p. 77–90.

Johnson, A.I., 1967, Specific yield—compilation of specific yield for various materials: U.S. Geological Survey Water-Supply Paper 1662-D, 74 p.

Kattenhorn, S.A., and Pollard, D.D., 2001, Integrating 3-D seismic data, field analogs, and mechanical models in the analysis of segmented normal faults in the Wytch Farm oil field, southern England, United Kingdom: American Association of Petroleum Geologists Bulletin, v. 85, p. 1183–1210.

Kalin, R.M., 2000, Radiocarbon dating of groundwater systems, *in* Cook, P.G., and Herczeg, A.L., editors, Environmental tracers in subsurface hydrology: Boston, Springer, p. 111–144.

Kendall, C., and Caldwell, E.A., 1998, Fundamentals of isotope geochemistry, *in* Kendall, C., and McDonnell, J.J. editors, Isotope tracers in catchment hydrology: Amsterdam, Elsevier Science, p. 51–86.

Knudsen, T.R., Biek, R.F., and Eaton, J.G., *in preparation*, Geologic map of Bryce Canyon National Park and vicinity: Utah Geological Survey Map, 2 plates, scale 1:24,000.

Kundzewicz, Z., and Doell, P., 2009, Will groundwater ease freshwater stress under climate change?: Hydrological Sciences Journal, v. 54, p. 665–675.

Lawton, T.F., Pollock, S.L., and Robinson, R.A.J., 2003, Integrating sandstone petrology and nonmarine sequence stratigraphy—application to the Late Cretaceous fluvial systems of southwestern Utah, U.S.A.: Journal of Sedimentary Research, v. 73, no. 3, p. 389–406.

Lindanger, M., Gabrielsen, R.H., and Braathen, A., 2007, Analysis of rock lenses in extensional faults: Norwegian Journal of Geology, v. 87, p. 361–372.

Lindsey, B.D., Jurgens, B.C., and Belitz, K., 2019, Tritium as an indicator of modern, mixed, and premodern groundwater age: U.S. Geological Survey Scientific Investigations Report 2019–5090, 18 p., https://doi.org/10.3133/sir20195090, April 1, 2020.

Mackin, J.H., and Rowley, P.D., 1976, Geologic map of The Three Peaks quadrangle, Iron County, Utah: U.S. Geological Survey Geologic Quadrangle Map GQ-1297, scale 1:24,000.

Maldonado, F., and Moore, R.C., 1995, Geologic map of the Parowan quadrangle, Iron County, Utah: U.S. Geological Survey Geologic Quadrangle Map 1762, 1 plate, scale 1:24,000.

Maldonado, F., and Williams, V.S., 1993a, Geologic map of the Parowan Gap quadrangle, Iron County, Utah: U.S. Geological Survey Geologic Quadrangle Map 1712, 1 plate, scale 1:24,000.

Maldonado, F., and Williams, V.S., 1993b, Geologic map of the Paragonah quadrangle, Iron County, Utah: U.S. Geological Survey Geologic Quadrangle Map 1713, 1 plate, scale 1:24,000.

Mook, W.G., 1972, On the reconstruction of the initial ^{14}C content of groundwater from the chemical and isotopic composition, *in* Eighth International Conference on Radiocarbon Dating: Royal Society of New Zealand, p. 342–352.

Mullet, D.J., 1989, Interpreting the early Tertiary Claron Formation of southern Utah: Geological Society of America Abstracts with Programs, v.21, p. 120.

Natural Resources Conservation Service, 2021,: National Water and Climate Center, Online: https://wcc.sc.egov.usda.gov/reportGenerator/view/customMultiTimeSeriesGroupByStationReport/annual_water_year/end_of_period/, accessed April 26, 2021.

National Climate Assessment, 2018a, Summary findings, Online: https://nca2018.globalchange.gov/downloads/NCA4_Ch01_Summary-Findings.pdf.

National Climate Assessment, 2018b, Chapter 25—Southwest, Online: https://nca2018.globalchange.gov/downloads/NCA4_Ch25_Southwest_Full.pdf.

Ott, A.L., 1999, Detailed stratigraphy and stable isotope analysis of the Claron Formation, Bryce Canyon National Park, Washington State University, unpublished M.S. thesis, 129 p.

Pan-American Center for Earth and Environmental Studies (PACES), 2012, Gravity database of the US: University of Texas, El Paso, Online, http://research.utep.edu/paces, last accessed June 2012.

Roberts, E.M., 2007, Facies architecture and depositional environments of the Upper Cretaceous Kaiparowits Formation, southern Utah: Sedimentary Geology, v. 197, p. 207–233.

Rowley, P.D., Mehnert, H.H., Naeser, C.W., Snee, L.W., Cunningham, C.G., Steven, T.A., Anderson, J.J., Sable, E.G., and Anderson, R.E., 1994, Isotopic ages and stratigraphy of Cenozoic rocks of the Marysvale volcanic field and adjacent areas, west-central Utah: U.S. Geological Survey Bulletin 2071, 35 p.

Rowley, P.D., Biek, R.F., Sable, E.G., Boswell, J.T., Vice, G.S., Hatfield, S.C., Maxwell, D.J., and Anderson, J.J., 2013, Geologic map of the Brian Head quadrangle, Iron County, Utah: Utah Geological Survey Map 263DM, 38 p., 2 plates, scale 1:24,000, https://doi.org/10.34191/M-263dm.

Rozanski, K., Araguás-Araguás, L., and Gonfiantini, R., 1993, Isotopic patterns in modern global precipitation, *in* Swart, P.K., Lohmann, K.C., McKenzie, J., and Savin, S. editors, Climate change in continental isotopic records: American Geophysical Union, p. 1–36.

Scholl, M.A., Ingebritsen, S.E., Janik, C.J., and Kauahikaua, J.P., 1996, Use of precipitation and groundwater isotopes to interpret regional hydrology on a tropical volcanic island—Kilauea volcano area, Hawaii: Water Resources Research, v. 32, no. 12, p. 3525–3537.

Solomon, D.K., and Cook, P.G., 2000, ^{3}H and ^{3}He, *in* Cook, P., and Herczeg, A.L. editors, Environmental tracers in subsurface hydrology: Boston, Kluwer Academic Publishers, p. 397–424.

Tamers, M.A., 1975, Validity of radiocarbon dates on groundwater: Geophysical Surveys, v. 2, no. 2, p. 217–239.

Theis, C.V., 1935, The relation between the lowering of the piezometric surface and the rate and duration of discharge of a well using ground-water storage: EOS, Transactions American Geophysical Union, v. 16, no. 2, p. 519–524.

Thiros, S.A., and Brothers, W.C., 1993, Ground-water hydrology of the upper Sevier River Basin, south-central Utah, and simulation of ground-water flow in the valley-fill aquifer in Panguitch Valley: Department of Natural Resources Technical Publication 102, 121 p.

Utah Automated Geographic Reference Center, 2018, Southern Utah LiDAR elevation data: Online, Utah Automated Geographic Reference Center, State Geographic Information Database, https://gis.utah.gov/data/elevation-and-terrain/2018-lidar-southern-utah/.

Utah Division of Water Quality, 2014, Standard operating procedure for collection of water chemistry samples: Salt Lake City, Utah Division of Water Quality unpublished report, 25 p.

Wallace, J., and Schlossnagle, T.H., *in preparation*, Petition for groundwater quality classification, Bryce Canyon area, Garfield County, Utah: Utah Division of Water Quality unpublished Aquifer Classification Petition Document, 46 p.

Wallace, J., Schlossnagle, T.H., and Payne, N., 2021, Analysis of septic-tank densities in a pristine aquifer: Johns and Emery Valleys near Bryce Canyon City, Garfield County, Utah: Utah Division of Water Quality unpublished contract deliverable, 58 p.

White, D.E., and Chuma, N.J., 1987, Carbon and isotopic mass balance models of Oasis Valley-Forty-Nine Mile Canyon ground water basin, southern Nevada: Water Resources Research v. 23, no. 4, p. 571–582.

Winter, T.C., Harvey, J.W., Franke, O.L., and Alley, W.M., 1998, Ground water and surface water—a single resource: U.S. Geological Survey Circular 1139, 79 p., online, https://pubs.usgs.gov/circ/circ1139/pdf/circ1139.pdf.

APPENDIX A:

Water Level, Discharge, and Water Chemistry Data

Link to supplemental data download:

https://ugspub.nr.utah.gov/publications/open_file_reports/ofr-733/ofr-733-a.pdf

APPENDIX B:

Drillers' Logs for Wells Completed in the Study Area

Link to supplemental data download:

https://ugspub.nr.utah.gov/publications/open_file_reports/ofr-733/ofr-733-b.pdf

APPENDIX C:

Description of Cuttings from Lion Bryce-Monsanto 1 Well

Link to supplemental data download:

https://ugspub.nr.utah.gov/publications/open_file_reports/ofr-733/ofr-733-c.pdf

APPENDIX D:

Gravity Data

Link to supplemental data download:

https://ugspub.nr.utah.gov/publications/open_file_reports/ofr-733/ofr-733-d.pdf

APPENDIX E:

Aquifer Properties

Link to supplemental data download:

https://ugspub.nr.utah.gov/publications/open_file_reports/ofr-733/ofr-733-e.pdf

APPENDIX F:

Precipitation and Snow Equivalent Graphs NRCS

Link to supplemental data download:

https://ugspub.nr.utah.gov/publications/open_file_reports/ofr-733/ofr-733-f.pdf

STRATIGRAPHIC COLUMN

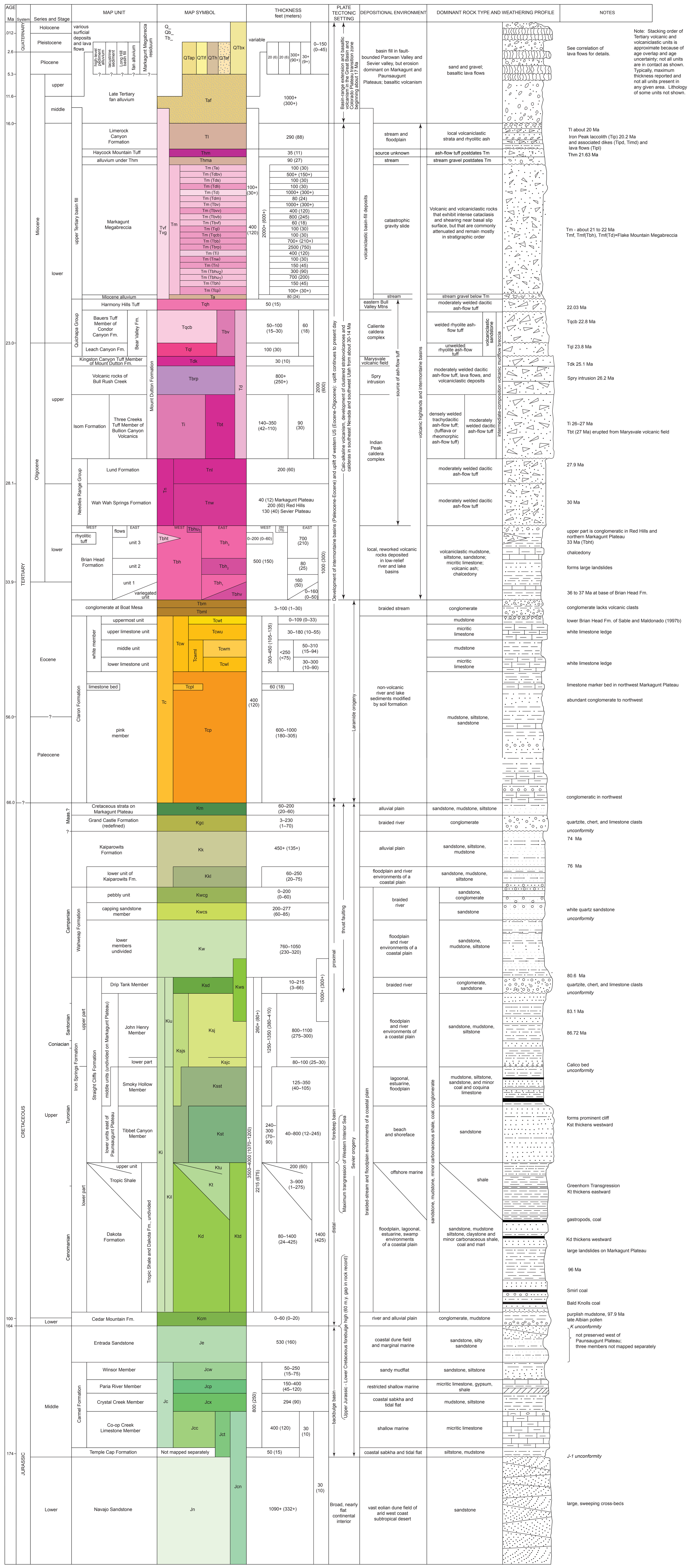

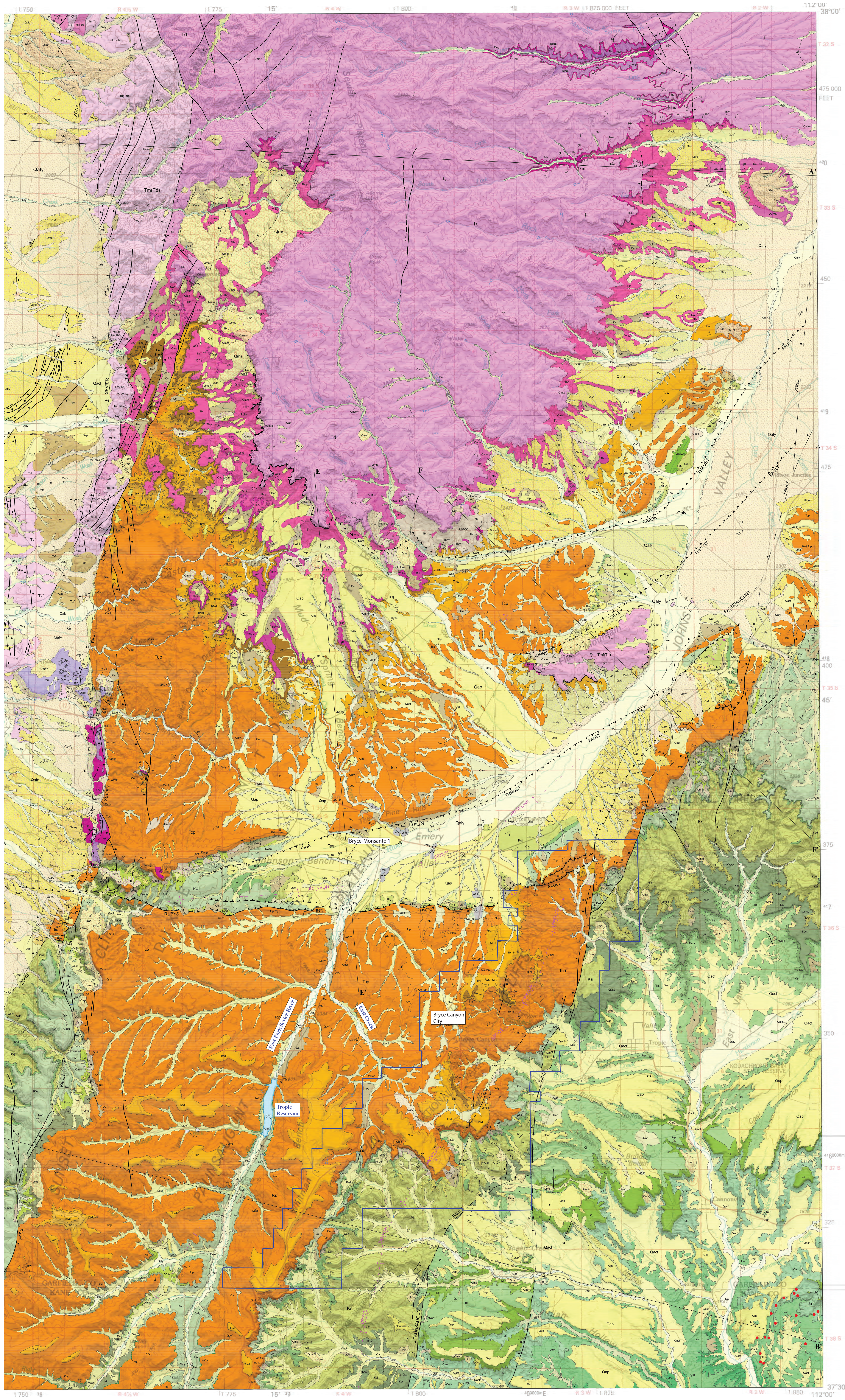

Plate 1 - Eastern One-Third of the Panguitch 30′ x 60′ Quadrangle
Utah Geological Survey Open-File Report 733
Hydrogeologic Study of the Bryce Canyon City Area, Including Johns and Emery Valleys, Garfield County, Utah

UTAH GEOLOGICAL SURVEY
a division of
Utah Department of Natural Resources
in cooperation with U.S. Geological Survey

THE CONTENTS OF THIS PLATE ARE DIRECTLY FROM UGS MAP M-270DM, EXCEPT FOR LABELS ADDED TO THE MAP FOR CLARITY. NOT ALL OF THE GEOLOGIC UNITS SHOWN IN THE STRATIGRAPHIC COLUMN AND CORRELATION CHART, NOR ALL OF THE MAP SYMBOLS LISTED, ARE SHOWN IN THIS PART OF THE GEOLOGIC MAP

GEOLOGIC MAP OF THE PANGUITCH 30' X 60' QUADRANGLE, GARFIELD, IRON, AND KANE COUNTIES, UTAH

2015

by

Robert F. Biek[1], Peter D. Rowley[2], John J. Anderson[3], Florian Maldonado[4], David W. Moore[4], David B. Hacker[5], Jeffrey G. Eaton[6], Richard Hereford[4], Harry Filkorn[7], and Basia Matyjasik[1]

[1] Utah Geological Survey, P.O. Box 146100, Salt Lake City, UT 84114-6100
[2] Geologic Mapping Inc., P.O. Box 651, New Harmony, UT 84757
[3] Kent State University, retired
[4] U.S. Geological Survey, retired
[5] Department of Geology, Kent State University Trumbull Campus, Warren, OH 44483-1998
[6] Department of Geosciences, Weber State University, Ogden, UT 84408-2507
[7] Department of Physics and Planetary Science, Pierce College, Woodland Hills, CA 91371

SCALE 1:62,500

1 0.5 0 1 2 3 4 MILES

1 0.5 0 1 2 3 4 5 6 KILOMETERS

CONTOUR INTERVAL 50 METERS

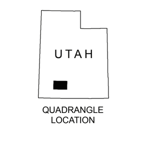

QUADRANGLE LOCATION

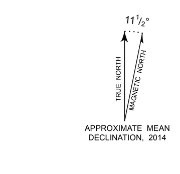

APPROXIMATE MEAN DECLINATION, 2014

Disclaimer

This geologic map was funded by the Utah Geological Survey and the U.S. Geological Survey, National Cooperative Geologic Mapping Program through USGS STATEMAP award numbers 08HQAG0096, G09AC00152, G10AC00386, and G11AC20249. The views and conclusions contained in this document are those of the authors and should not be interpreted as necessarily representing the official policies, either expressed or implied, of the U.S. Government.

CORRELATION OF MAP UNITS

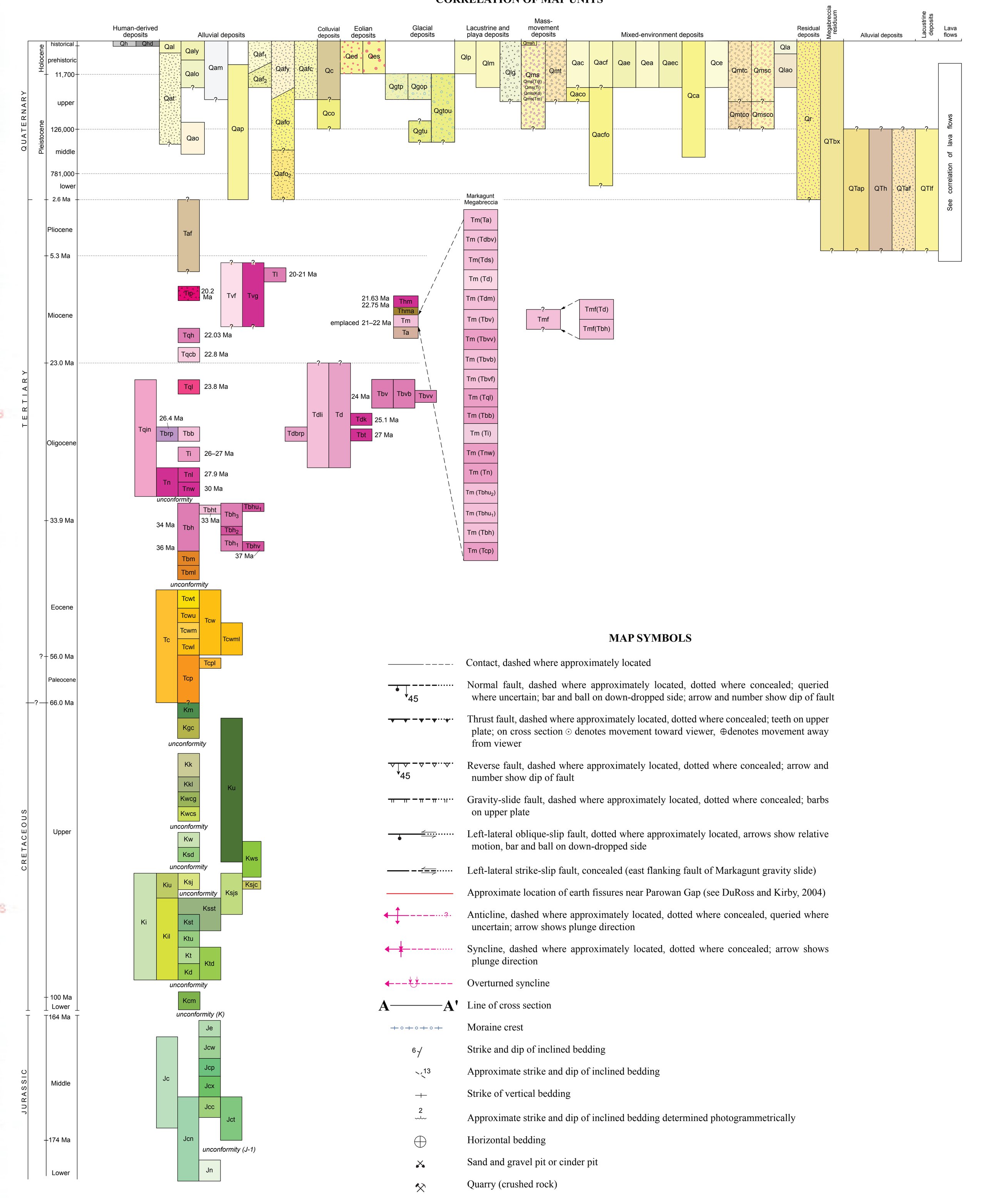

MAP SYMBOLS

- Contact, dashed where approximately located
- Normal fault, dashed where approximately located, dotted where concealed; queried where uncertain; bar and ball on down-dropped side; arrow and number show dip of fault
- Thrust fault, dashed where approximately located, dotted where concealed; teeth on upper plate; on cross section ⊙ denotes movement toward viewer, ⊕denotes movement away from viewer
- Reverse fault, dashed where approximately located, dotted where concealed; arrow and number show dip of fault
- Gravity-slide fault, dashed where approximately located, dotted where concealed; barbs on upper plate
- Left-lateral oblique-slip fault, dotted where approximately located, arrows show relative motion, bar and ball on down-dropped side
- Left-lateral strike-slip fault, concealed (east flanking fault of Markagunt gravity slide)
- Approximate location of earth fissures near Parowan Gap (see DuRoss and Kirby, 2004)
- Anticline, dashed where approximately located, dotted where concealed, queried where uncertain; arrow shows plunge direction
- Syncline, dashed where approximately located, dotted where concealed; arrow shows plunge direction
- Overturned syncline
- A——A' Line of cross section
- Moraine crest
- Strike and dip of inclined bedding
- Approximate strike and dip of inclined bedding
- Strike of vertical bedding
- Approximate strike and dip of inclined bedding determined photogrammetrically
- Horizontal bedding
- Sand and gravel pit or cinder pit
- Quarry (crushed rock)
- Volcanic vent
- Sinkhole; although an inventory has not been done, countless sinkholes, not readily visible on aerial photographs and so not shown on this map, are known to be on the Markagunt Plateau
- Marker bed
- Timd Mafic dike, bar and ball on down-dropped side of fault intruded by dike
- Tipd Feeder dike of Iron Peak intrusion
- Oil and gas exploration drill hole, plugged and abandoned; number refers to table 4
- Spring
- Radiometric age sample (see table 3)
- Geochemical sample (see http://geology.utah.gov/online/analytical_data.htm)
- Palynomorph sample (see table 2)
- Selected sedimentary pipes in and near Kodachrome Basin State Park (see Baer and Steed, 2010)
- Bryce Canyon National Park boundary

Base from USGS Panguitch 30' x 60' Quadrangle (1980)
Projection: UTM Zone 12
Datum: NAD 1927
Spheroid: Clarke 1866

Project Manager: Douglas A. Sprinkel

GIS and Cartography: Jay C. Hill, and Basia Matyjasik

Utah Geological Survey
1594 West North Temple, Suite 3110
P.O. Box 146100, Salt Lake City, UT 84114-6100
(801) 537-3300
geology.utah.gov
Geologic Map Portal
https://doi.org/10.34191/OFR-733

UTAH GEOLOGICAL SURVEY
a division of
Utah Department of Natural Resources

CROSS SECTIONS IN THE BRYCE CANYON CITY STUDY AREA

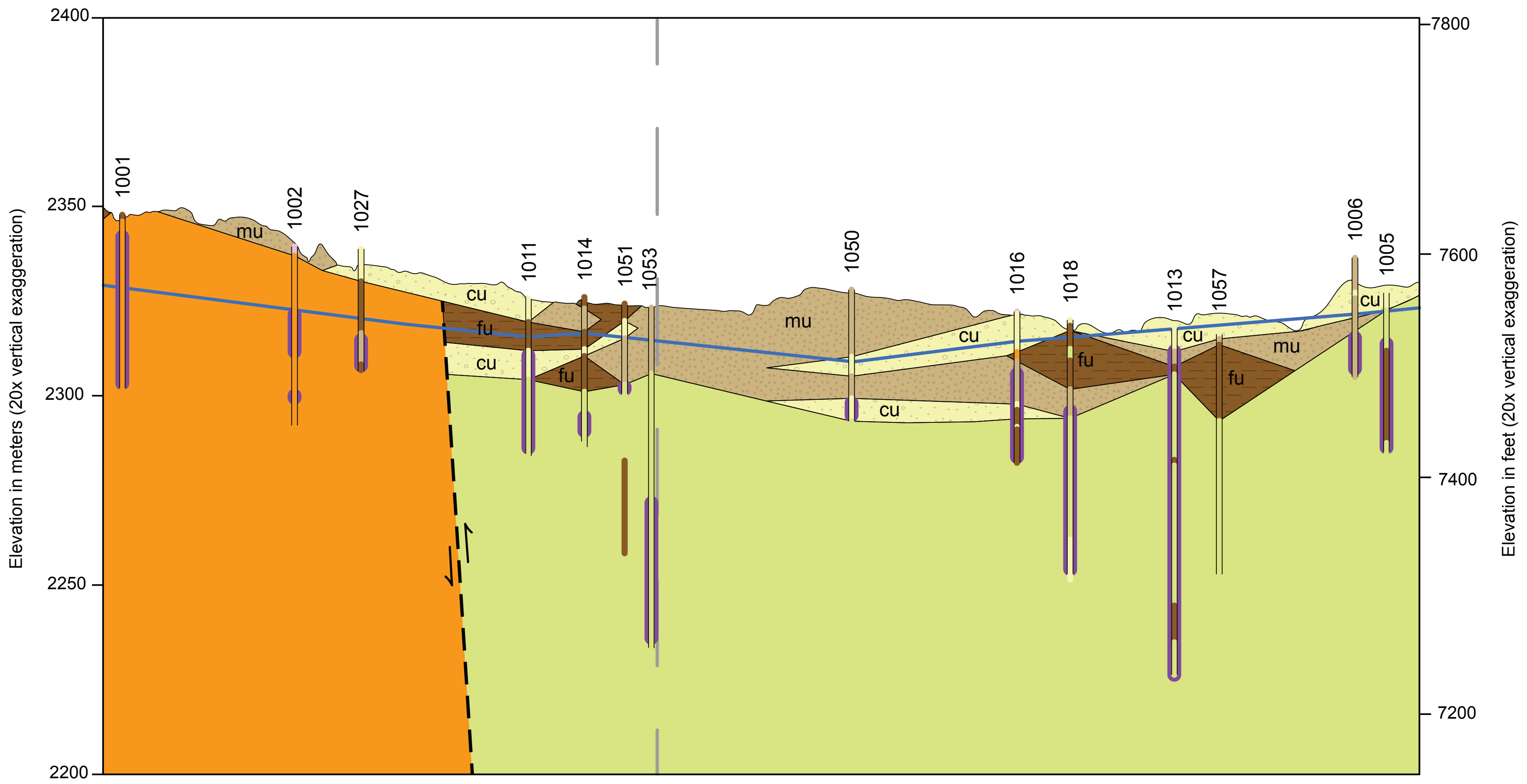

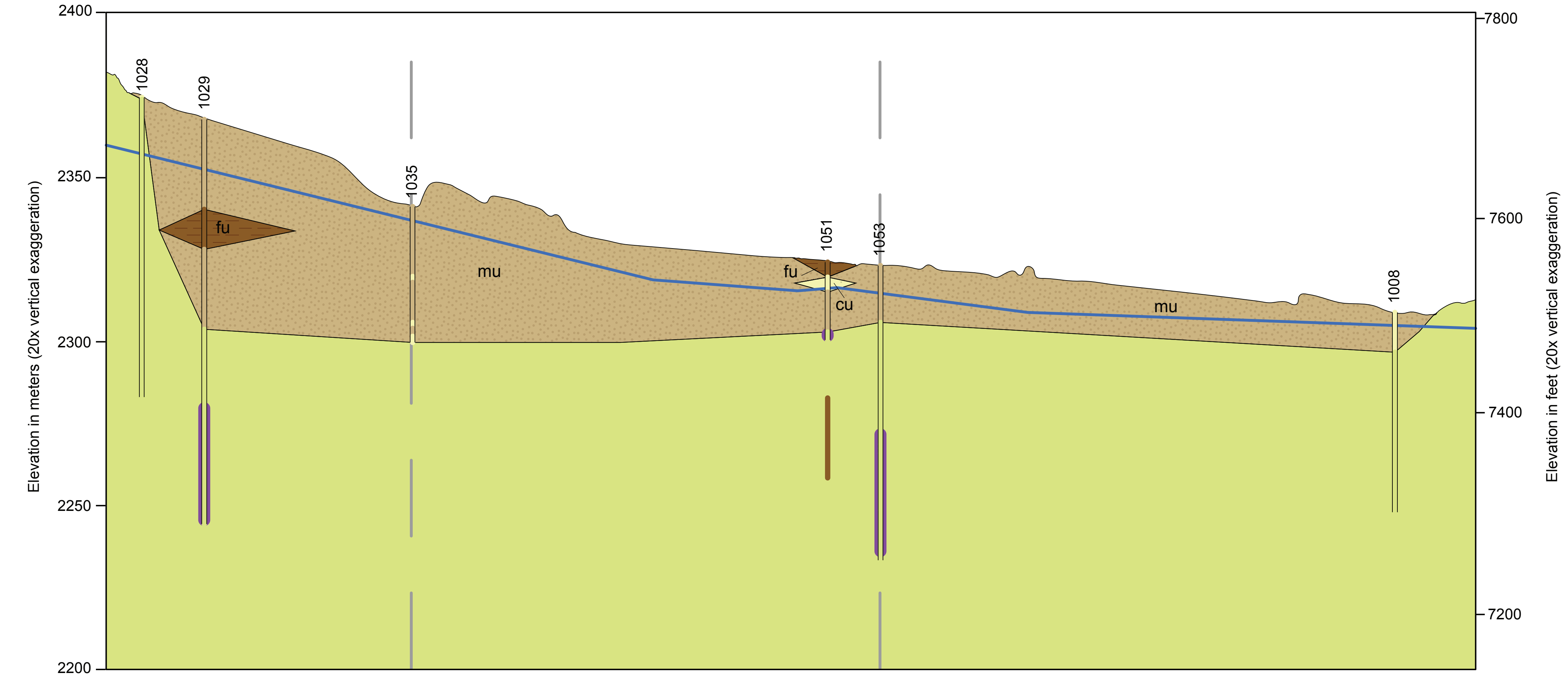

LITHOLOGIC UNITS

Valley Fill

- Topsoil
- cu — Coarse-grained unconsolidated
- mu — Mixed-grained unconsolidated
- fu — Fine-grained unconsolidated

Bedrock Units

- Claron Formation
- Cretaceous, undivided

Symbols

- Fault with arrows showing relative displacement (Vertical exaggeration artificially increases fault dips)
- 2019 potentiometric surface
- Bend in section
- Approximate valley-fill boundary

Wells - projected at actual elevation onto section lines

- 85 — Well ID
- Borehole lithology by color
- Perforated or screened interval

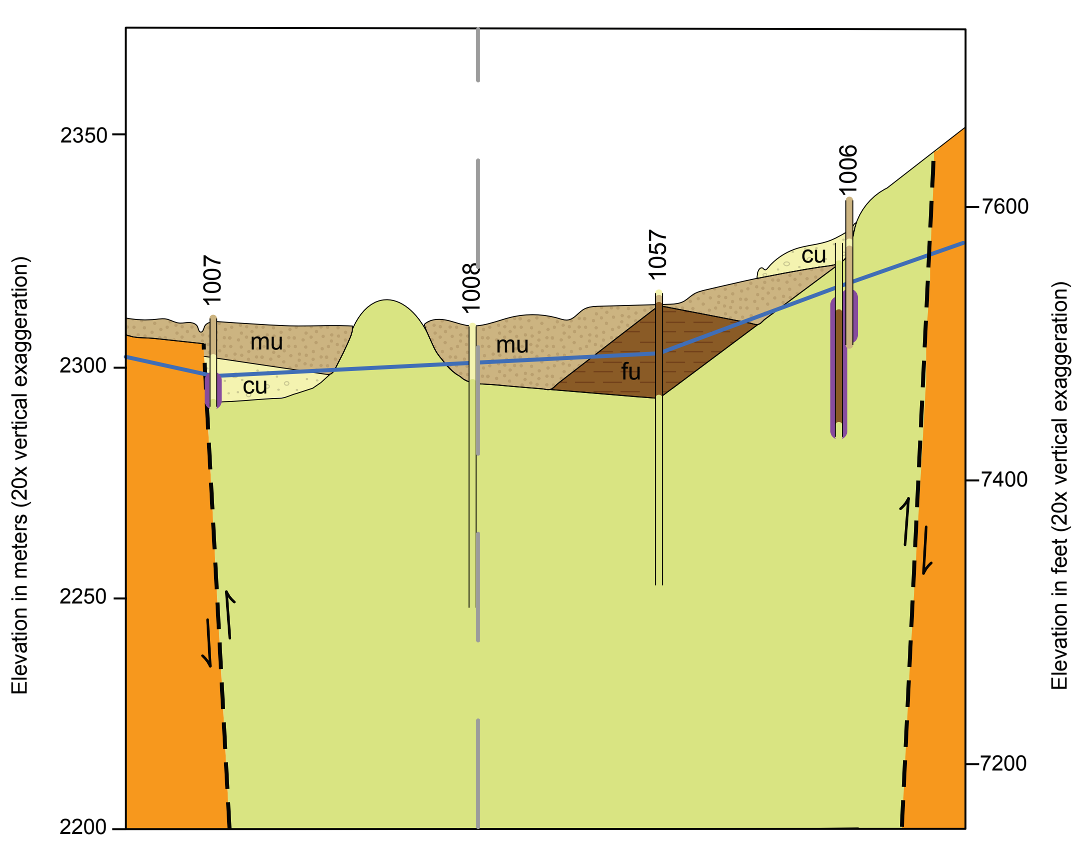

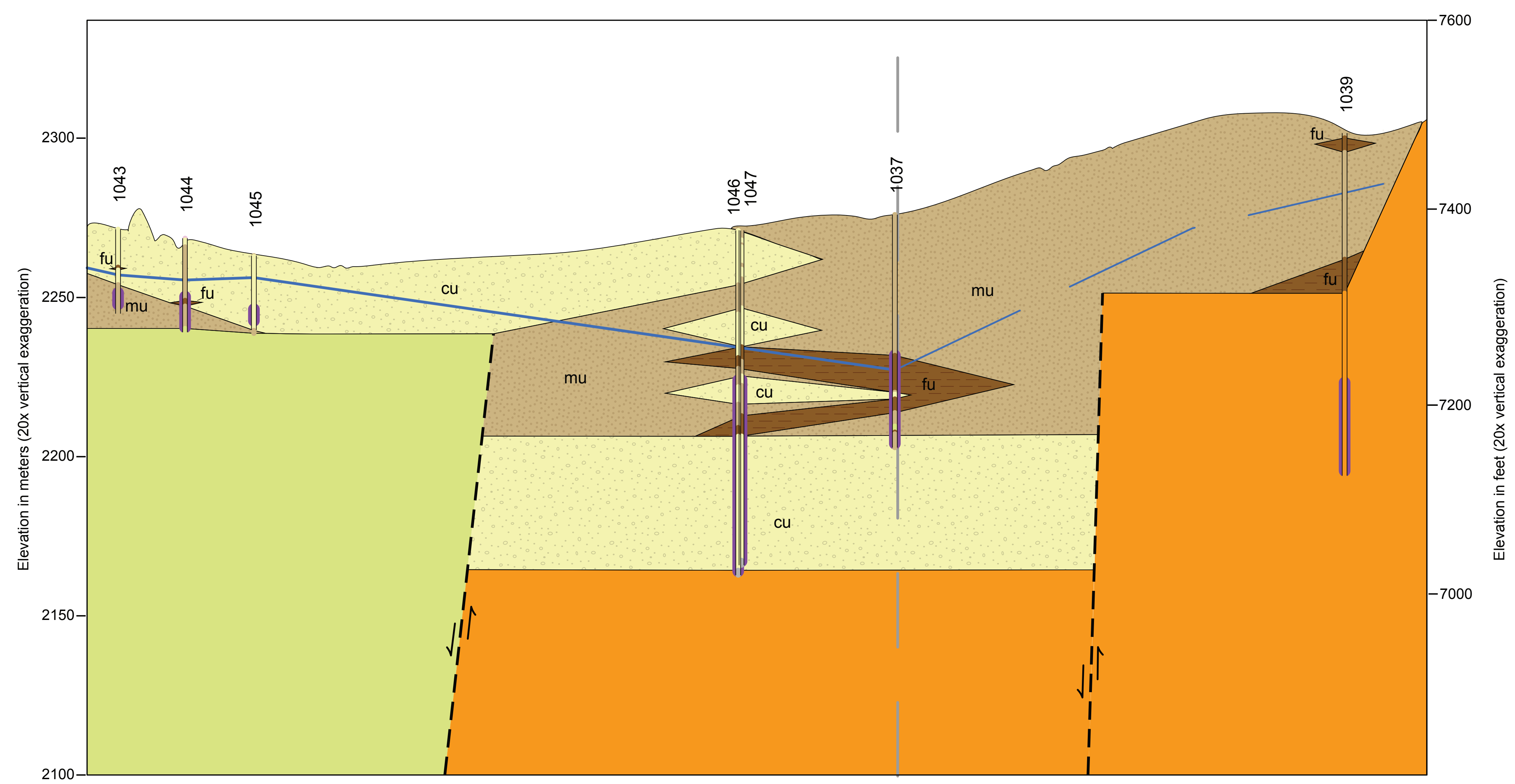

CROSS SECTION LOCATION MAP